



Annual Symposium on Research and Industrial Training  
of Department of Electronics

# **9<sup>th</sup> Annual Symposium on Research and Industrial Training of Department of Electronics**

**24<sup>th</sup> Feb. 2023**



**Department of Electronics**

Faculty of Applied Sciences

Wayamba University of Sri Lanka

Kuliyapitiya, 60200

Sri Lanka.



**Proceedings of**  
**9<sup>th</sup> Annual Symposium on Research and Industrial Training**  
**of**  
**Department of Electronics**

24<sup>th</sup> February 2023



**Department of Electronics**  
Faculty of Applied Sciences  
Wayamba University of Sri Lanka  
Kuliyapitiya, 60200  
Sri Lanka



## **Editorial board**

### ***Editor-in- chief***

Mr. K.K.C.S. Kiriella

### **Board Members**

Dr. M.A.A. Karunarathna

Snr. Prof. K.P. Vidanapathirana

Snr. Prof. (Mrs.) G.A.K.S. Perera

Prof. L.D.R.D. Perera

Prof. (Mrs.) J.M.J.W. Jayasinghe

Dr. Y.A.A. Kumarayapa

Dr. W.A.S. Wijesinghe

Ms. U.A.D.N. Anuradha

Mr. K.K.C.S. Kiriella

### **Review Panel**

Prof. L.D.R.D. Perera

Prof. (Mrs.) J.M.J.W. Jayasinghe

Dr. M.A.A. Karunarathna

Dr. Y.A.A. Kumarayapa

Dr. W.A.S. Wijesinghe

Ms. U.A.D.N. Anuradha

Mr. K.K.C.S. Kiriella

©Department of Electronics, Faculty of Applied Sciences,  
Wayamba University of Sri Lanka, 2022

**ISSN 2362 0560**

Designing and Printing at Department of Electronics,  
Faculty of Applied Sciences, Wayamba University of Sri Lanka , Kuliypitiya



## **Foreword**

It is with great pleasure that I write this foreword for the proceedings of the ASRITE-2022, the 9th Annual Symposium on Research and Industrial Training of the Department of Electronics at the Faculty of Applied Sciences, Wayamba University of Sri Lanka. This symposium provides a good platform for the undergraduates to showcase their research findings and industrial solutions from their final year research and six-month industrial training.

ASRITE-2022 embodies the hard work and dedication of many individuals. I extend my heartfelt gratitude to Vice-Chancellor of Wayamba University of Sri Lanka, Snr. Prof. Udith K. Jayasinghe and Dean of the Faculty of Applied Sciences, Prof. L.D.R.D. Perera for their invaluable guidance and support. I also should thank to Research Coordinator of the Department of Electronics, Prof. (Mrs.) J.M.J.W. Jayasinghe and Industrial Training Coordinator of the Department of Electronics, Dr. Y.A.A. Kumarayapa and the Coordinator of ASRITE-2022, Mr. K.K.C.S. Kiriella, for their diligent efforts in organizing this event.

The symposium offers a unique opportunity for the department's undergraduates to exchange their research ideas, knowledge, and expand the professional network. I hope that this symposium will continue to inspire and encourage future graduates to pursue research and innovation in the field of electronics and contribute to the advancement of the industry and society.

I wish all participants and attendees a productive and fulfilling experience at ASRITE-2022.

**Dr. M.A.A. Karunarathna**

Head - Department of Electronics

## CONTENTS

### Individual Research Papers

	Page
<b>01 IOT-BASED REMOTE SENSING TECHNIQUE WITH MACHINE LEARNING APPROACH FOR EARLY FLOOD RISK ASSESSMENT</b>	<b>1</b>
E.G.A.S. Bandara, Y.A.A. Kumarayapa	
<b>02 STUDY OF CHAOTIC BEHAVIOR IN ELECTRONIC CIRCUITS</b>	<b>9</b>
K.A.D. Sandeepa, W.A.S. Wijesinghe	
<b>03 DESIGNED A PRINTED ANTENNA WITH CIRCULAR POLARIZATION FOR GPS APPLICATIONS</b>	<b>17</b>
P.S.S. Witharana , J.M.J.W. Jayasinghe	
<b>04 LP GAS DETECTION AND NOTIFICATION SYSTEM</b>	<b>25</b>
R. D. Rasangika, M. A. A. Karunarathna	
<b>05 AUTOMATED REGISTER POSTAL MACHINE SYSTEM</b>	<b>32</b>
Y.G. Chandrasiri, U.A.D.N. Anuradha, K.K.C.S. Kiriella	
<b>06 DESIGN AND IMPLEMENTATION OF IOT BASED PATIENT BIO-MEDICAL PARAMETER MEASURING AND CRITICAL CONDITION ALARMING SYSTEM</b>	<b>40</b>
S.H.D.Dananjani , Y.A.A. Kumarayapa	
<b>07 DESIGN AND BUILD AN IOT-BASED FULLY- AUTOMATED MINI-GREENHOUSE FOR THE CULTIVATION OF VEGETABLES</b>	<b>48</b>
K.P. Gunaratne , J.M.J.W. Jayasinghe	

<b>08 MULTIFUNCTIONAL LABORATORY POWER SUPPLY</b>	<b>56</b>
L.S.K. Gunasinghe , L.D.R.D. Perera	
<b>09 DEVELOPMENT OF A SMART PILL DISPENSER</b>	<b>64</b>
M.A. Pathiraja , W.A.S. Wijesinghe	
 <b>Industrial Training Research Papers</b>	
<b>10 ARDUINO BASED RECHARGEABLE BATTERY TESTER</b>	<b>72</b>
Y.G Chandrasiri , K.K.C.S Kiriella	
<b>11 IOT BASE REAL TIME VEHICLE TRACKING SYSTEM</b>	<b>80</b>
S.H.D. Dananjani , M.A.A. Karunarathna	
<b>12 QUALITY CHECKING AND DATA ANALYZING HARDWARE SYSTEM WITH IOT FOR APPAREL INDUSTRY</b>	<b>88</b>
K.P. Gunaratne , Y.A.A. Kumarayapa	
<b>13 SMART MONKEY REPELLENT SYSTEM FOR TELECOM WIRES</b>	<b>96</b>
L.S.K. Gunasinghe , J.M.J.W. Jayasinghe , K.G. Welagedara	
<b>14 DEVELOPMENT OF A SMART AGRO SOIL ANALYZER</b>	<b>103</b>
M.A. Pathiraja , W.A.S. Wijesinghe , A.P. Kumara	

# **IOT-BASED REMOTE SENSING TECHNIQUE WITH MACHINE LEARNING APPROACH FOR EARLY FLOOD RISK ASSESSMENT**

E.G.A.S. Bandara<sup>\*</sup>, Y.A.A.Kurmarayapa

*Department of Electronics, Wayamba University of Sri Lanka, Kuliyaipitiya, Sri Lanka*

<sup>\*</sup>anushkabandara41@gmail.com

## **ABSTRACT**

Although there is a high population density due to the fertility of the river basins, even in the case of minor floods, these settlements are constantly at risk due to the flow of this excess water to the dry areas. When such over-flooding occurs in the river basins, it is important to have real-time remote mapping, early flood detection, and analyzing methods to prevent disaster and to deploy emergency response teams to rescue human lives and their property. Nevertheless, the use of radio and television news alert systems with announced flood risk communications are slow and less efficient methods that exist with heavy rainfall and other environmental disturbances. To circumvent such obstacles, in this study we propose a novel early flood risk assessment automation application with machine learning implementation to defend human lives. Compared to the other early flood risk assessment systems, the proposed system implemented Time series-based ARIMA model to predict flood risk assessment and IoT based SMS alert system with a GEE-based flood mapping and rainfall forecasting method to improve its validity and usability. Thus, the general public without much technical knowledge can use our early flood alert system on their own. Hence, this research study with our new risk awareness method will protect those living near flood-risky areas of major river basins.

**Keywords:** Remote sensing, Time series data prediction, Internet of Things

## **1.0 INTRODUCTION**

Floods are a natural disaster that occurs regularly in many parts of the world. Generally, a flood occurs when the water level of a river exceeds its maximum water level. This excess water flowing into dry areas is called a flood. When consider the dusters in globe, floods are the most unfavorable structure in nature. This is actually in phrases of every loss of existence and property damage. In Sri Lanka too, floods are more common than any other natural hazard [1]. According to the statistics, rainfall is the main environmental factor to influence the probability

of flood. Hence, designing, an early flood alerting system that operates based on the variation of rainfall patterns is a critical factor to deploy an emergency response team to rescue human lives [2]. At present, there are different types of flood hazard early detection and awareness system exists. However, there is a delay in notifying the message of settlements about whether the situation is dangerous or not.

This study has developed a flood-alerting system that consists of automated IoT-based applications, Remote sensing-based rainfall data analysis, and flood mapping techniques that also combine machine learning methods to predict the flood warning. The main objective of the proposed research study is to design a smart IoT and RS-based flood alert system with a time series analysis-based flood risk predictor to secure human lives and their property.

These prediction results were used for pre-flood risk notifications as SMS alerts to the public for their safety. Also, in the hardware part, the newly calibrated rain gauge sensor and the water level measurement sensor are proposed to utilize for measuring the main parameters that caused for the flood risk hazard.

## **2.0 EXPERIMENTAL**

### **2.1 Study Area**

Most of the rivers originate from Sri Lanka's mountainous central location and go with the flow outwards in all instructions down to the sea. According to the data of the disaster management system of Sri Lanka, the Kelani and Kalu Ganga river basins are the most flood-prone areas which illustrate in figure 2.1.

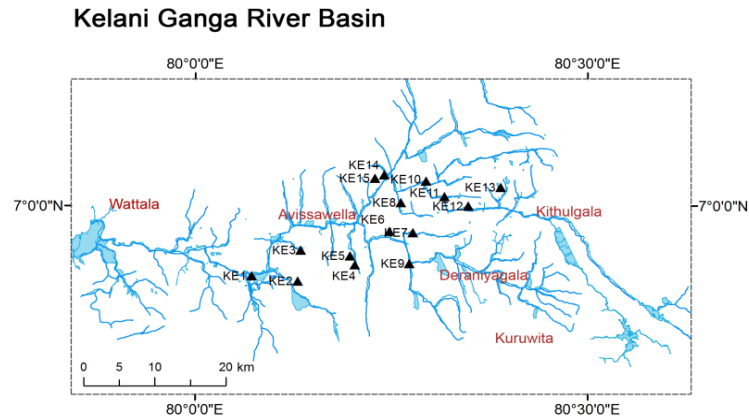


Figure 2.1: Kelani River basin

## 2.2 The Proposed System overview

The implemented automation part mainly consists of two parts, the transmitter device, and the receiver device. The machine learning model is deployed on the server side and the prediction results provide immediate alerts on whether the considered area is treated on flood or not.

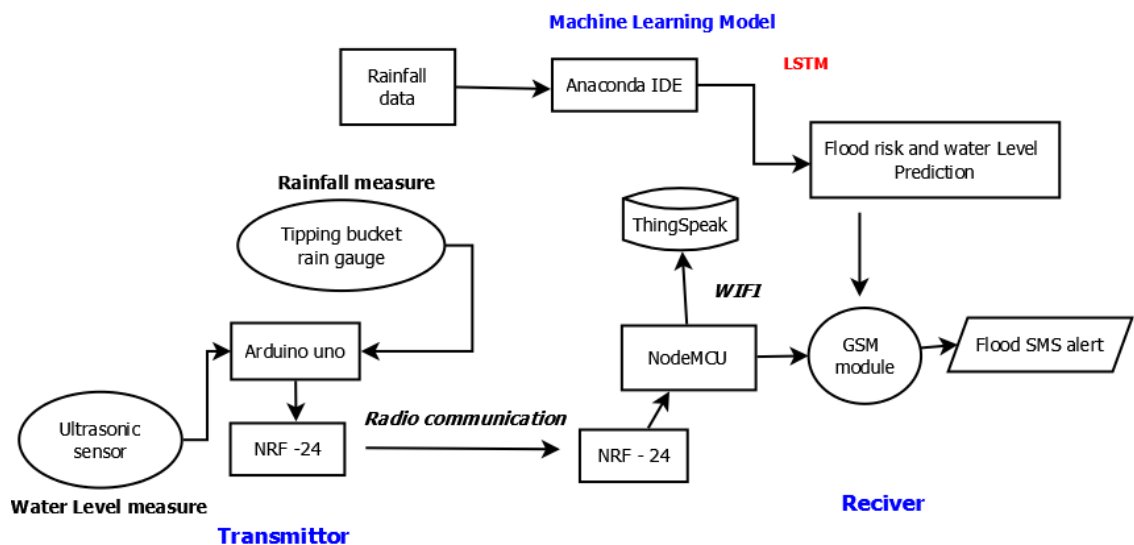


Figure 2.2: Block diagram of the complete Communication system

Figure 2.2 shows the complete block diagram of the overall designed system. On the transmitter side, the sensors are mounted to detect the variation of physical properties and the data send through Radio Frequency communication protocol. The IoT-based platform is implemented on the receiver side with a combine machine learning prediction model to improve the validity of the automated system.

### 2.3 Hardware implementation of the proposed system

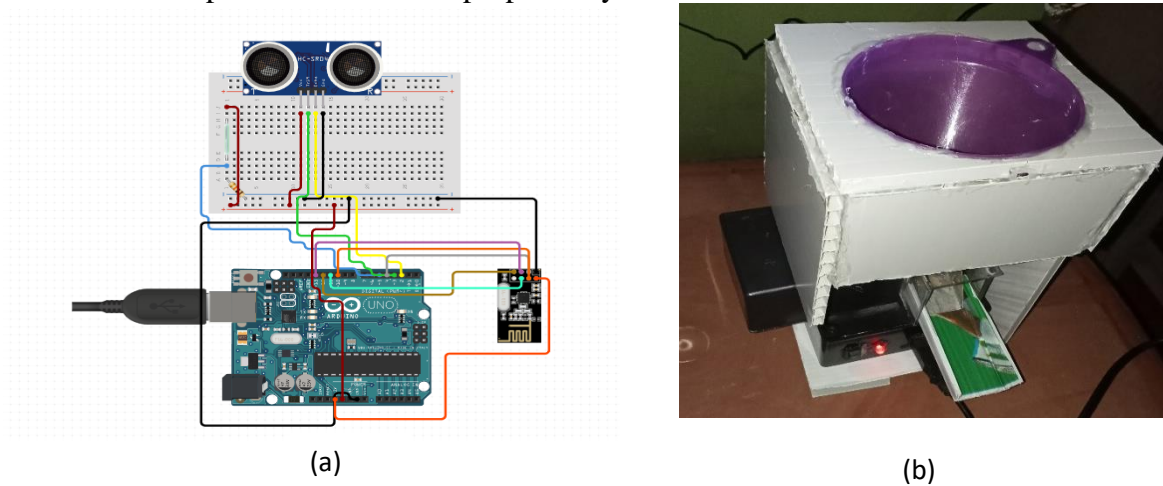


Figure 2.3: (a) Circuit diagram of the transmitter. (b) Hardware design of the transmitter device

Figure 2.3 shows the transmitter device of the flood alert warning system based on IoT and Radio communication. In the transmitter part, the Arduino Uno development board is used as the main controller, an ultrasonic sensor is used to measure the water level of the river, and a tipping bucket rain gauge is used to measure the rainfall. Finally, the measured data was transmitted through the NRF24 module based on radio communication protocol.

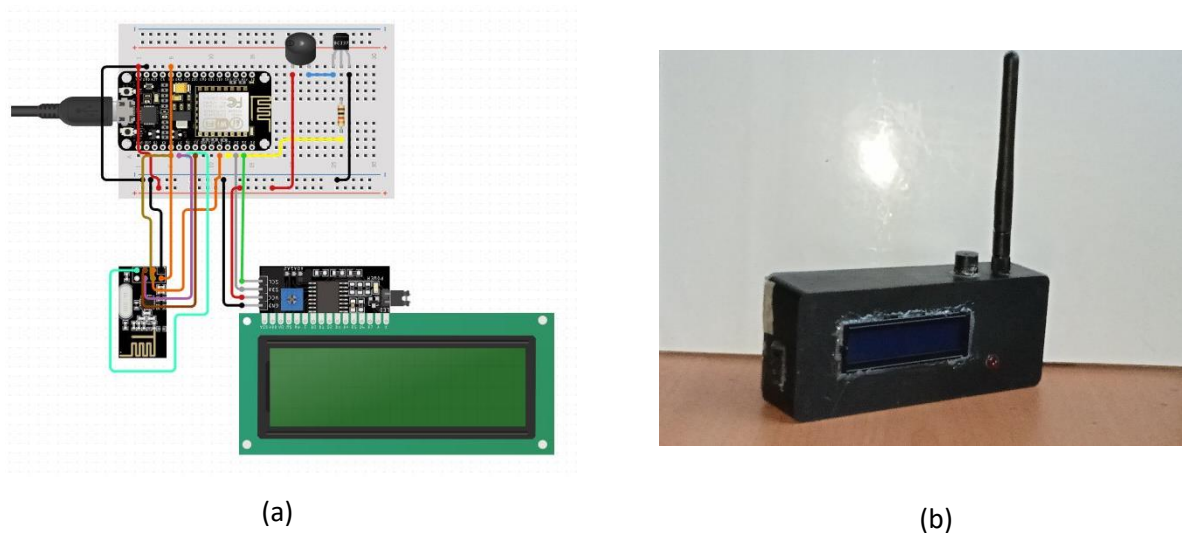


Figure 2.4: (a) Circuit diagram of the receiver. (b) Hardware design of the receiver device

Figure 2.4 shows the receiver device of the flood alert warning system. This device captures the water level and rainfall data that transmit to the transmitter and this data is real-time monitored in Thingspeak sever through the IoT platform. The Nodemcu ESP 8266

development board act as the main controller and the sim800C GSM module is used to send the message as a flood alert for the social. Also, this device contains a buzzer which helps to generate a sound signal as a warning alert.

### 3.0 RESULTS AND DISCUSSION

The ultimate aim of this system is to detect the water level and daily rainfall of the entire area by using the ultrasonic sensor and rain gauge sensor mounted on the transmitter device in order to predict the discharge of the river and notify about flood risk for human safety.

#### 3.1 The Rain Gauge calibration



Figure 3.1: Tipping bucket rain gauge sensor calibration

Figure 3.1 shows the calibration testing process of the rain gauge sensor, in this process, an injection syringe is used to measure the volume of each bucket, and the results are used to calculate the rainfall of the catchment area.

The receiver device contains a 16x2 LCD module and it's displayed the received parameters as figure 3.2 and also this parameter can be visualized and analysis IoT based ThingSpeak server.





Figure 3.2: received parameter display in the LCD panel of receiver device

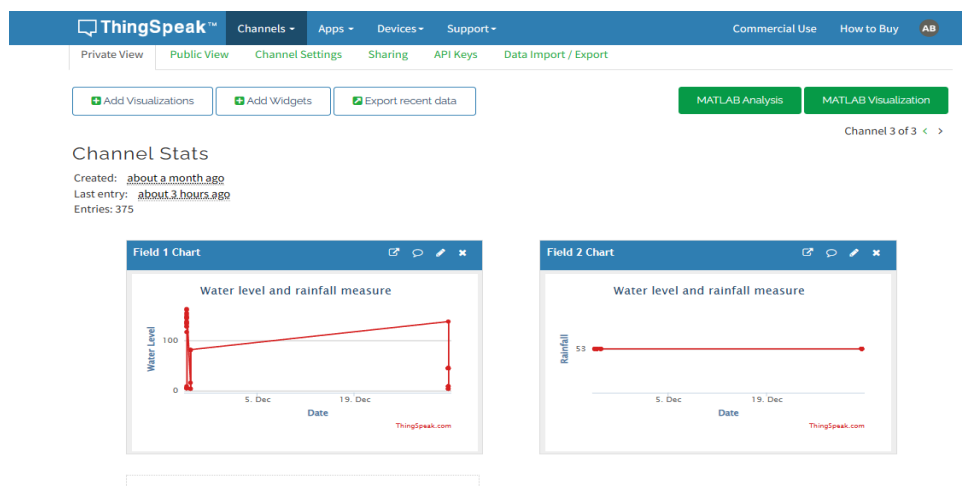


Figure 3.3: The Real-time updated data on the ThingSpeak server

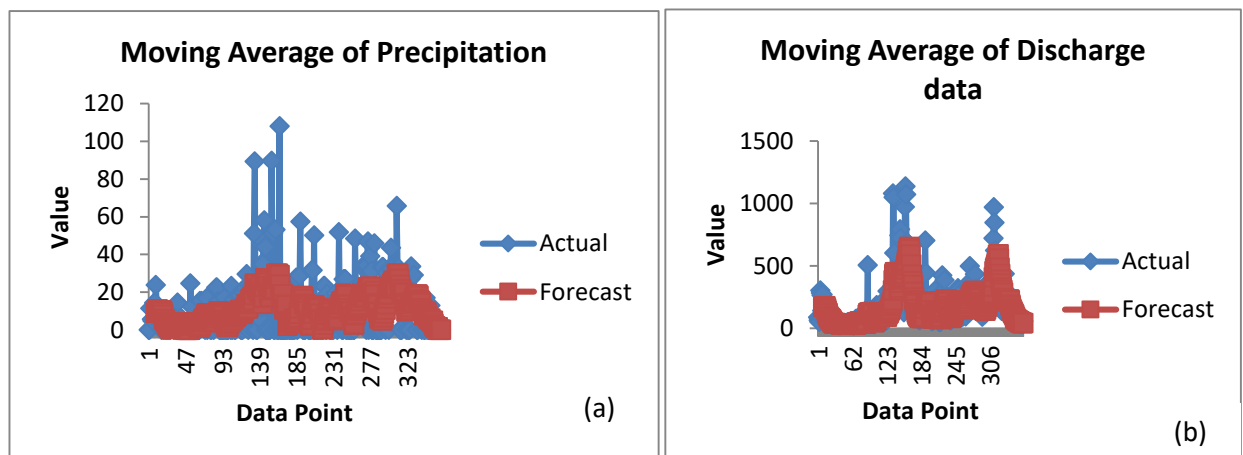


Figure 3.4: Time series plot of centered moving average in (a) The Precipitation data. (b) The discharge data

Figure 3.4 shows the time series plot of precipitation data in the Hanwella station of the

Kelani River basin and the change of discharge data at Kelani River Hanwella station throughout the year 2021. According to the charts, the precipitation and discharge data vary according to the nonlinear pattern. To identify the trend component of the linear model the time series analysis-based moving average method is used to implement the machine learning approach for predicting the data.

#### **4.0 CONCLUSION**

Flood is one of the major natural disasters that cannot be avoided in the period of heavy rainfall. The major flood hazards are risky and it's affects so many lives and properties. At present there are different types of flood avoidance techniques and early flood detection system implemented for saving lives and their properties. However, these systems were developed only focusing on a unique property. Nevertheless, in the proposed and constructed method use IoT, remote sensing method and machine learning assessment to improve the validity of early flood monitoring and notification system.

This project mainly focuses on the Kelani River basin and analysis of rainfall and discharge data at Hanwella station. The developed flood monitoring and early warning system aim to detect flood hazards by using IoT and remote sensing technique with data prediction method. In future studies, it can be implemented for different weather stations of major flood-affected river basins. Moreover, the machine learning model can be improved by using different time series data prediction methods.

#### **ACKNOWLEDGEMENTS**

Department of irrigation is highly acknowledged for providing data sets of discharge data of this study. Authors of the journals and the academic staff of Faculty of Applied Sciences, Wayamba University of Sri Lanka would also thanks and appreciation.

#### **REFERENCES**

- [1]. Sivakumar, S.S., Flood Mitigation Strategies Adopted in Sri Lanka A Review. March. *International Journal of Scientific & Engineering Research*, Volume 6, Issue 2, 2015, 607

- [2].UNDP, UNDP BOOK CHAP 04\_ Flood .pdf, pp. 64–89, 2010,[http://www.Dmc.gov.lk/images/hazard / hazard/Report/UNDP%20BOOK%20CHAP%2004\\_ %20Flood.pdf](http://www.Dmc.gov.lk/images/hazard/hazard/Report/UNDP%20BOOK%20CHAP%2004_%20Flood.pdf)
- [3]. Khalaf, M., Alaskar, H. , Hussain, A. J., IoT-Enabled Flood Severity Prediction via Ensemble Machine Learning Models. *IEEE Access* 8, , 2020, 70375–70386
- [4]. Kim, H. I.L. ,Kim, B. H., Flood Hazard Rating Prediction for Urban Areas Using Random Forest and LSTM, *KSCE J. Civ. Eng.*, vol. 24, no. 12, pp. 3884–3896, (2020), doi: 10.1007/s12205-020-0951-z

## STUDY OF CHAOTIC BEHAVIOR IN ELECTRONIC CIRCUITS

K.A.D. Sandeepa\*, W.A.S. Wijesinghe

*Department of Electronics, Wayamba University of Sri Lanka, Kuliypitiya, Sri Lanka*

\*97kadsandeepe@gmail.com

### ABSTRACT

Chaos theory is a branch of mathematics and physics that studies the behavior of dynamic systems that are highly sensitive to initial conditions. This means that small differences in initial conditions can lead to vastly different outcomes over time. One of the key concepts in chaos theory is the idea of a strange attractor. A strange attractor is a geometric object that is formed by the trajectory of a dynamic system over time, and it is characterized by its fractal structure and its sensitivity to initial conditions. Evidence for chaotic behavior was observed by experiments and computer simulations. The purpose of the diode inductor resistor (DLR) experiment was to construct a simple circuit with a resistor, diode, and inductor in series driven by a sinusoidal signal to create chaotic behavior within the circuit. The logistic map was iterated for different values of  $\lambda$  and the Bifurcation diagram was observed for chaotic behavior of the DLR circuit. The bifurcation diagram shows a periodic doubling; hence the circuit shows chaotic behavior. By calculating the Feigenbaum  $\delta$  constant (the ratio of distance between successive bifurcations), the chaotic nature of the circuit can be proved. Chaotic behavior of Chua's circuit that was observed closely matches the original Chua attractor.

**Keywords:** Attractor, Chua's circuit, Feigenbaum  $\delta$  constant

### 1.0 INTRODUCTION

Chaos belongs to the ancient terms usually connected with a high degree of disorder. There are two necessary conditions under which chaos can evolve: three degrees of freedom (valid for autonomous systems; driven systems need to be of at least second order) and the presence of some nonlinearity [1]. The field of chaos theory was founded by a meteorologist named Edward Lorenz in the 1960s, and it has since grown to become a central concept in the study of complex systems in many different fields, such as physics, mathematics, biology, economics, and even the social sciences. In recent decades mathematical chaos used in electronic circuits to generate random numbers for security purposes. One-time passwords and pseudo-random numbers can

be generated using chaotic electronic circuits. The long-time unpredictability of a chaotic data sequence makes it very useful in the field of spread spectrum communication, secure communication channels, and cryptography. One of the mostly used ways to exhibit chaotic behavior is Linsay's experimentation which was done in response to Feigenbaum's theory of non-linear systems that exhibit period doubling, which states that their behavior, and specifically their bifurcation and period doubling patterns, follow universal laws independent of the equations that describe their particular behavior. Here usage of logistic map is very important: computer simulations of the logistic map can be observed by using Mathematica software. Then measured Feigenbaum  $\delta$  constant to ensure that the circuit shows the chaotic behavior.

## 2.0 METHODOLOGY

### 2.1 The DRL circuit

The DRL circuit is a very simple kind of circuit that contains a diode, an inductor, and a variable resistor. This circuit can be found in many household electronic devices such as TV, DVD player, etc.

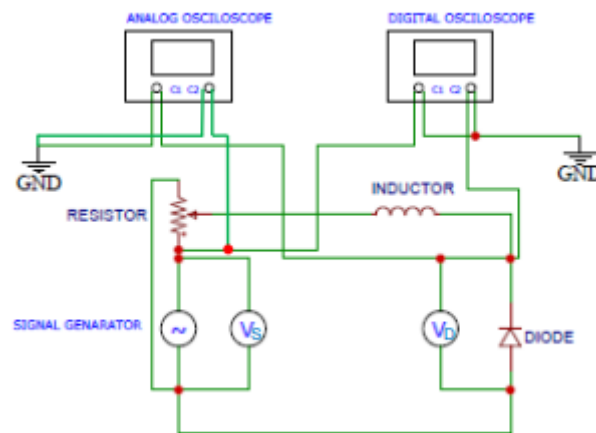


Figure 2.1: DLR circuit

We can obtain a relationship between the voltages of each component in the circuit as.

$$V_s = V_R + V_L + V_D \quad [1]$$

Where,

$V_s$  = Input voltage

$V_R$  = Voltage across the Resistor

$V_L$  = Voltage across the Inductor

$V_D$  = Voltage across the Diode

Table 2.1: Component values of DLR circuit

Component	Value
Variable Resistor	10 k $\Omega$
Inductor	2 mH
Diode	IN4007

Each voltage can be expressed as follows to get a more detailed idea of the circuit,

$$V_0 \sin(2\pi ft) = RI(t) + L \frac{dI}{dt} + V_D \quad [2]$$

Where,  $V_s$ , is the varying voltage of the signal generator,  $V_R$  is the voltage across the resistor,  $V_L$  is the voltage across the inductor, and  $V_D$  is the voltage across the diode. The phenomenon of period doubling is evidenced by measuring the voltage drop across the diode and varying the frequency,  $f$ , or amplitude,  $V_0$ , of the driving voltage. An analogous model can be attributed to current driven back and forth within a pipe whose frequency and amplitude are modulated by some incoming signal. A damping component of the pipe acts like a resistor in the circuit, a propeller takes the place of the inductor, and a flap valve replaces the diode.

For current flowing in one of the directions, the propeller builds up the momentum that resists the backward flow of the current until it begins spinning in the opposite direction. In combination with the diode, the inductor picks out a range of frequencies and amplitudes that allow period doubling to occur. If we imagine the output signal as the pressure drops across the flap valve, then, for small amplitudes, the flap valve opens and closes at the same rate as the driving frequency. However, for larger amplitudes, the backward surge is unable to close the flap valve completely before the next forward surge pushes it open again. Consequently, the pressure across the valve is lower than it would be if the valve was completely closed. However, this incoming surge must overcome the momentum of the last backward surge and does not open the valve as much as the first surge. Thus, the next backward surge can completely close the valve, and so the cycle repeats. In this way, the output signal can achieve higher periodicity than the input signal.

In the beginning, the DRL circuit (Figure 2.1) was created by using a signal generator, Digital and Analog oscilloscopes, Diode, Inductor, and a Variable resistor along with wires on the breadboard. A sinusoidal signal was passed through the circuit, and both channels of the Digital oscilloscope were connected to the input and Diode voltages. The Analog oscilloscope was connected to the voltage through the diode and the input voltage again like in the Digital Oscilloscope, and then XY button was pressed in the analog one to see the cycles on it. After finding the cycles of the LCR circuit output signal, the variable resistor was changed to adjust

the input voltage to the circuit while the frequency was 205 kHz and found the 1 cycle. Likewise, after almost 4 cycles, chaos was found by changing the input voltage.

After that, Feigenbaum  $\delta$  was calculated by using our data, and after that, by using Mathematica software computer simulation part was done. The program was written to logistic map equation,  $X_{n+1} = 4\lambda x_n(x_0 - x_n)$  using Mathematica software. The logistic map was iterated for different values of  $\lambda$  ( $\lambda = 0.5, 1.0, 2.0, 3.0, 3.5, 3.55, 4.0$  and  $4.05$ ) and initial value  $x_0 = 0.95$  was chosen. Graph of  $x_n$  Vs  $n$  was plotted using Mathematica software. Then a bifurcation diagram was plotted for the logistic map by plotting some values of  $x_n$  after about 200 to 205 iterations as a function of  $\lambda$ . The  $\lambda$  values were 0.5, 1.0, 2.0, 3.0, 3.2, 3.4, 3.6, and 3.8. A value of  $\lambda$  was found for which the logistic map was chaotic by looking at the bifurcation diagram.

## 2.2 Chua's Circuit

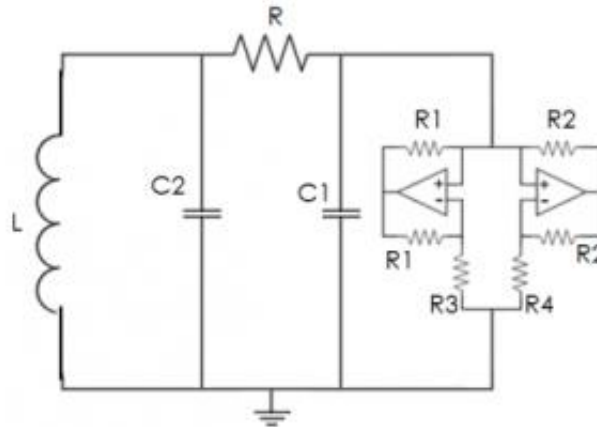


Figure 2.2: Chua's circuit

Chua's circuit is made out of capacitors ( $C1, C2$ ), an inductor ( $L$ ), and several resistors ( $R, R1, R2, R3, R4$ ). We obtain suitable values for the circuit element and provide a signal from the signal generator.

In the beginning, Chua's circuit was created by using a signal generator, Digital and Analog oscilloscopes, capacitors, Inductor, and a Variable resistor along with wires on the breadboard. Signal generator was connected across the inductor, and sinusoidal signal was passed through the circuit. Then channels of the digital oscilloscope were connected to the input and load (Resistor sub circuit). The XY mode was activated on the oscilloscope, and observed the output by varying the frequency given by the signal generator. Also, the circuit was built using simulator software, and observed the output of the circuit [2], [3].

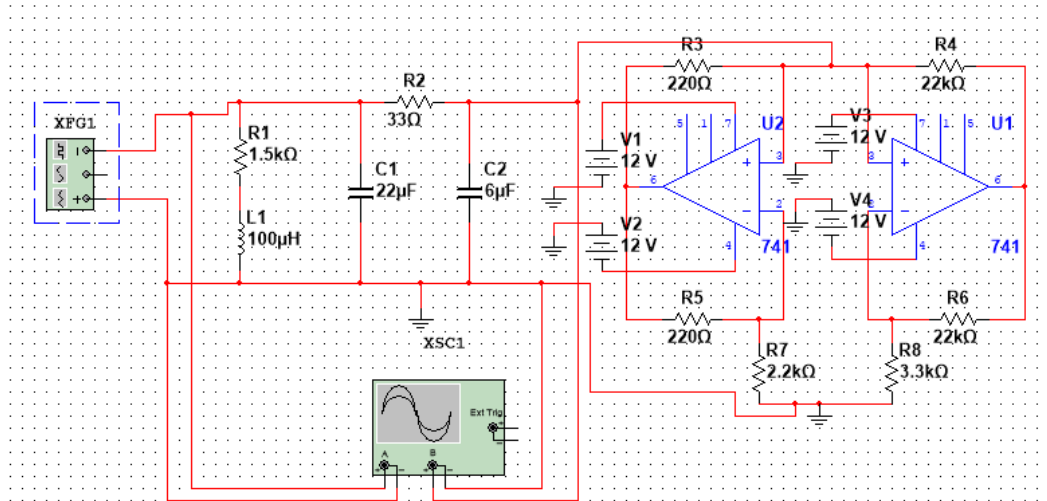


Figure 2.3: Chua's circuit for software simulation

### 3.0 RESULTS AND DISCUSSION

#### 3.1 Phase- space plot of diode voltage vs. driving voltage for DLR circuit

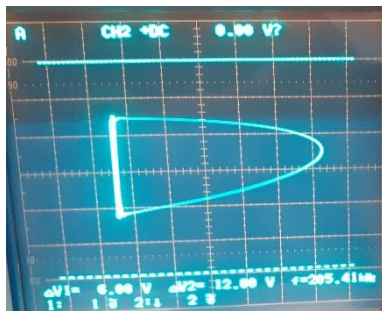


Figure 3.1: Phase - space plot of diode voltage vs. driving voltage for period 1

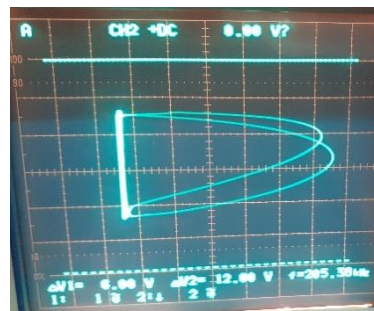


Figure 3.2: Phase - space plot of diode voltage vs. driving voltage for period 2

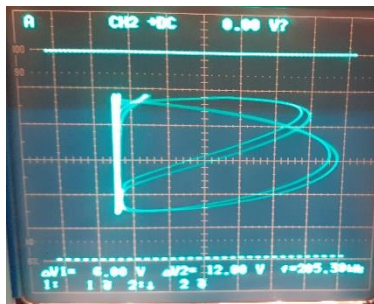


Figure 3.3: Phase - space plot of diode voltage vs. driving voltage for period 3

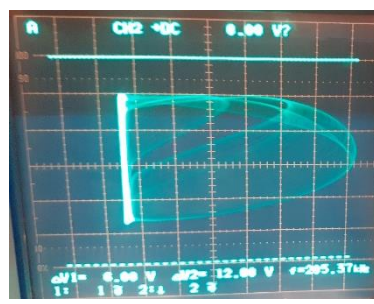


Figure 3.4: Phase - space plot of diode voltage vs. driving voltage for chaos

By changing the input voltage, there were regions with periods 1, 2, 3, and chaos. These outputs were taken using the XY mode of the oscilloscope. The periodic doubling can be seen; hence the circuit shows chaotic behavior [4].



### 3.2 Computer Simulations for logistic map equation

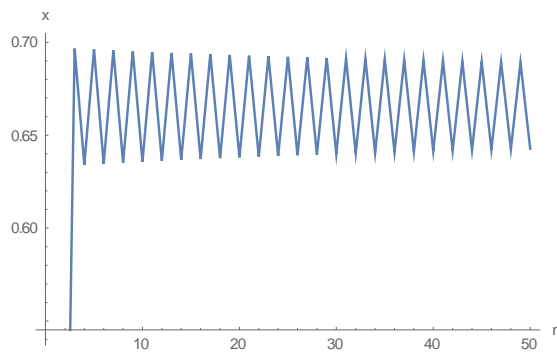


Figure 3.5: the graph of  $x_n$  vs  $n$  for  $\lambda=3.0$

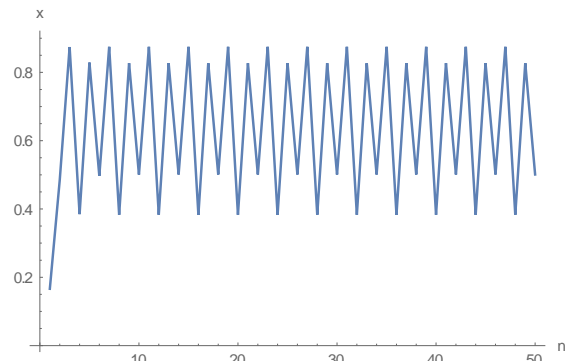


Figure 3.6: the graph of  $x_n$  vs  $n$  for  $\lambda=3.5$

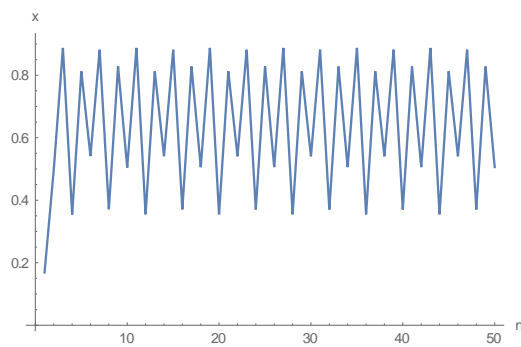


Figure 3.7: the graph of  $x_n$  vs  $n$  for  $\lambda=3.55$

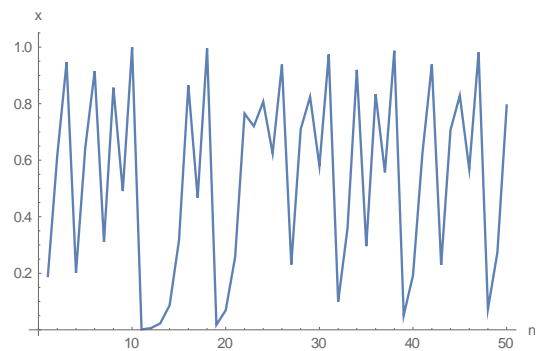


Figure 3.8: the graph of  $x_n$  vs  $n$  for  $\lambda=4.0$

The logistic map was iterated for different values of  $\lambda$  and took above computer simulations for the logistic map using Mathematica 11.2 software.

### 3.3 Bifurcation Diagram

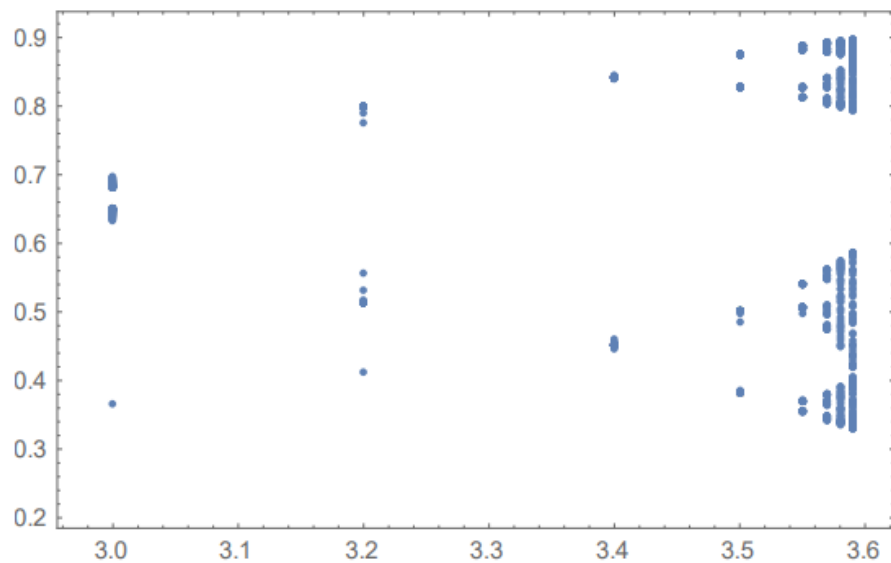


Figure 3.9: Bifurcation Diagram

A clear period-doubling can be seen from the bifurcation diagram, which proves the circuit shows chaotic behavior.

### 3.4 Calculating Feigenbaum $\delta$ Constant

$$\delta = \lim_{n \rightarrow \infty} \left( \frac{\lambda_n - \lambda_{n-1}}{\lambda_{n+1} - \lambda_n} \right) \quad [3]$$

$$\delta = \frac{820 - 560}{900 - 820}$$

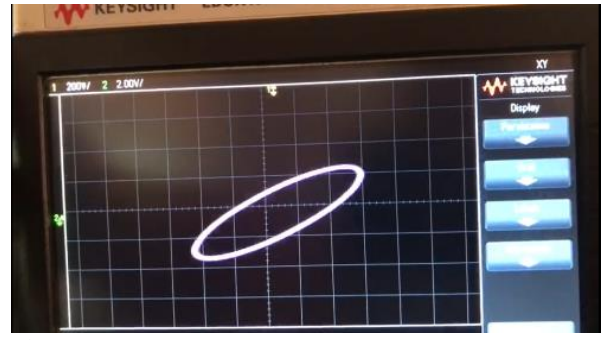
$$\delta = 3.25$$

Numerical calculations show that  $\delta \approx 4.66920$ . In the expression for the  $\delta$ ,  $\lambda_n$  refers to the  $\lambda$ , which demonstrates the onset of a  $2^N$  cycle. Here Feigenbaum  $\delta$  constant is calculated by taking the ratio of distance between successive bifurcations [4].

### 3.5 Output of Chua's circuit



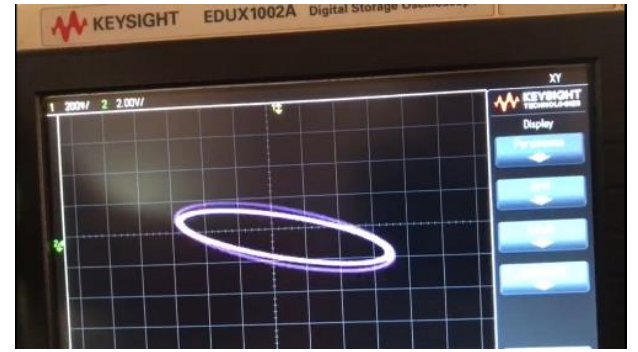
(a)



(b)



(c)



(d)

Figure 3.10: Outputs of the Chua's circuit when the input frequencies are (a) 8.5 MHz, (b) 14.5 MHz, (c) 15 MHz, (d) 18 MHz

### 3.6 Discussion

The purpose of the DLR experiment was to construct a simple circuit with a resistor, diode, and inductor in series driven by a sinusoidal signal to create chaotic behavior within the circuit. Due to the nonlinear dynamics of a diode, when a DLR circuit is created and driven by a sinusoidal signal whose amplitude is continually increased, chaotic behavior can be observed.

The Feigenbaum  $\delta$  constant value we calculated was close to the actual value. At the sensitive region of the system, we could get a chaotic situation: by a very small change of input voltage, the waveform was highly distorted, which means that chaotic behavior was applied. In the computer simulations, the  $\lambda$  value was changed from 0.5 to 4.05. Here  $X_0$  was taken as 0.95. Code was run around 205 iterations. When the iteration process is increased, the function started to show a special pattern introduced as Bifurcation.

It was difficult to find suitable values to operate Chua's circuit. Using Multisim software, the circuit (Figure 2.3) was tested for values that can give proper circuit iterations as Chua's attractor. When considering the outputs (in Figure 3.10 (c) and (d)), we can see chaos. But the output is not perfect as the Chua attractor.

#### 4.0 CONCLUSION

Chaotic behavior was theoretically identified by plotting Logistic maps and Bifurcation diagram using mathematical software. The Bifurcation diagram has clear periodic doubling, which is a sign of chaotic behavior. And it was practically recognized by observing the outputs of the DLR circuit. The Feigenbaum  $\delta$  constant practical value that has been gained is 3.25. Chua's circuit has shown chaotic behavior when observing the outputs on the Oscilloscope.

#### ACKNOWLEDGEMENTS

The authors would like to express their sincere gratitude to everyone who helped to carry out this project successfully.

#### REFERENCES

- [1] Collin Sparrow, *The Lorenz Equations Bifurcations, Chaos, and Strange Attractors*, 1<sup>st</sup> Ed., Springer New York, 1982
- [2] Matsumoto T., A Chaotic Attractor from Chua's Circuit, *IEEE Transactions on Circuits and Systems. IEEE*, (1984), CAS-31 (12), 1055-1058, doi:10.1109/TCS.1984.1085459
- [3] Chua Leon O., Matsumoto T., Komuro M., The Double Scroll, *IEEE Transactions on Circuits and Systems. IEEE*. (December 1984), CAS-32 (8): 798–818.
- [4] Stankevich N. V., Kuznetsov N. V., Leonov G. A., Chua L., Scenario of the birth of hidden attractors in the Chua circuit, *International Journal of Bifurcation and Chaos*, 27 (12), (2017), 1730038–188.
- [5] Hilborn, Robert C., *Chaos and Nonlinear Dynamics; an Introduction for Scientist and Engineers*, Oxford University Press, Oxford, 19

## DESIGN A PRINTED ANTENNA WITH CIRCULAR POLARIZATION FOR GPS APPLICATIONS

P.S.S. Witharana\*, J.M.J.W. Jayasinghe

<sup>1,2</sup>*Department of Electronics, Wayamba University of Sri Lanka, Kuliyaipitiya, Sri Lanka.*  
\*punsarasandali96@gmail.com

### ABSTRACT

A small antenna with advanced features has become a very versatile device in the contemporary world. This project presents the design of a microstrip patch antenna for a GPS application operating at 1.575 GHz. the major objective of this research was to design a low-cost, compact microstrip antenna with sufficient bandwidth, an Omnidirectional radiation pattern, and right-hand polarization. The proposed antenna has dimensions of 63.5 mm x 75.3 mm x 1.6 mm which is fabricated using Duroid 5880 with a dielectric constant of 2.2. The microstrip patch antenna design was simulated in High-frequency simulation software (HFSS). This research discusses the impedance bandwidth, gain, radiation pattern, and circular polarization of the proposed antenna. In this research, an edge truncated microstrip patch antenna was proposed. The simulation gave results good enough to satisfy our requirements to fabricate it on hardware that can be used wherever needed.

**Keywords:** circular polarization, GPS applications, edge truncated

### 1.0 INTRODUCTION

#### 1.1. Overview

Today, production vehicles are fitted with a multitude of antennas to facilitate communication and enable a moving vehicle to connect with the outside world [1]. To achieve polarization matching, the transmitter and receiver must have the same frequency range, axial ratio, spatial orientation, and sense of polarization. Circularly polarized antennas are reconcilable with these requirements because they can reduce multipath effects and provide flexibility in the orientation angle between transmitting and receiving antennas, thus circularly polarized antennas are widely used in mobile and wireless communication such as global navigation systems and satellite communication systems [2].

### 1.2. Research objectives for vehicular applications

According to studies, there are many patch antennas with circular polarization. This study is mainly focused on designing a low-cost, compact microstrip antenna, to enhance the performance, increase the bandwidth, and make the antenna work efficiently by using an Omnidirectional radiation pattern and right-hand polarization.

### 1.3. Literature review

A pentagonal microstrip antenna has been designed in [3] for dual resonance frequencies at L1 (1.575 GHz) and L2 (1.227 GHz) with Right Hand Polarization. It was designed using IE3D simulation software. The coaxial feed has been used as the feeding technique for the antenna [3]. The drawback of the design is it does not cover the required bandwidth of GPS. A single cross-dipole microstrip antenna with enhanced low-elevation gain has been investigated. Two perpendicular dipoles were printed on two separate substrates and vertically placed inside a cylindrical back cavity. The antenna was designed to operate in GPS L1 (1.575 GHz) band. An L-shaped microstrip feed line was used as the feeding technique [4]. To generate RHCP fields, the signals applied to the two dipoles are equal in amplitude and  $90^\circ$  out of phase. This antenna can be used for applications that require a broad beamwidth and good low-elevation gain with fewer constraints on size and weight. In [5], A self-matched printed hemispherical helical antenna for potential use in global positioning system receivers has been introduced. This introduced antenna can be used in GPS receivers. Even though, it gives good angular coverage for the GPS requirements it covers the GPS L2 band. A novel compact antenna has been proposed for CP operations just using the feedline and the ground plane. The proposed design offers advantages in structure, size, weight, fabrication, and performance, which make the proposed antenna suitable for integration into RF circuitry and a good candidate in commutation systems [6].

## 2.0 EXPERIMENTAL

### 2.1. Theory and Diagrams

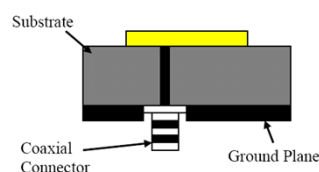


Figure 2.1: Microstrip antenna with a coaxial cable

To design a microstrip patch antenna, we have to select the resonant frequency and a dielectric medium for which the antenna is to be designed. The width of the patch is calculated using the equation,  $W = \frac{C_0}{2f_r} \sqrt{\frac{2}{\epsilon_r + 1}}$ . Where,  $W$ = patch width,  $C_0$  = speed of light,  $f_r$ =resonance frequency, and  $\epsilon_r$ =value of the dielectric substrate. The refractive index is calculated using the equation,  $\epsilon_{reff} = \frac{\epsilon_r + 1}{2} + \frac{\epsilon_r - 1}{2} \left[1 + \frac{12h}{W}\right]^{-\frac{1}{2}}$ . where,  $\epsilon_{reff}$  = Effective Dielectric Constant,  $\epsilon_r$  = relative permittivity,  $h$  = height of the substrate,  $w$  = width.  $W/h > 1$ . patch length can be calculated using the equation,  $\frac{\Delta L}{h} = 0.412 \frac{(\epsilon_{reff} + 0.3) \left(\frac{W}{h} + 0.264\right)}{(\epsilon_{reff} - 0.258) \left(\frac{W}{h} + 0.8\right)}$ . Where,  $h$  = height of the substrate. The length ( $L$ ) of the patch is now to be calculated using the mentioned equation,  $L = \frac{C_0}{2f_r \sqrt{\epsilon_{reff}}} - 2\Delta L$ . The length and width of a substrate are equal to that of the ground plane. The length of a ground plane ( $L_g$ ) and the width of a ground plane ( $W_g$ ) is calculated using the given equations,  $L_g = 6h + L$  and  $W_g = 6h + W$ . Where,  $L_g$  = length of the ground and  $W_g$  = width of the ground [7]

There are several methods to achieve circular polarization. They are a fractal boundary, square patch with shaped slots, embedding cross slots in the metallic patch, stacking antennas, Truncating the edges, etc. In this research, truncating edges method was selected to achieve circular polarization.

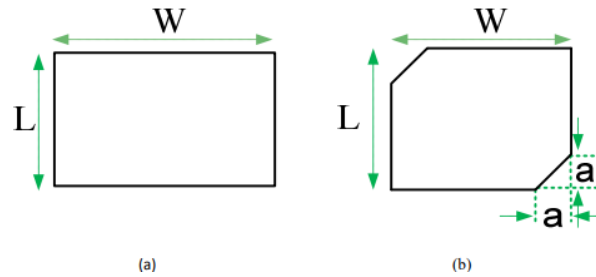


Figure 4.1: Truncating edges of a patch antenna

The truncating length was calculated from the given equations.  $a = L \sqrt{\Delta s/s}$ ,  $\frac{\Delta s}{s} = \frac{1}{2Q_0}$ ,  $Q_0 = \frac{c\sqrt{\epsilon_r}}{4f_0 h}$ ,

Where,  $a$  = length of truncating,  $L$  = patch length,  $\frac{\Delta s}{s}$  = truncating ratio,  $Q_0$  = unloaded quality factor,  $f_0$  = frequency [8]

## 2.2. Procedure:

Rectangular microstrip antenna was designed using the values obtained by calculations. Then the designed antenna was truncated at the edges. Finally, the truncated antenna fine-tuned the dimensions and observed the results. This proposed antenna achieves circular polarization in the form of truncating two opposite edges of a basic rectangular patch antenna.

## 3.0 RESULTS AND DISCUSSION

The calculations were made from the equations given in section 2.

Table 3.1: Design parameters of the patch antenna

Patch shape	rectangular
Patch length	63.5 mm
Patch width	75.3 mm
Substrate length	94.9 mm
Substrate width	106.7 mm
Height of substrate	1.6 mm
Frequency	1.575GHz
Dielectric constant	2.2
Feeding technique	Coaxial cable

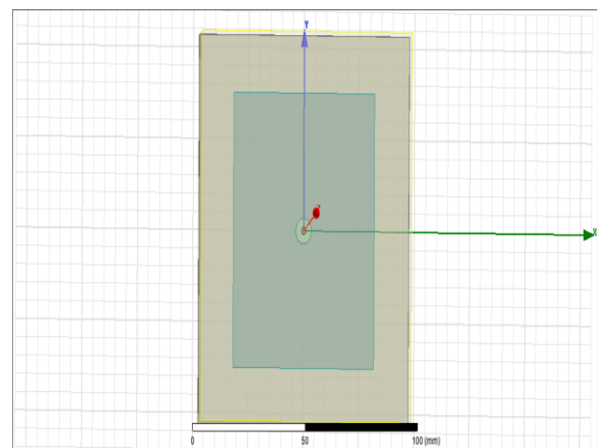


Figure 3.1: Top view of the microstrip antenna

At the beginning of the experiment, the coaxial probe was kept at the (0,0) position of the patch. Then, the feeding position was changed across the y-axis from 0 mm to 30 mm.

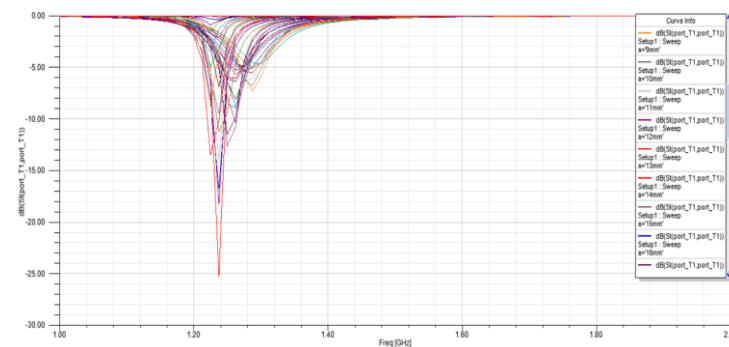


Figure 3.2: S11 plot when changing the probe through the y-axis

According to the results obtained by changing the probe through the y-axis, the best peak value was found when the probe position is 13 mm. When the probe position is 13mm the frequency was observed as 1.2 GHz. However, the experiment's objective was to provide a GPS band,

whereas the desired frequency should be within the range of 1.5635 GHz-1.5868 GHz. As per the above result, it was not within the range. Therefore, it was decided to change the patch width in order to gain the desired frequency. The S11 plot when changing the patch width is shown in figure 3.3.

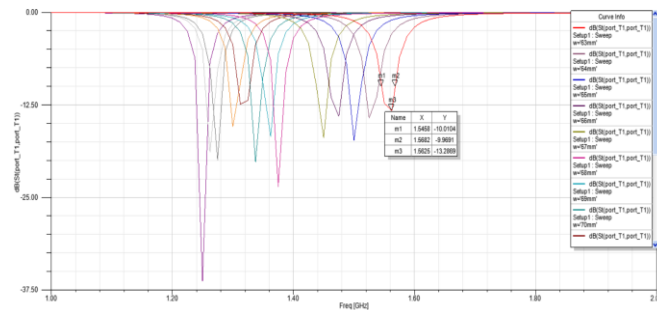


Figure 3.3: S11 plot for changing the patch width

When the patch width is 62.2 mm and the probe position is 11.1 mm, the frequency range was observed as 1.5635 GHz-1.5868 GHz.

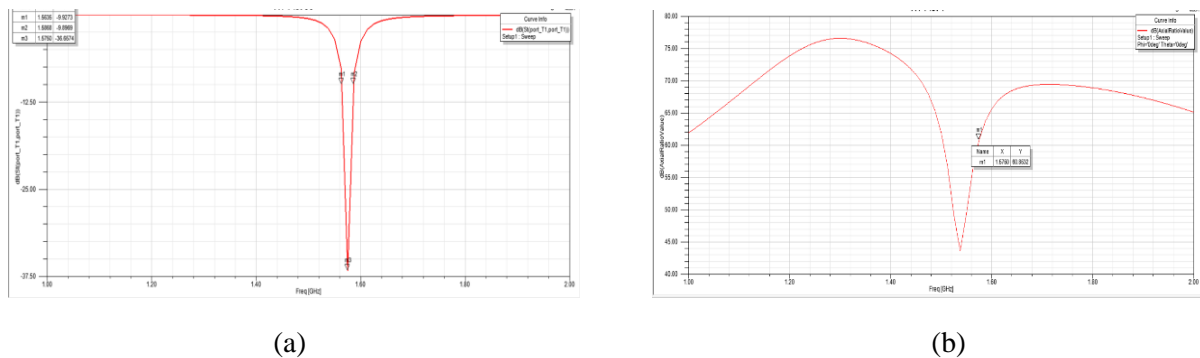


Figure 3.4: Antenna performance for the patch width 62.2 mm and probe position 11.1 mm (a) S11 plot (b) the axial ratio plot

Even though the frequency range was observed as 1.5635 GHz - 1.5868 GHz, the axial ratio was observed as 60.85 dB when changing the probe through Y-axis. This is far beyond circular polarization. Then, the next decision was to change the probe position along the x-axis to see whether there are any changes.

When changing the probe through the x-axis, the desired frequency range was achieved for the probe position 12.6 mm, and for the patch length 62.1 mm, the frequency range was 1.5631-1.5865 GHz.



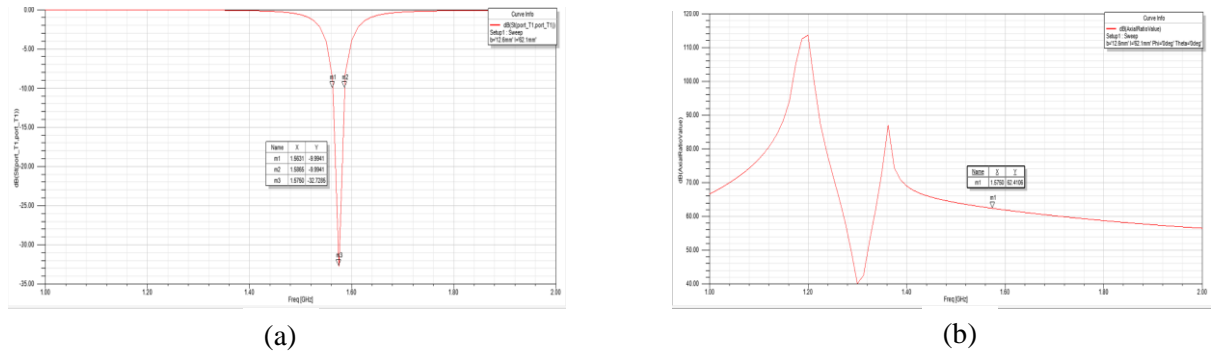


Figure 3.5: Antenna performance for the patch length 62.1mm and probe position 12.6mm (a) S11 plot (b) the axial ratio plot

Even though the desired frequency range was achieved by changing the dimension of the patch, the axial ratio was high in value (62.41 dB). The Next objective was to reduce the axial ratio to get a circular polarization for the antenna. The antenna was decided to truncate diagonally to test whether the axial ratio is changing.

The calculations were made from the equations given in the theory and diagrams section, and 6.8 mm was selected as the truncating length. The S11 plot and the axial ratio for the truncating length of 6.8 mm were given below.

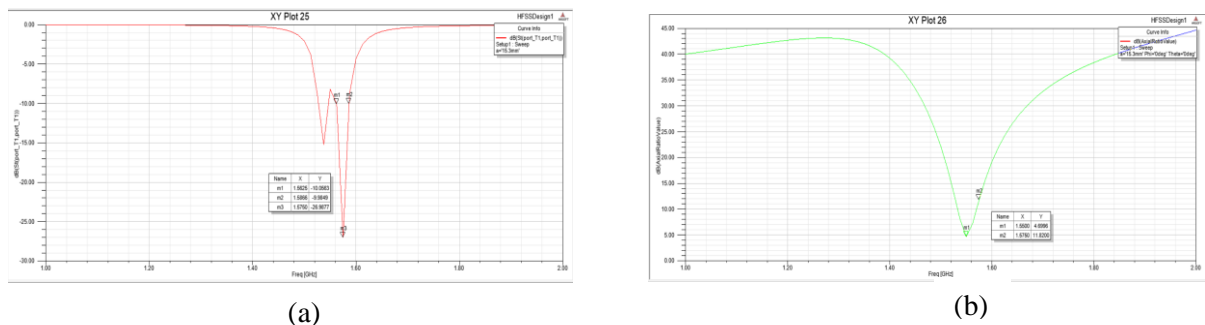


Figure 3.6: Antenna performance for the truncating length 6.8mm (a) S11 plot (b) the axial ratio plot

For the 6.8 mm, the frequency range was 1.5625 - 1.5866 GHz. The axial ratio was reduced to a considerable value (11.82 dB). The truncating length was changed from 5-10 mm. When the truncating length is 9 mm, the axial ratio was 9.73 dB. The axial ratio and the S11 plots when truncating length is 9 mm were given below.

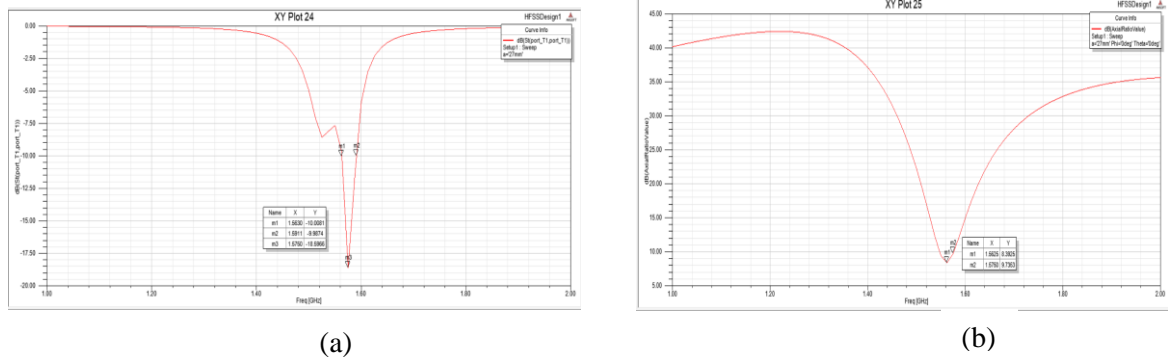


Figure 3.7: Antenna performance for the truncating length 9 mm (a) S11 plot (b) the axial ratio plot

From the above graphs, the 9 mm truncating length gave the axial ratio as 9.73 dB, and also the frequency range was 1.5630-1.5911 GHz which covers the desired GPS bandwidth.

The same procedure was carried out for the opposite diagonal as well.

For the opposite diagonal the results were not very much changed. For the truncating length of 9 mm, the frequency range was 1.5625-1.5866 GHz. The axial ratio was reduced to a considerable value (11.93 dB). The truncating length was changed from 5-10 mm. When the truncating length is 9 mm, the axial ratio was 9.58 dB.

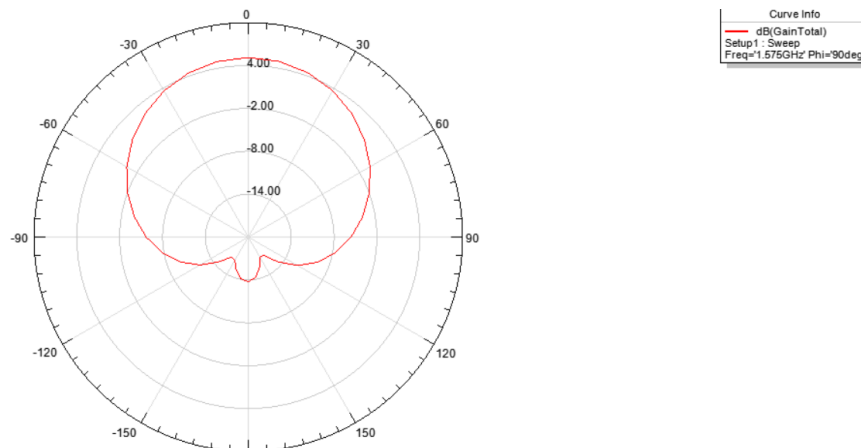


Figure 3.8: Radiation pattern for the truncating length 9 mm where center frequency 1.575 GHz  $\pi = 90^\circ$

#### 4.0 CONCLUSION

GPS antenna requires the performance of circular polarization because circular polarization can reduce the polarization mismatch and misalignment between the transmitter and receiver. The microstrip patch antenna design for circular polarization has been completed using High-frequency simulation software. As the final design, the microstrip patch antenna's parameters were 63.5 mm x 65.5 mm x 1.6 mm. and the truncating length was 9 mm. The center frequency

of the antenna was 1.575 GHz and the required bandwidth was 1.563-1.587 GHz which matched with the simulated bandwidth 1.5632-1.5911GHz. The axial ratio was 9.58 dB. The simulation gave results good enough to satisfy our requirements to fabricate it on hardware that can be used wherever needed.

## REFERENCES

- [1] Li, W. M., Jiao, Y. C., & Huang, J., A novel compact printed antenna with circularly polarized characteristics. *Progress In Electromagnetics Research Letters*, 28, (2012), 83-90.
- [2] Phyto, Z. M., Nway, T. M., Win, K. K. K., & Tun, H. M., Development of Microstrip Patch Antenna Design for GPS in Myanmar. *American Journal of Electromagnetics and Applications*, 8(1), (2020), 1-11.
- [3] Bukhori, M. F., Misran, N., Islam, M. T., Yunus, M. M., Shakib, M. N., Design of microstrip antenna for GPS application, *2008 IEEE International RF and Microwave Conference* , (2008), 464-466.
- [4] Sun, Y. X., Leung, K. W., & Lu, K., Broadbeam cross-dipole antenna for GPS applications. *IEEE Transactions on Antennas and Propagation*, 65(10), (2017), 5605-5610.
- [5] Zhang, Y., & Hui, H. T., A printed hemispherical helical antenna for GPS receivers. *IEEE microwave and wireless components letters*, 15(1), (2005), 10-12.
- [6] Li, W. M., Jiao, Y. C., & Huang, J., A novel compact printed antenna with circularly polarized characteristic. *Progress In Electromagnetics Research Letters*, 28, (2012), 83-90.
- [7] Afridi, M. A., Microstrip patch antenna– designing at 2.4 GHz frequency, *Biol. Chem. Res*, (2015), 128-132.
- [8] Aung, K. S., & Mon, S. S., Comparison of rectangular and truncated rectangular patch antenna for ku-band. *International Journal of Electronics and Computer Science Engineering*, 3(02), (2012).

## LP GAS DETECTION AND NOTIFICATION SYSTEM

R. D. Rasangika\*, M. A. A. Karunarathna

*Department of Electronics, Wayamba University of Sri Lanka, Kuliyaipitiya, Sri Lanka*

\*dilshanirasangika96@gmail.com

### ABSTRACT

Liquid petroleum gas (LP gas) explosions and gas leak mishaps involving residential LP gas cylinders have caused dread, worry, and social unrest throughout Sri Lanka last year. LP gas leaks are extremely dangerous since even a little one might eventually lead to a gas concentration that explodes. Operators in the vicinity of the leak can be alerted by a gas detector, giving them the choice to rectify the problem or leave. This system not only detects LP gas leakages but also indicates it using a buzzer alarm and sends a call to the respective owner. But sometimes the user may not be within reachable distance. In such situations indication of the risk is not enough. This system has an exhausting fan so it can remove leaked gas from the home. This system uses an Arduino UNO microcontroller as the processor, processing data from the MQ 5 gas sensor and transmitting it to a GSM module to send a call alert to the user. The advantage of these initiatives is that they can stop fires before they start, which can stop explosions caused by gas leaks.

**Keywords:** Arduino UNO, MQ5 Gas Sensor, GSM Module

### 1.0 INTRODUCTION

Liquefied petroleum gas (LPG) is a combustible blend of hydrocarbon gases. Propane and butane are among the hydrocarbons that make up gas. LPG is generated during the refining of petroleum (crude oil) or it is taken from petroleum or natural gas streams as they emerge from the earth. Liquefied petroleum gas leaks have caused considerable harm, including the death of people. In the last year, several occurrences of gas explosions have been reported in Sri Lanka and all over the world. Since LP gases are heavier than air, when a leak occurs in a confined area, a layer of gas rises above the floor. Such circumstances provide an immediate threat since even the smallest ignition trigger might create an explosion and fire. When there is more than 4-6% LPG in the air, an explosion is possible.

Considering previous studies Yekini N. Asafe et al. proposed a gas leakage detector and monitoring system but it was only the monitoring system. In some urgent situations gas leakage

indication is not enough to remove the risk [1]. Vasudev Yadav et al. presented the MQ-9 embedded system computer circuit. These systems occasionally lack a keyboard, screen, disks, printers, or other recognizable I/O devices of a personal computer, as well as any means of human interaction. MQ-9 sensor that, in the case of gas leakage, will ring a buzzer and alert the semiconductor diode [2].

This research project aims to find LP gas leaks, show them on LCDs, alert the owner using IOT technology, and take appropriate action to reduce the risk [3],[4].

This project can divide into 2 parts.

1. LP gas detection system with gas amount representation.
2. Automated leaked gas removing system.

## **2.0 EXPERIMENTAL**

The system works by detecting levels of LPG gas which is in the room source/engine using an MQ-5 LPG sensor. If there is an LPG gas is detected, the tool will first be issued the indicator of the LPG ppm value on the LCD, and if it increases, the buzzer will turn on to alarm. Furthermore, leakage of data will be sent to the GPS module to send a call to the house owner's mobile phone. Meanwhile, sends the signal to turn on the exhaust fan to reduce the levels of LPG in the room. However, if the LPG gas levels continue to reduce to the normal level, the system shut the exhaust fan and turns off the buzzer. The overall action of this system is processed under two parts.

1. LP gas detection and gas amount representation.
2. Remove leaked gas from the area.

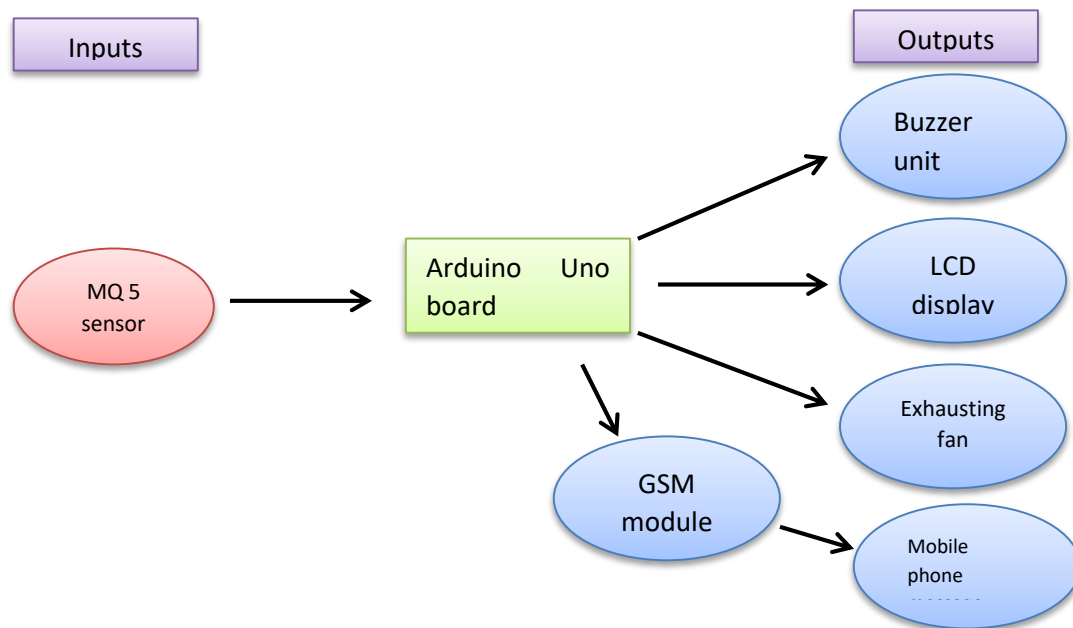


Figure 2.2.1: Hardware Flow chart

### 2.1 LP gas detection system with gas amount representation

The first part of this project is to detect the leaked LP gas with an MQ-5 gas sensor and notify it using the buzzer. Then the LCD indicates the gas leakage and at the same time, it sends an SMS to the owner's mobile via the GSM module. This part is the risk identification system of this project. Mainly the MQ-5 gas sensor senses the LP gas leakage and it gives the signal to the microcontroller (Arduino UNO). Then the microcontroller will activate the buzzer while displaying the current situation of the area on the LCD. Then the gas leakage notification will be sent to the owner via SMS or a Call as they prefer.

### 2.2 Automated safety leaked gas removing system

The second part of this system is the safety action system. This system is used to remove the leaked LP gas from the considered area. An exhausting fan is used to remove leaked LP gas. After notifying them about the gas leakage to the owners, they try to enter the area fill with LP gas. It will be a risky situation as there are possibilities of sudden fire, explosions, breathing issues, etc. So, to overcome that problem up to a certain extent, the system removes the gas from the area using an exhaust fan. It also starts to work according to the instructions given by the microcontroller.

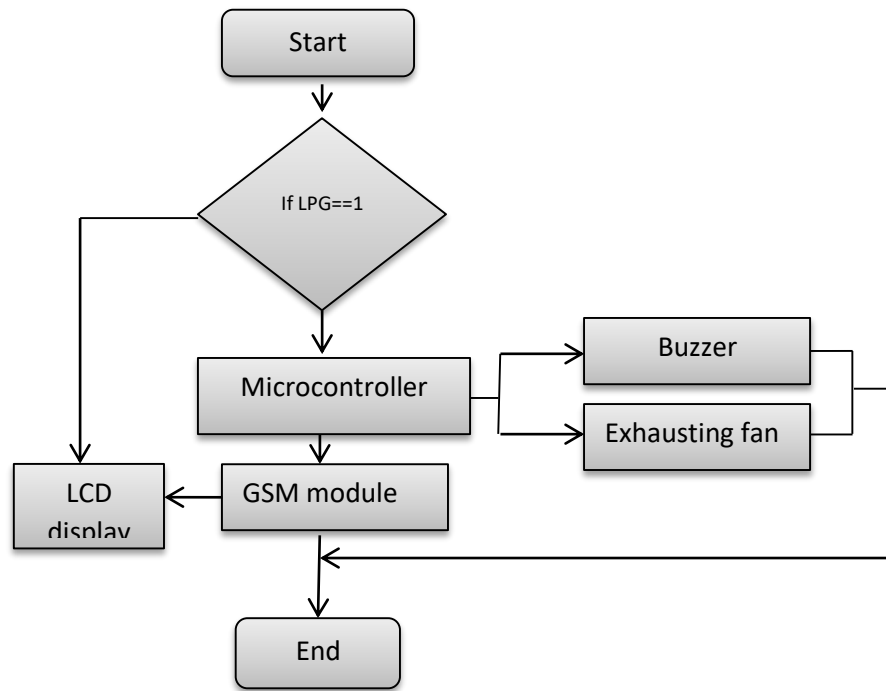


Figure 2.2.2: Functional Flow chart

### 3.0 RESULTS AND DISCUSSION

#### 3.1 Experimental Results

By using MQ-5 sensor LP gas detection can be done at the range 300 ppm – 10000 ppm. Hence, the LP gas detection level was set to 295 ppm. Because practically when the gas cooker was turned on, sometimes the flame won't ignite at once. At that missing time, LP gas level comes to the 100-250 ppm range. Then by avoiding that situation, this 295-ppm level was initiated [5],[6].

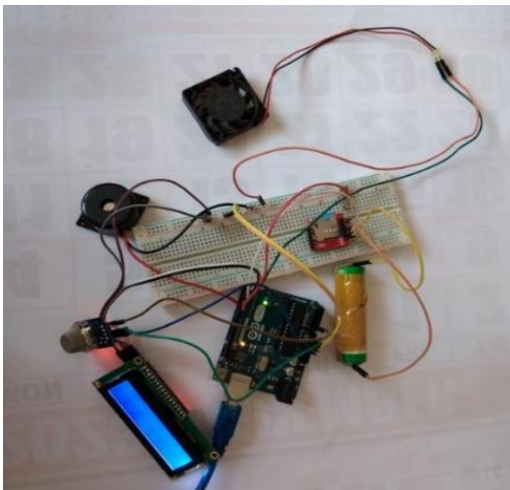


Figure 3.1: Hardware view of the circuit

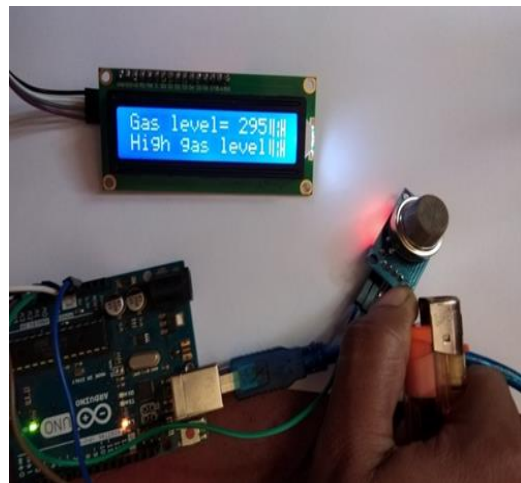


Figure 3.2: LP gas detected display on LCD

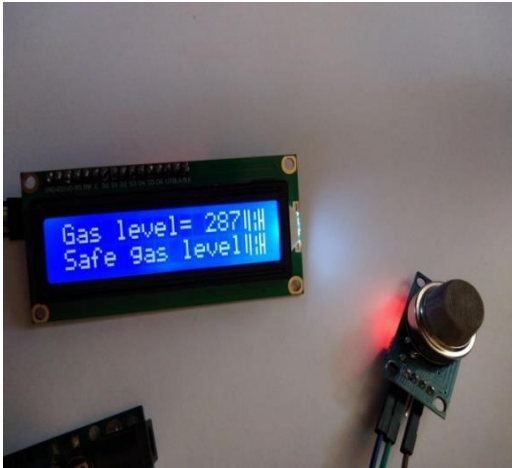


Figure 3.3: No LP gas detected display on LCD

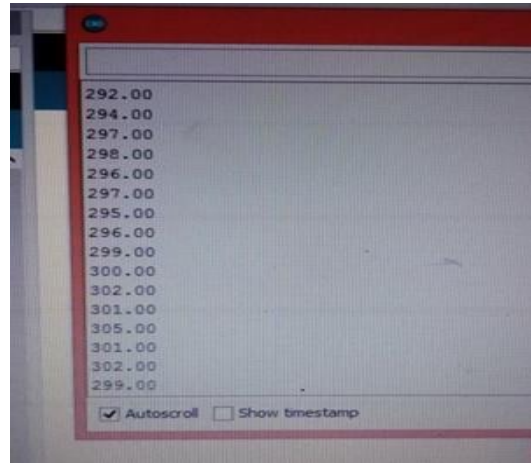


Figure 3.4: LP gas detection with ppm values in the serial monitor

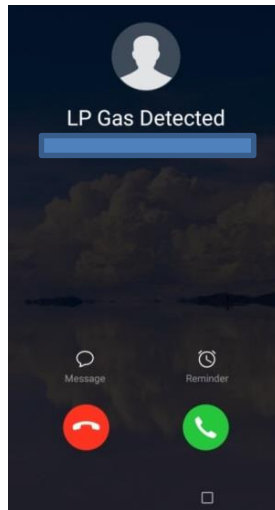


Figure 3.5: Receiving a call when a gas leak detected

### 3.2 Advantages of the proposed system

This automated detection and alerting system have several advantages over the manual method. Quick response times, accurate emergency detection, and a faster spread of critical situations. The gas detection and alteration system developed is a highly economical technique to find any gas leaks. In addition to detecting gas leaks, it also warns by making noises like alarms, etc. It has uses in several different contexts, including schools, colleges, universities, residences, and industries. With this system in place, not only would a timely alert have been useful for evacuation but the source of the gas leakage could have also been stopped, saving many lives. It is especially useful when leakage occurs when no one is around. In this case, the MQ5 gas sensor detects the leakage, and the system alerts by producing a sound. When no one is at home the message from the GSM module sends the message to the owner. That is very beneficial.



This system not only detects the leaked LP gases but also this system acts as a safety action-taking system. Sometimes the owner of the home may not be within reachable distance, in such situations even though the mobile phone indication may not be useful. In such situations taking immediate actions to minimize the risk is very useful. The exhausting fan removes the leaked gases from the risky area to the open area to minimize the risk. Three separate locations a ventilated area, an airtight environment, and an open space are used for sensor testing. The open room detected gas amount is at the minimum level. The sensitivity of the MQ-5 sensor is depending on the distance from the sensor to the gas-leaking object and also the type of area. Then other factors that influence sensitivity are wind factors such as testing in open spaces, if the wind blows hard enough then the detected gas levels will decrease / not be detected. A sensitive  $\text{SnO}_2$  filament is used in the MQ5 gas sensor. The conductivity of the filament increases in the presence of flammable gas, such as LPG, and the degree of this change in conductance or resistance may be utilized to calculate the equivalent gas concentration [2-11].

#### **4.0 CONCLUSION**

In conclusion, Gas leaks might cause catastrophic incidents that cause property damage and deaths. Poor maintenance and people's lack of awareness are the primary causes of gas leakage and explosions. LPG escape detection, therefore, helps to prevent accidents and the loss of human life. This system was created to find any LP gas leaks, notify the user of them and take safety action to minimize the risk. In the future, this system will have a feature that can notify the emergency to the emergency services o police stations. And with this system, a mobile app can develop to monitor the working condition of the system with guidance to the people to minimize the risk. This system can be developed as a gas-sensing walking robot to sense the leaked LP gas and go to the target point where gas leakage occurs and identify the leaked amount in ppm because LP gas is a heavy gas and the sensitivity of the sensor depend on the distance among gas detector and leaked gases.

#### **ACKNOWLEDGEMENTS**

The authors would like to thank all the staff of the Department of Electronics, Faculty of Applied Sciences, Wayamba University of Sri Lanka.

## REFERENCES

- [1] N. Asafe, Y., J. Oyeranmi, A., A. Olamide, O. and O. Abigael, A., *Gas Leakage Detector and Monitoring System*, 12(5),(2022),56–65, doi:10.5815/ijem.2022.05.05.
- [2] Vasudev Y., Akhilesh S., Sofiya B., Vipin K., Ubais A., Suraj K., U. G. Scholar U. G., *A Review On Microcontroller Based Lpg Gas Leakage Detection & Controlling System Using Iot & Gsm Module*, IEEE 2nd International Conference On Electronics Technology (ICET), 2016.
- [3] Tukkoji, C., Kumar, A. N. S., *LPG Leakage Detection Using IOT*, 4, (2020),603-609, doi: 10.33564/IJEAST.2020.v04i12.108.
- [4] C. Hou, J. Li, D. Huo ., *A portable embedded toxic gas detection device based on a cross-responsive sensor array*, *Sensors and Actuators B: Chemical*, 161,(2012), 244–250.
- [5] circuitdigest.com. (n.d.). MQ-5 Combustible Gas Sensor Interfacing with Arduino., <https://circuitdigest.com/microcontroller-projects/interfacing-mq5-gas-sensor-with-arduino>, (Accessed date: 2022.07.13).
- [6] Grove -Gas Sensor (MQ5) User Manual. [https://www.mouser.com/datasheet/2/744/Seed\\_1010056-1217478.pdf](https://www.mouser.com/datasheet/2/744/Seed_1010056-1217478.pdf) (Accessed date: 2022.10.05).
- [7] Evalina, N. and A Azis, H., *Implementation and design gas leakage detection system using ATmega8 microcontroller*, 821,(2020), p.012049, doi:10.1088/1757-899x/821/1/012049.
- [8] Nahid, S.I., Anjum, N., Chowdhury, N.Z., Anni, L.T., Mahmud, Md.T., Khan, M.M. and Ashique, R.H., *Development of a Smart Automatic Gas Leakage Detector and Alarming System*, (2021), doi:10.1109/iemcon53756.2021.9623207.
- [9] C, Ramya.K., M, N., R, M. and S, H., *LPG Leakage Detector with Smart SMS Alert using Microcontroller*, (2021), doi:10.1109/icces51350.2021.9489037.
- [10] Last Minute Engineers, *Interface an I2C LCD with Arduino*, (2020), <https://lastminuteengineers.com/i2c-lcd-arduino-tutorial/>. (Accessed 2022.11.03).
- [11] Last Minute Engineers, *Send Receive SMS & Call with SIM800L GSM Module & Arduino.*, (2018). <https://lastminuteengineers.com/sim800l-gsm-module-arduino-tutorial/>, (Accessed date 2022. 11. 03).

## **AUTOMATED REGISTER POSTAL MACHINE SYSTEM**

Y.G. Chandrasiri\*, U.A.D.N. Anuradha, K.K.C.S. Kiriella

*Department of Electronics, Wayamba University of Sri Lanka, Kuliypitiya, Sri Lanka*

\*gayanchandrasiri12all@gmail.com

### **ABSTRACT**

Postal service is one of the demanding services in Sri Lanka due to the reliability and affordability. Therefore, most of the people as well as companies are using the postal services frequently. But physical labor service is used to conduct all the activities which are not tally the larger demand. Because of this, lots of inefficiencies can be identified. This research study addresses the issue by automating the package registration process in the package handling department. The weights of the packages are measured by the automated system and automatically displayed on the website. Customers must interact, add the information from the registration document, and pay for the storage of this information together with other pertinent information. A QR code is produced automatically with the payment receipt to verify the transaction and clear up any misunderstandings among clients. Without using any effort, the parcel is automatically carried to storage. The efficiency can be substantially boosted and all processes can be automated in this way. Additionally, this technology greatly lowers the labor costs associated with this operation. The system is shown to be efficient and cost-effective when all the information is taken into account.

**Keywords:** Payment, Postal service, QR code

### **1.0 INTRODUCTION**

#### **1.1 Problem Identification**

The Sri Lanka Postal Department offers registered postal services, which are in higher demand in urban areas compared to rural areas due to their widespread use by government and private organizations. However, the manual processing of this service results in long wait times and increased costs, making it inefficient. Additionally, the shortage of labor and social factors makes it challenging to provide an integrated service.

To improve the efficiency and cost-effectiveness of the registered postal service, it is recommended to implement an automated system. The adoption of automation can reduce

waiting times for customers and provide an efficient service without the social and labor-related challenges associated with manual processing. Furthermore, an automated system can attract more customers and enhance the image of the postal department.

## 1.2 Proposed System

This procedure can be made simpler by using an automated postal system for package/letter registration and processing. Urban post offices handle more registered mail than rural post offices, thus automated methods are more appropriate for these stations, according to the data gathered. Additionally, this technology gets rid of mistakes made by people when processing a package's weight and when calculating prices, increasing the process's dependability. The system is also simple to maintain and can be updated to reflect changes in technology, laws, and taxation. Customers can follow their deliveries owing to the user-friendly interface, which also makes it more convenient to pay with ATM cards. The technology also helps postal workers because it eliminates the need for them to manually enter or type transaction data and instead provides them with a user-friendly interface that makes it simple to retrieve information on any transaction. This design incorporates a database that holds all the necessary data and can be backed up to ensure data loss in an emergency is prevented.

## 2.0 EXPERIMENTAL

### 2.1 Hardware Requirements

This passage discusses various hardware components being utilized in a project. These components include the ESP8266 Wi-Fi module, HX711 load cell amplifier, RC522 RFID reader, relay switch, and pneumatic piston. The ESP8266, a popular and affordable Wi-Fi module that is gaining popularity among hardware designers, can be programmed using the user-friendly Arduino Integrated Development Environment (IDE) [1]. The HX711 is a high-precision analog-to-digital converter that was designed for use with bridge sensors in industrial applications [2]. The RC522 RFID reader is being used in the project and has a reading range of 10cm-3m, depending on the implementation [3]. A relay is an electromechanical component that utilizes the electromagnetic principle to switch between low power voltage and high voltage. Lastly, a pneumatic piston powered by compressed air is being utilized to move packages into storage [4].

## 2.2 Software Development

The system's software has been developed using various programming languages and database management systems. The back end of the system was built with Node.js, a JavaScript platform that's used for creating scalable network applications that are fast and efficient in handling real-time data across multiple devices [5]. On the other hand, the front end was developed with Angular, a TypeScript platform that's known for its scalability in building web applications. Angular comes with a framework that's component-based and a set of libraries that handle different features such as client-server communication, forms management, and routing [6]. Lastly, MongoDB was chosen as the database management system for the system. MongoDB is a flexible document database that utilizes JSON-like storage and provides full indexing support and replication features. With its simple APIs, MongoDB is well-suited for storing unstructured data [7].

## 2.3 Project Design

When the user places the package on the weight sensor, the automated system detects it and enters the delivery details first (Sender address and name, Receiver address and name). By using NodeMCU, the weight sensor will take a reading and transmit it to the database. The cost will be decided in the backend of the programming, and the information will be kept in the database.

The RFID card reader will read the RFID tag card and then charge the appropriate amount. A receipt with transaction information (a QR code) will thereafter be generated. The user must adhere the receipt to the packaging.

Before proceeding, the package's weight will be once more verified. The package will be moved to storage by the pneumatic piston if the weights are equal and the data in the QR code matches.

The system's block diagram is depicted in Figure 2.1.

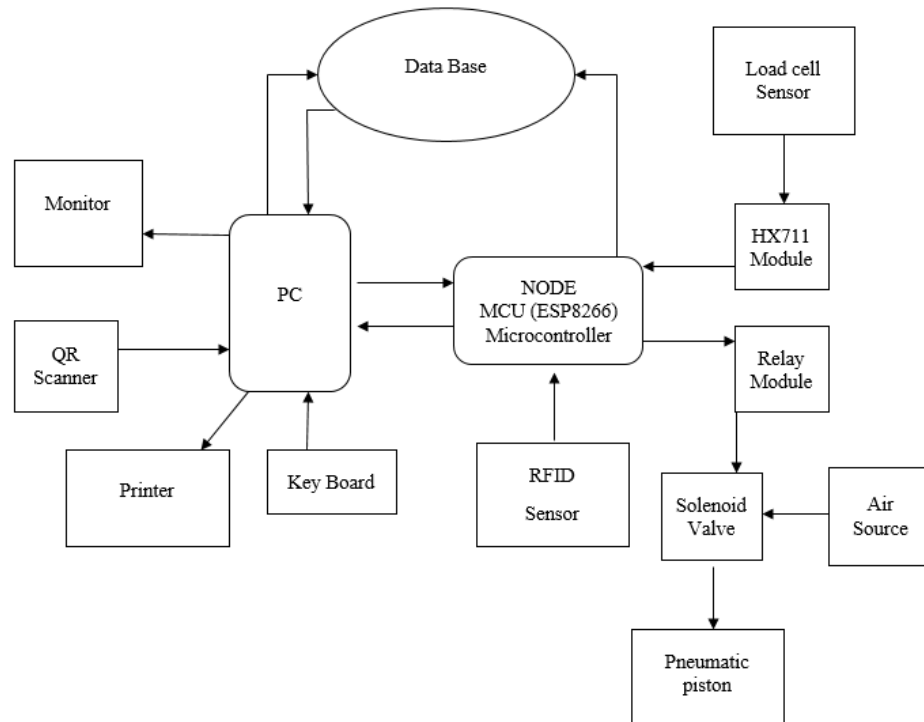


Figure 2.1: Block Diagram of the Design

Weight is measured by a load cell sensor, amplified by a HX711 weighing sensor, and transmitted to an Arduino to be computed. A MongoDB database is then updated with the weight value. The user enters the sender and recipient addresses into the system, makes a payment using an RFID card reader, and receives a receipt with a QR code. After being put on the package, the QR code is scanned with a QR code reader. If the data is correct, a pneumatic piston driven by a microprocessor moves the package to storage. Figure 2.2 illustrates this procedure.

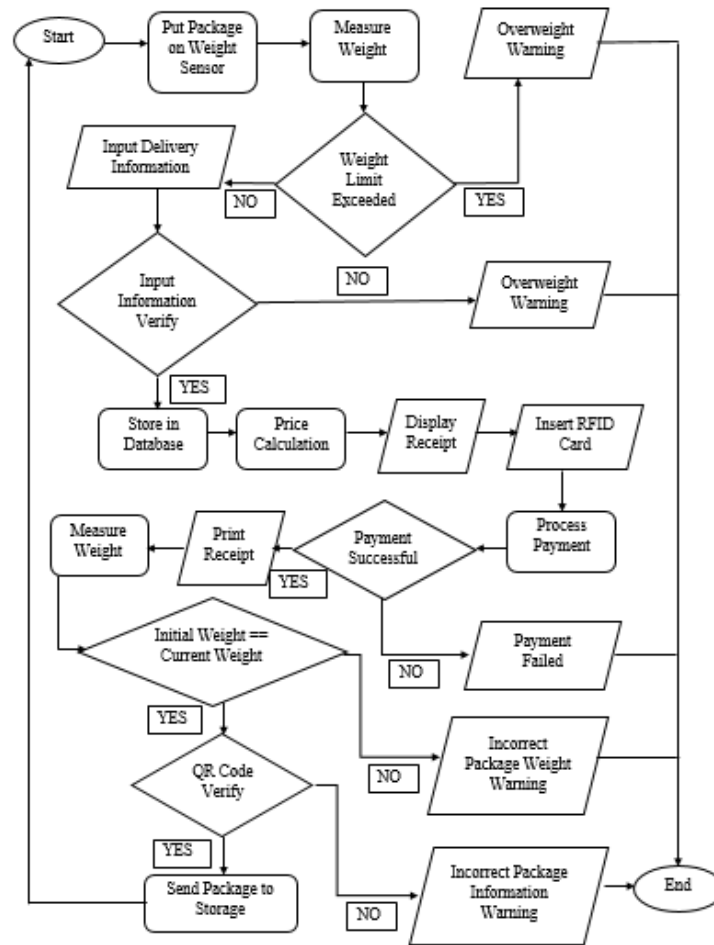


Figure 2.2: Flow Chart of the System

### 3.0 RESULTS AND DISCUSSION

#### 3.1 Results

Hardware implementation of this system is shown in Figure 3.1. A package's weight is recorded when it is placed on the weighing plate, and the information is then communicated to the online interface. The price is determined and shown in accordance with the weight. Customers can use the web interface to enter the required information and register a package. Registration is not accessible until the payment has been received. Using an RFID tag card and reader, the customer can make a purchase. The customer can access the register after making a payment. The receipt is printed after registration, as seen in Figure 3.2. The receipt must be adhered to the package by the customer. The information about the package is contained in the QR code. Once verification is complete, the package is transferred.

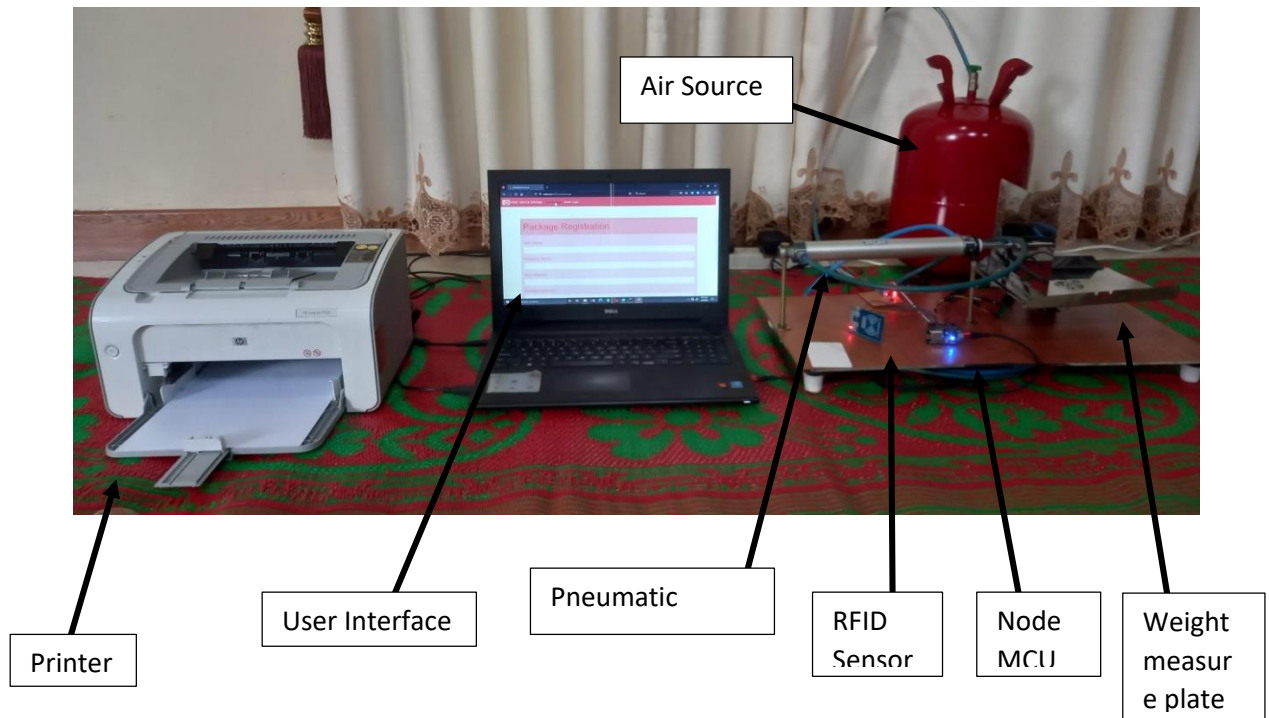


Figure 3.1: Overall Hardware System

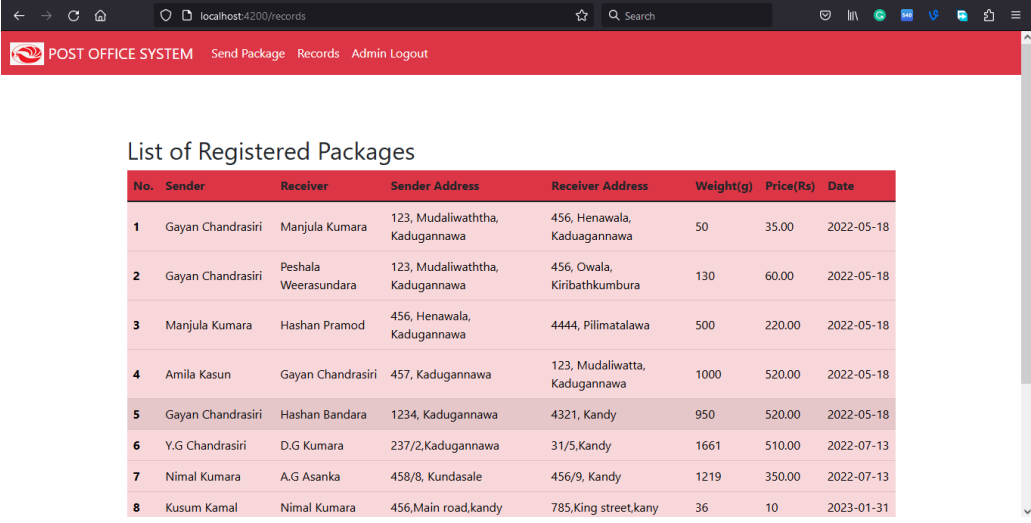


Figure 3.2: The Printing Receipt

In this system, the Node MCU is powered by 5 volts and is used to operate the load cell sensor and RFID sensor, which are supplied with 3.3 volts from the Node MCU board. The pneumatic piston, on the other hand, is powered by 24 volts and is controlled by a 5-volt relay module. The load cell calibration factor is 285.5, which was determined using the Arduino calibration code. The range of air pressure for the pneumatic piston is between 2 and 8 bars, with the most suitable pressure range for this system being between 5.5 and 6 bars. Additionally, the weight measuring plate and the pneumatic piston was built on an



iron plate holder in order to achieve accurate and sensitive weight measurements. Figure 3.3 shows the result of registration completed detail on real time database.



No.	Sender	Receiver	Sender Address	Receiver Address	Weight(g)	Price(Rs)	Date
1	Gayana Chandrasiri	Manjula Kumara	123, Mudaliwattha, Kadugannawa	456, Henawala, Kadugannawa	50	35.00	2022-05-18
2	Gayana Chandrasiri	Peshala Weerasundara	123, Mudaliwattha, Kadugannawa	456, Owala, Kiribathkumbura	130	60.00	2022-05-18
3	Manjula Kumara	Hashan Pramod	456, Henawala, Kadugannawa	4444, Pilimatalawa	500	220.00	2022-05-18
4	Amila Kasun	Gayana Chandrasiri	457, Kadugannawa	123, Mudaliwattha, Kadugannawa	1000	520.00	2022-05-18
5	Gayana Chandrasiri	Hashan Bandara	1234, Kadugannawa	4321, Kandy	950	520.00	2022-05-18
6	Y.G Chandrasiri	D.G Kumara	237/2, Kadugannawa	31/5, Kandy	1661	510.00	2022-07-13
7	Nimal Kumara	A.G Asanka	458/8, Kundasale	456/9, Kandy	1219	350.00	2022-07-13
8	Kusum Kamal	Nimal Kumara	456, Main road, kandy	785, King street, kany	36	10	2023-01-31

Figure 3.3 Image of the System Database

The database for this project was created in a MongoDB environment. The database contains a variety of data, including the sender's name, address, recipient's name, address, package weight value, and service charge cost. The database contains a security feature with a username and password that only the admin (postal officer) can access.

### 3.2 Discussion

The outcome of this research provided an automated system for the process of sending a parcel or document using registered post. In this system, weight measurement is done using a load cell sensor. The sensitivity of the weight measurement value was found to be high, the web interface was user-friendly, and the use of an online database management system ensured that customer details were not lost during power outages. The system prevents illegal activity by customers through the implementation of a weight-matching feature that compares the weight of the package initially input by the customer to the weight re-checked upon delivery. However, there were some weaknesses such as the system does not support connectivity with an ATM card reader in an industrial setting, the activation of the pneumatic piston increasing complexity and occasional communication issues that may arise between the NodeMCU and the web interface within the system. Despite these challenges, the system was able to function effectively and achieve its goal of accurate weight measurement. The same methodology can be implemented in a system of production, where weighing of the package, attaching of receipts and their subsequent transfer to the store is done.

#### 4.0 CONCLUSION

The project's aim was to automate the package registration process for postal workers handling registered mail by using a web interface for customers to register their packages, which is powered by a NodeMCU module and a load cell sensor for measuring weight, and an RFID sensor for payment. The implemented system utilized the MongoDB database to store customer information and was protected by password and user access for added security. The system has been designed to operate in low-power and affordable technique using reliable and accurate sensors, and a pneumatic piston powered by compressed air. Overall, with the implementation of an automated postal registration system, reducing the amount of time spent in the postal registration line, customers can save precious time. and a low-cost, low-energy package registration option is also provided by the system.

#### ACKNOWLEDGEMENTS

The authors would like to express their sincere gratitude to everyone who helped to carry out this project successfully.

#### REFERENCES

- [1]. Firmansyah R., The prototype of infant incubator monitoring system based on the internet of things using NodeMCU ESP8266, *Journal of Physics*, (2019), <https://iopscience.io-p.org/article/10.1088/1742-6596/1171/1/012015/pdf> (Accessed 2022.11.12)
- [2]. Load Cells: Types, How It Works, Applications, & Advantages, *encardio*, (2020), <https://www.encardio.com/blog/load-cells-types-how-it-works-applications-advantages> (Accessed 2022.11.10)
- [3]. what is RFID? How It Works? Interface RC522 RFID Module with Arduino, *last minute engineers*, (2020), <https://lastminuteengineers.com/how-rfid-works-rc522-arduino-tutorial/> (Accessed 2022.11.15)
- [4]. Pneumatic Solenoid Valves, *iqs directory*, (2019), <https://www.iqsdirectory.com/articles/solenoid-valve/pneumatic-solenoid-valve.html> (Accessed 2022.11.17)
- [5]. Taha Sufiyan, What is Node.js: A Comprehensive Guide, *Simplilearn*, (2021), <https://www.simplilearn.com/tutorials/nodejs-tutorial/what-is-nodejs>, (Accessed 2022.11.06)
- [6]. Thakur, I., Understanding Angular, *Analytics Vidhya*, (2021), <https://medium.com/analytics-vidhya/understanding-angular-2775383eac99>, (Accessed 2022.10.30)
- [7]. Botelho, B., Mongo DB, *tech target*, (2021), <https://www.techtarget.com/search-data-management/definition/MongoDB>, (Accessed 2022.11.03)

# **DESIGN AND IMPLEMENTATION OF IOT BASED PATIENT BIO-MEDICAL PARAMETER MEASURING AND CRITICAL CONDITION ALARMING SYSTEM**

S.H.D.Dananjani\*, Y.A.A. Kumarayapa

*Department of Electronics, Wayamba University of Sri Lanka, Kuliyaipitiya, Sri Lanka*

\*dananjani955@gmail.com

## **ABSTRACT**

By employing an interconnected network, the Internet of Things (IoT) enabled healthcare system is useful for properly monitoring Critical Conditions (Eg: - COVID-19) patients. This technology helps to increase patient satisfaction in the hospital or home care patients. Monitoring individuals' health in day-to-day life has become an important concern given Covid19. It would help us to come to know some changes that could happen inside a human body. This project will monitor the heartbeat, temperature, and oxygen level of Critical Condition patients at its preliminary stage. Then special attention is paid to those patients who are receiving treatment at home and also can be monitored often by a physician. If the sensor records any value going beyond the bad reading then will generate an alert message and email and send it to the hospital or concerned person stating the patient's status for a medical emergency. So IoT-based patient health monitoring systems effectively use the internet to monitor patients' health metrics and save lives and time in this patient's condition for obtaining previous records. This proposed system is set up to be very easy and consists of high performance and counts on a timely response. This paper presents an IoT-based healthcare system that makes it easier for patients to control an alternative method of reducing hospital traffic while at home. These patient-specific applications of the proposed system as supplemental devices may have a significant effect on their own lives. This suggested some health parameter monitoring system using IoT, then the authorized person may access these saved data are watching any IoT platform and based on these values then treat the patients, the diseases are diagnosed by the physicians from a distance.

**Keywords:** ESP32, IoT, Patient parameter, temperature, heartbeat, oxygen level

## **1.0 INTRODUCTION**

This paper is about an IoT-based health monitoring system. In particular, for COVID-19

patients, high blood pressure patients, hypertension patients, diabetic patients, etc. in a country territory, in rural areas, the number of doctors is not the same as in urban areas. Medical equipment is not readily available in rural areas, except for government medical centers. In comparison to government hospitals, these clinics see a higher percentage of patients. Similarly, the equipment has mostly been used up. As a result, in the situation of an emergency, this hardware component will transmit a report as soon as possible to the doctors or medical specialists. The remaining work will be done by doctors based on their reports. The IoT health-monitoring platform has provided us with a significant benefit in the advancement of contemporary medicine [01]. IoT devices are widely used in the medical sector. And the technology we are talking about is a patient health monitoring system that uses the IoT. A sensor in this health monitoring system will collect information about the patient's health condition. It is smaller in size, faster, and more affordable. This system can be used to measure the oxygen saturation level, heart rate, and temperature of the human body and display the results on a web-based platform. The physical, logical, and application layers are the three layers of the system. The development of an IoT-based health monitoring system is described in this study. The paper's main contribution is to create an IoT-based real-time health monitoring system. Various sensors have been used to measure the data of patients in real time. A mobile application has also been developed. It was tested after the entire system had been developed. In this investigation, three separate real-life human test volunteers were used [02].

## **2.0 EXPERIMENTAL**

The core objective of this project study is to design and implement a smart patient health tracking system. Figure 2.1 shows the overview of the proposed system. The sensors are embedded in the patient's body to sense the temperature, Oxygen Level, and heartbeat of the patient. Two more sensors are placed at the patient's residence to monitor the temperature, oxygen level, and heartbeat [04]. These sensors are connected to a control unit, which calculates the values of all sensors. These calculated values are then transmitted through an IoT cloud to the base station. From the base station, the values are then accessed by the doctor at any other location. Thus, based on the temperature, Oxygen Level and heartbeat values, and room sensor values, the doctor can decide the state of the patient and appropriate measures can be taken. Also, if the sensor records any value going beyond the set threshold, then will generate an alert message and email and send it to the concerned person stating about the medical emergency [03].

Figure 2.1 shows the block diagram of the proposed system and figure 2.2 shows the Process of the proposed system below.

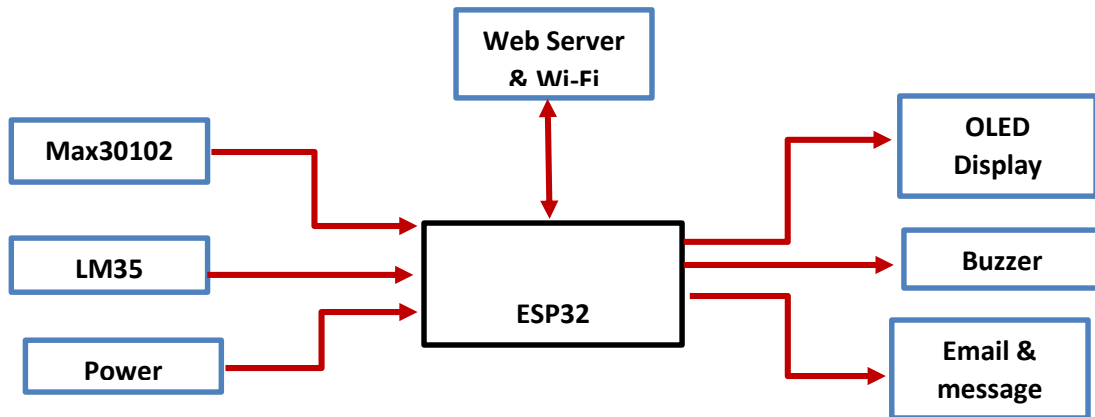


Figure 2.1 : Block Diagram of the System

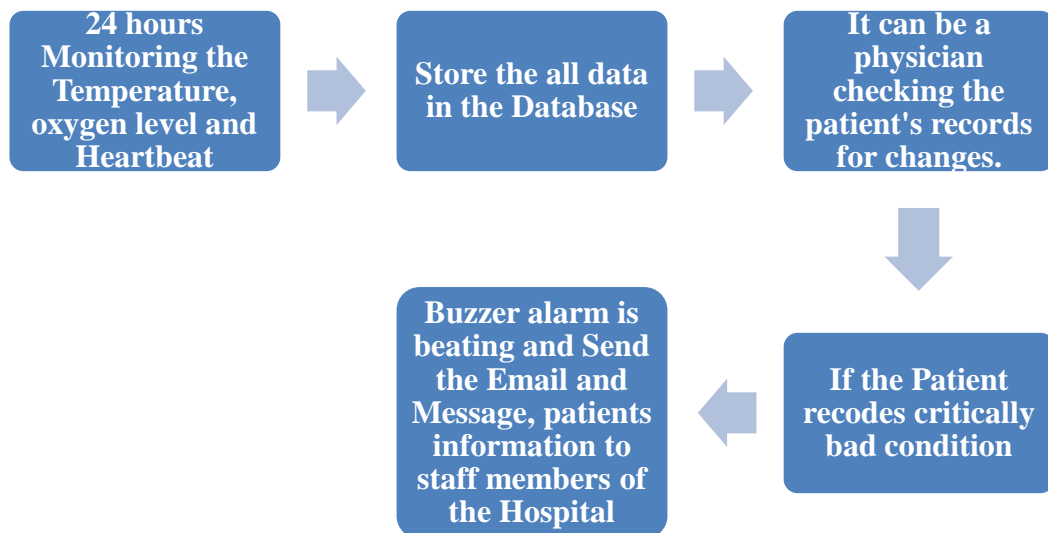


Figure 2.2 : Process of the proposed system

Then Figure 2.3 shows the Circuit Diagram of the proposed System and it shows that all components are connected to other. Then Figure 2.4 shows the Flow Chart of the Proposed System below. First starting the system, then the instructions are displayed on OLED Display to the patient how to use them. Then parameters are measured and stored all data in the database. It can be a check of the recodes of the patient's details by a physician. If the Patient records a critically bad condition, then a Buzzer alarm is activated, and Send the Email Message, and the patient's information to staff members of the Hospital.

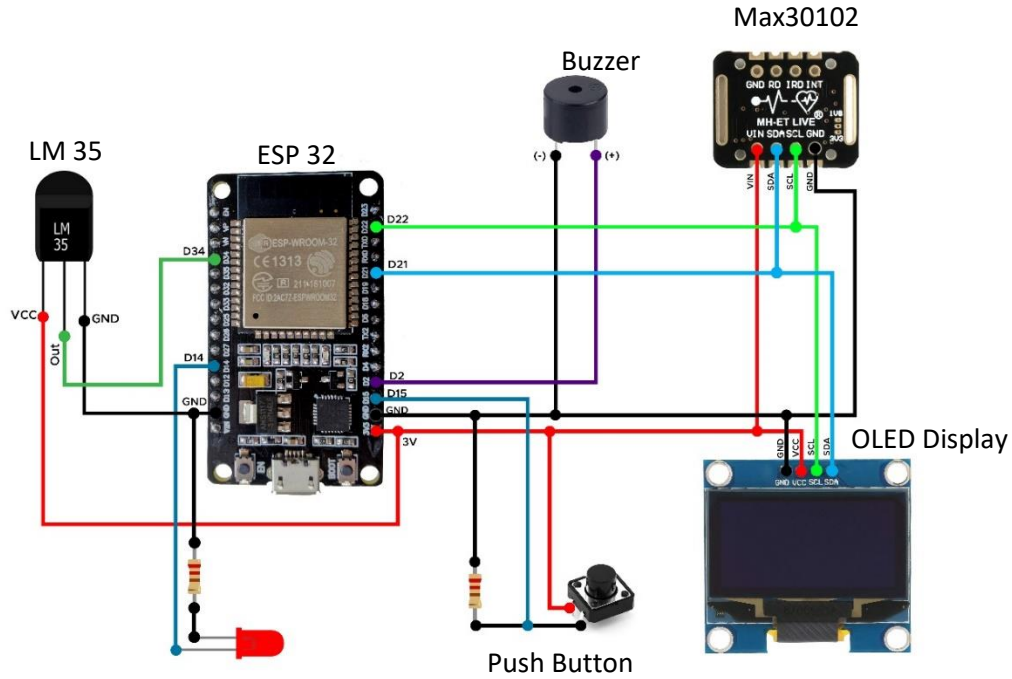


Figure 2.3 : Circuit Diagram of the proposed System

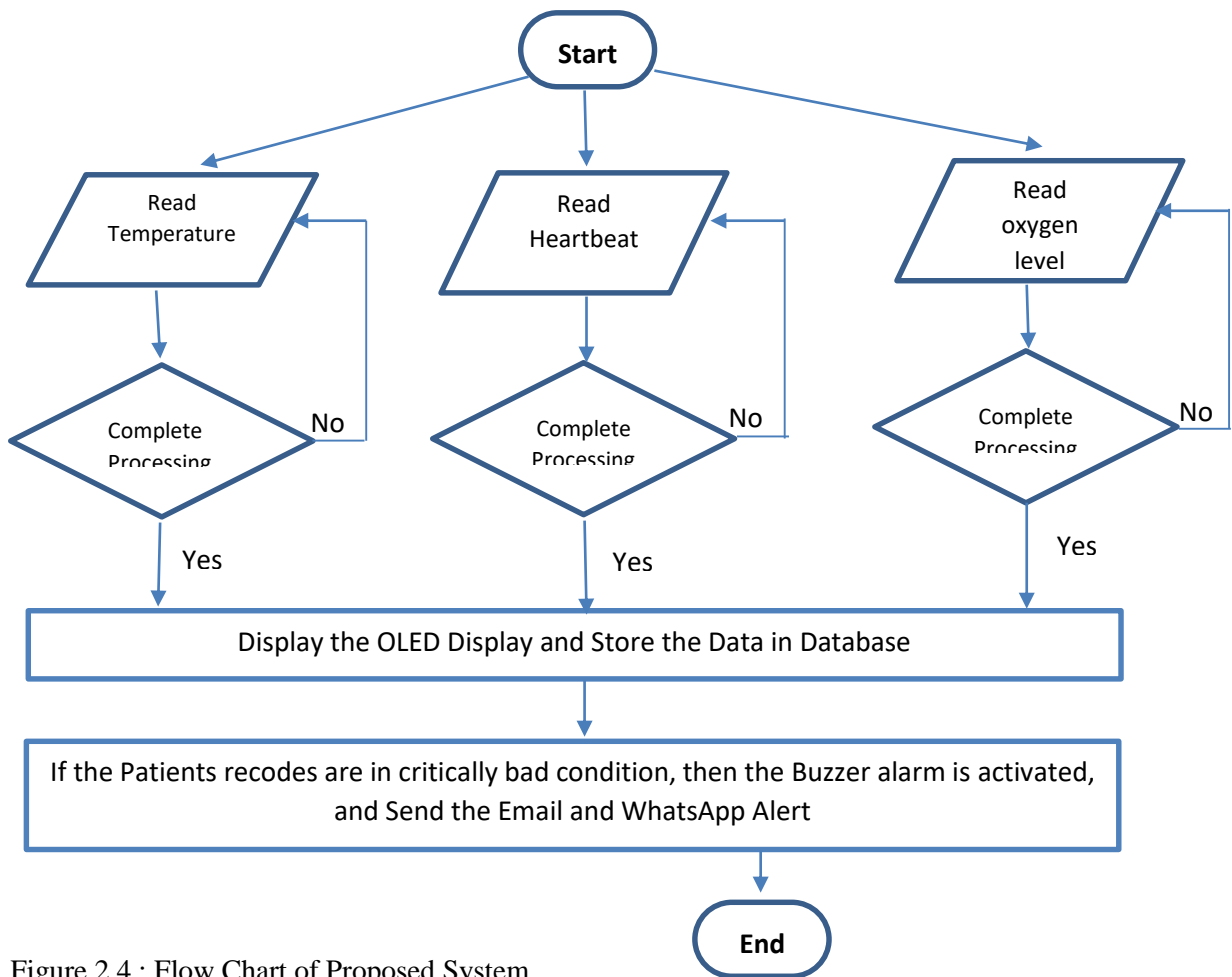


Figure 2.4 : Flow Chart of Proposed System

### 3.0 RESULTS AND DISCUSSION

#### 3.1 Graphical User Interface

The system created for this research study is shown in this section, along with the results obtained using the system. Then data is uploaded to ESP32, the system starts working, and the measurement data was acquired. The web page is then stored in this data shows Figure 3.1. The goal of this project is to ensure that web pages are simple to read and have user-friendly interfaces.

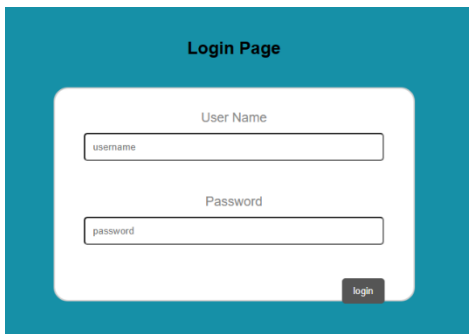


Figure 3.1 : Login Web Page

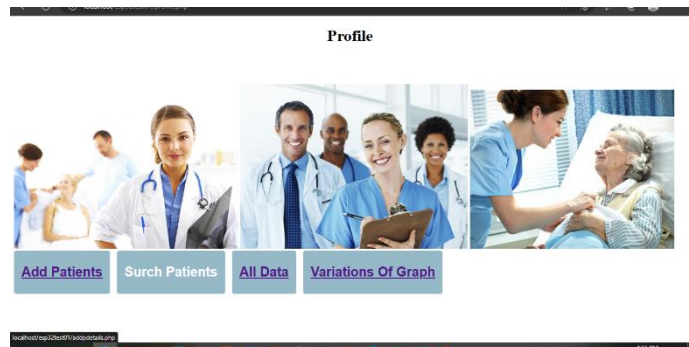


Figure 3.2 : Profile Web Page

Figure 3.4 shows the doctor can see the history of patient vitals that has been recorded and stored on the server in tabular form.

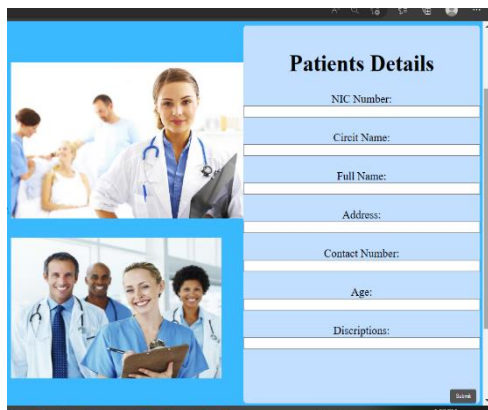


Figure 3.3: Web Page of adding patients

Unit No	Temperature	Heart Beat	Oxygen Level	Date	Time
4	30.00	70.00	95.00	2023-01-07	19:57:49
4	30.00	70.00	95.00	2023-01-07	19:57:55
4	32.00	80.00	94.00	2023-01-07	19:58:00
4	35.00	80.00	92.00	2023-01-07	19:58:05
4	38.00	82.00	90.00	2023-01-07	19:58:10
4	39.00	85.00	89.00	2023-01-07	19:58:15
4	40.00	85.00	88.00	2023-01-07	19:58:21
4	40.00	82.00	90.00	2023-01-07	19:58:26
4	39.00	80.00	90.00	2023-01-07	19:59:44
4	40.00	80.00	84.00	2023-01-07	19:59:49
4	45.00	50.00	80.00	2023-01-07	19:59:54
4	34.00	55.00	78.00	2023-01-07	19:59:59
4	30.00	70.00	95.00	2023-01-07	20:00:05
4	30.00	70.00	95.00	2023-01-07	20:00:10
4	30.00	70.00	95.00	2023-01-07	20:00:15
4	30.00	70.00	95.00	2023-01-07	20:00:21
4	30.00	70.00	95.00	2023-01-07	20:00:26
4	30.00	70.00	95.00	2023-01-07	20:00:31
4	30.00	70.00	95.00	2023-01-07	20:00:37
4	35.00	75.00	100.00	2023-01-07	20:02:19
4	35.00	75.00	100.00	2023-01-07	20:02:24
4	37.00	78.00	97.00	2023-01-07	20:02:30

Figure 3.4 : Store that Patients Details

Figure 3.5, Figure 3.6, Figure 3.7, and Figure 3.8 Show the time Series of Measured Vales of temperature, Oxygen Level, and heartbeat vs time.

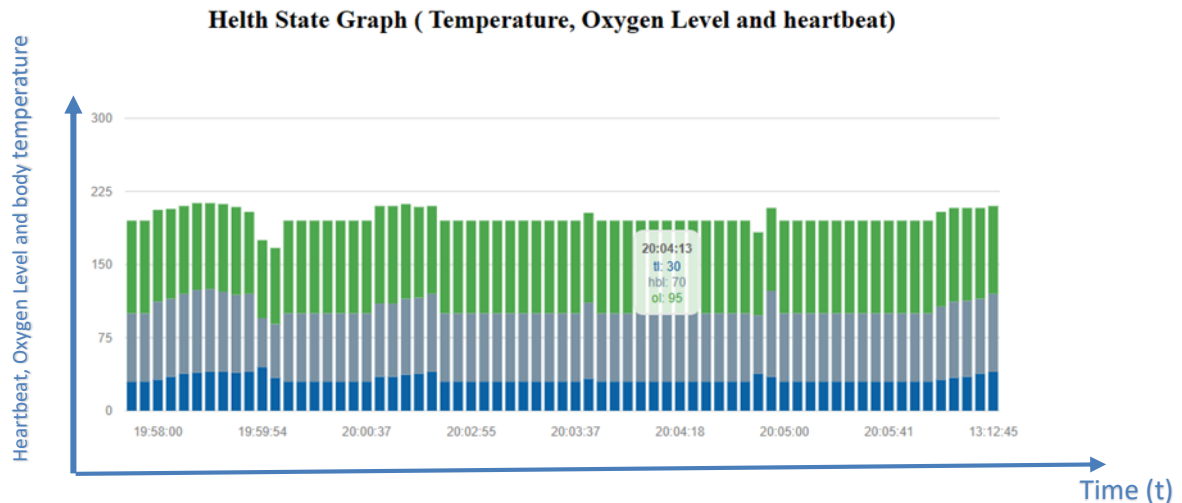


Figure 3.5 : Graph of temperature, Oxygen Level and heart rate vs time

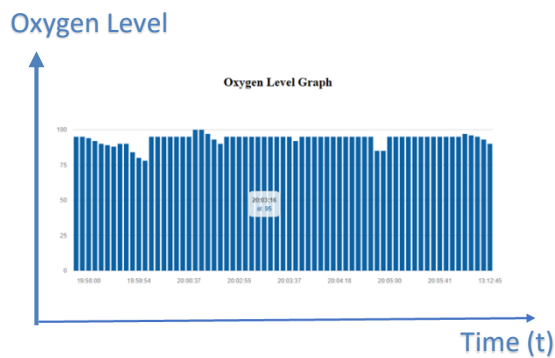


Figure 3.6 : Graph of Oxygen Level vs time

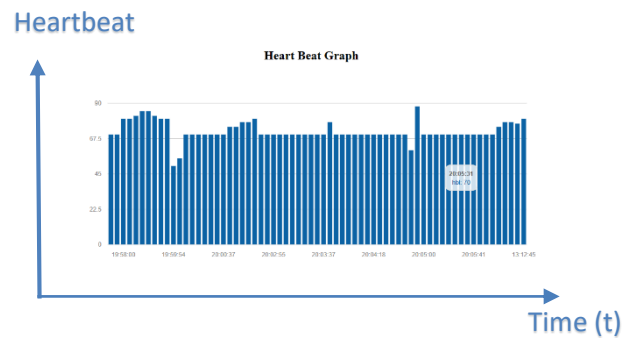


Figure 3.7 : Graph of Heartbeat vs time

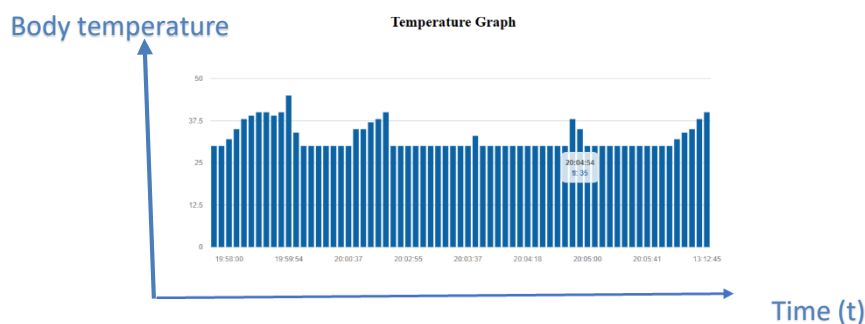


Figure 3.8 : Graph of Body temperature vs time

The data is also updated and stored in the Cloud which allows doctors, nurses, and patients' relatives to monitor their health from anywhere via the internet. When these values are not normal, they are sent to the Email Alert and SMS Alert. Figure 3.9 shows the Email Alert and Figure 3.10 shows the WhatsApp message.





Figure 3.9 :Email Alert

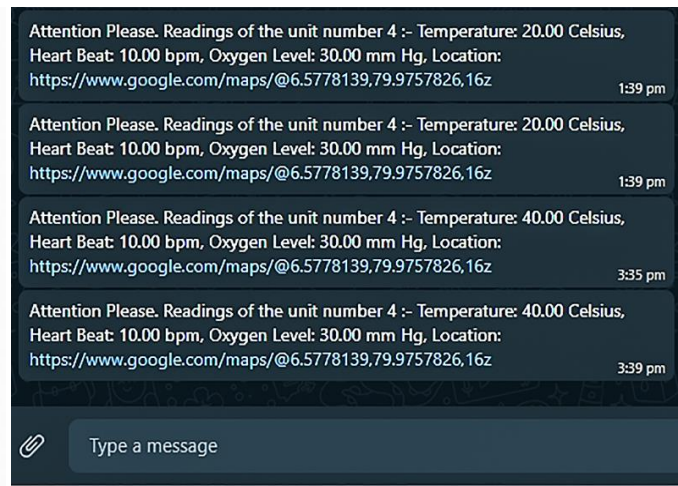


Figure 3.10 : WhatsApp Message

In our proposed and constructed IOT-based system, When the doctor or caretaker would need to know the patient, their location can be tracked down by clicking on the track patient location link. Then the Text Message and Email clicking that link is redirected to a Google maps page with the current patient's location details (Figure 3.5).

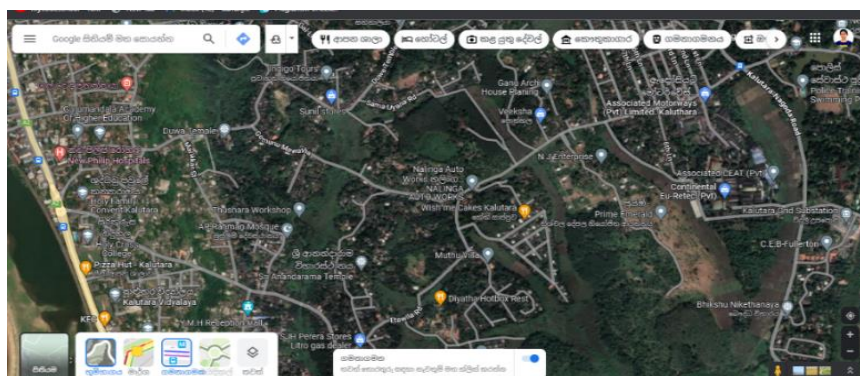


Figure 3.11 : Google Location

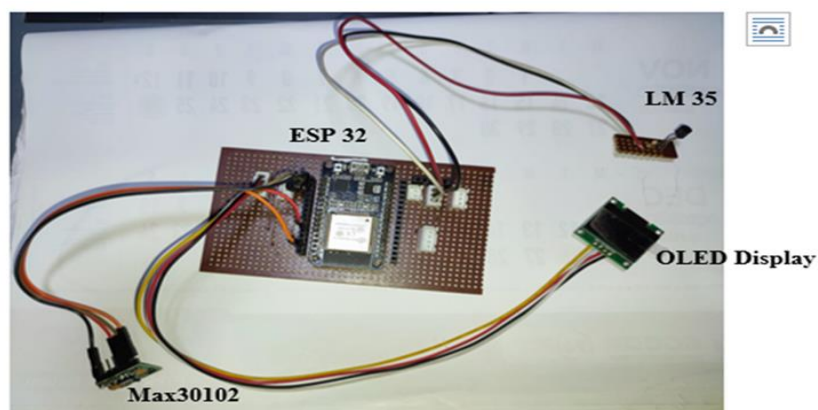


Figure 3.12 : The constructed system Setup for the task

#### 4.0 CONCLUSION

This paper explains the design and implementation of a health monitoring system for the temperature, Heartbeat, and oxygen level of humans with the use of IoT. This IoT-based device allows users to determine their health parameters, which could help regulate their health over time. Once the diseases are virtually recognized by doctors utilizing the internet, this suggested IoT health parameter monitoring system will allow the authorized person to access these saved data, recode patient data, and treat patients based on these values. A patient monitoring system has been implemented into an IoT-based prototype system which will measure the heart rate, oxygen level, and temperature of the patient continuously and will display the output on the OLED screen one by one and stored in the Cloud. If the sensor records any value going beyond the bad reading, then it will generate an alert message and email and send it to the hospital or concerned person stating the patient's status for a medical emergency.

#### ACKNOWLEDGEMENTS

The authors would like to thank all the staff of the Department of Electronics, Faculty of Applied Sciences, Wayamba University of Sri Lanka, and others who have supported to make this research a success.

#### REFERENCES

- [01] Md. Milon Islam, Ashikur Rahaman, and Md.Rashedul Islam, *Development of Smart Healthcare Monitoring System in IOT Environment*, <https://www.ncbi.nlm.nih.gov/pmc/articles/PMC7250268/>, (Accessed 2022-07-08)
- [02] Patient Monitoring System, [https://www.draeger.com/en\\_sea/Hospital/Patient-Monitoring-Systems](https://www.draeger.com/en_sea/Hospital/Patient-Monitoring-Systems), (Accessed 2022-08-20)
- [03] Development of IoT Heartbeat and Body Temperature Monitoring System for Community Health Volunteer, <https://ieeexplore.ieee.org/document/9090692>, (Accessed 22-08-20)
- [04] IoT Based Health Monitoring System, <https://ieeexplore.ieee.org/abstract/document/9074192> (Accessed 2022-08-20)
- [05] IoT-Based Health Monitoring System Development and Analysis, <https://www.hindawi.com/journals/scn/2022/9639195/> (Accessed 2022-12-20)
- [06] Patient Monitoring System Based on Internet of Things, <https://www.Sciencedirect.com/science/article/pii/S1877050916301260> (Accessed 2022-12-20)

## **DESIGN AND BUILD AN IOT-BASED FULLY- AUTOMATED MINI-GREENHOUSE FOR THE CULTIVATION OF VEGETABLES**

K.P. Gunaratne\*, J.M.J.W. Jayasinghe

*Department of Electronics, Wayamba University of Sri Lanka, Kuliyaipitiya, Sri Lanka*

\*fas172061@kul.wyb.ac.lk

### **ABSTRACT**

Modernization of agriculture is essential to generate sufficient income and attract the youth in Sri Lanka [3]. When the available space is very limited or no outside room is available, the perfect option is using an indoor mini greenhouse. The mini greenhouses, which are manually controlled, are popular among householders in Sri Lanka. Therefore, main objective of this study to design and build an IoT (Internet of Things)-based fully automated mini-greenhouse for the cultivation of vegetables specially with fertigation system. The pot experiment was carried out to compare the two different cropping systems i.e., automated mini- glasshouse and traditional out-door growing systems with two different crops. In mini-greenhouse the environmental factors such as soil moisture, temperature, light intensity, humidity, and fertigation were automated supplying ideal growing environment. In outdoor condition, constant monitoring and adjustment were done to manage environmental factors as well as pest and diseases control with paying more attention and much time. The prototype has successfully demonstrated its capability to sense environmental factors in mini greenhouse. The prototype also managed to implement the data gathered by the sensor and sent signal to devices and to take action, when the threshold was reached. As far as crop performance is concerned, the lettuce plants grown in two different cropping systems showed similar performance in relation to crop growth and nitrogen uptake and the capsicum plants grown in green house showed higher performance compared with the plant kept in outdoor. Therefore, this design helps to ease much of the burden and challenge growers face having to manage every single environmental factor, without the need for constant monitoring and adjustment.

**Key words:** Automation, Mini greenhouse, IoT

### **1.0 INRODUCTION**

The mini greenhouses which are manually controlled are popular among house holders in Sri Lanka mainly for ornamental plants and cut flowers, but less popular among house holders for vegetables. However, automatically controlled mini greenhouses are still not popularized among households in Sri Lanka even for ornamental plants and cut flowers.

Moreover, most of the house holders living in urban areas of Sri Lanka are employed, there is no time to watch mini green house.

Cruz *et al.* [1] and Kodali *et al.* (2016) [2] have carried out research on IoT-based automated greenhouse where temperature, light intensity, and humidity were automated but not fertigation.

Therefore, the objective of this study was to design and build an IOT-based fully-automated mini-greenhouse for the cultivation of vegetables specially with fertigation system.

## 2.0 EXPERIMENTAL

The mini greenhouse (prototype) was constructed using wood and glass panes with dimension of length \* width \* height were 3' \* 2' \* 2.8' (Figure 1).



Figure 2.1: Mini greenhouse with plants

### 2.1 Control system

The control system was designed mainly to handle 5 tasks. They were temperature control, light intensity control, water irrigation control, and fertigation control. NodeMCU ESP8266 microcontroller development board was used as the main control unit which was responsible for taking sensor input and control outputs. Also, it was used to link the user interface with control system by connecting to internet via Wi-Fi router (Figure 2.1).

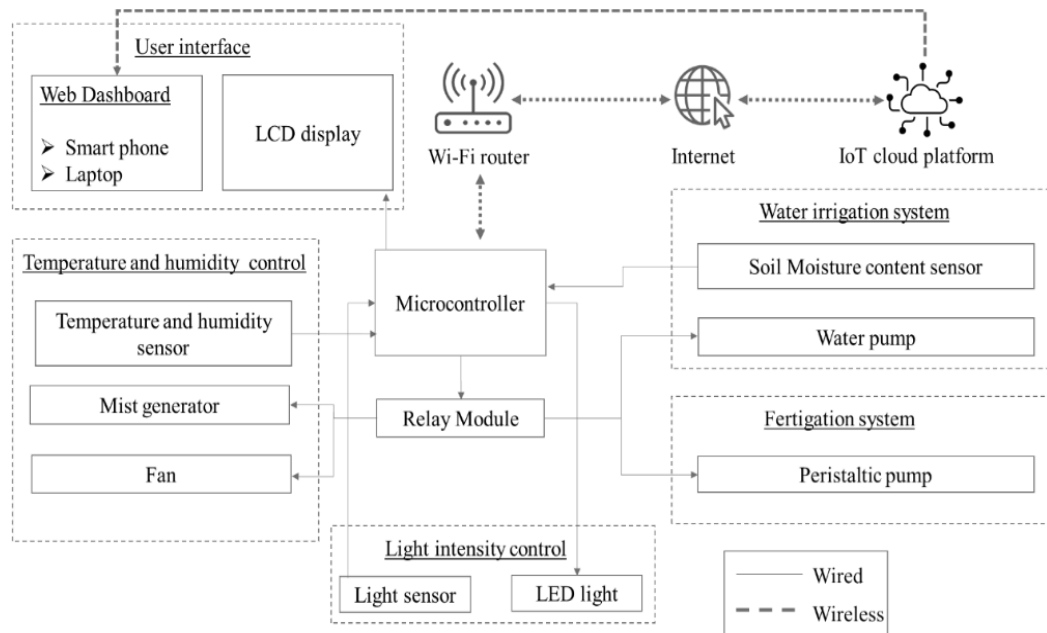


Figure 2.2: Block diagram of the control system

The temperature and humidity control section were designed to monitor temperature and humidity by DHT 11 humidity and temperature sensor, control temperature by fan, and control humidity by mist generator. The light intensity control section was designed to monitor the light intensity using an LDR sensor and supply light intensity by LED lights. Water irrigation system was designed to monitor soil moisture content by capacitive soil moisture sensor and supplement of water to plants by operating water pump. Fertigation system was designed to dispense pre-determined amount of fertilizer solution to the plants in pre-determined time intervals by using peristaltic pump.

## 2.2 Crop study

Cropping system (automated mini green house, Outdoor) and crop type (Lettuce, Capsicum) were used as factors of this study. Completely randomized design (CRD) with 3 replicates was used as experimental design. Moist soils containing around 35% water (which was considered as plant available water content) were filled into pots of 4.5 L capacity each holding 4.0 kg soil separately. Then, 6 pots were sown with Lettuce seeds and Capsicum seeding were transplanted in 6 pots. Three pots from each crop were put in mini greenhouse and 3 pots of each crop was put outside as control to comparison. The plants kept in outdoor was exposed to natural environment. Therefore, constant monitoring and adjustment were needed. Managing environmental factors including temperature, humidity, light levels, water requirement and ventilation to be take care of. Pest and diseases control was the other very important

management practice to be carried with paying more attention under outdoor condition. The Albert' solution was used for fertigation and fertigation was done in one week intervals.

At the end of experiment, pots were dismantled. Before dismantling, height of plant, number of leaves, number of flowers, number of pods were measured. The roots of uprooted samples were washed properly by using tap water. Fresh weights of plants were measured by using analytical balance. After that the samples were kept in oven at 80°C for overnight. Then dry weight of samples was taken. Then, samples were ground by using willy mill for nitrogen determination. Total nitrogen contents of the plant were measured using Kjeldahl method[4] . The data collected were statistically analyzed using the Statistical Analysis System (SAS) package, version 6 [5].

### 3.0 RESULTS AND DISCUSSION

#### 3.1 Control system performance

Fan automatically turned on and off depending on the set temperature. The fluctuation of inside temperature on day 2022-12-31 during 7:00:00 to 18:00:00 was given in Figure 3.1.

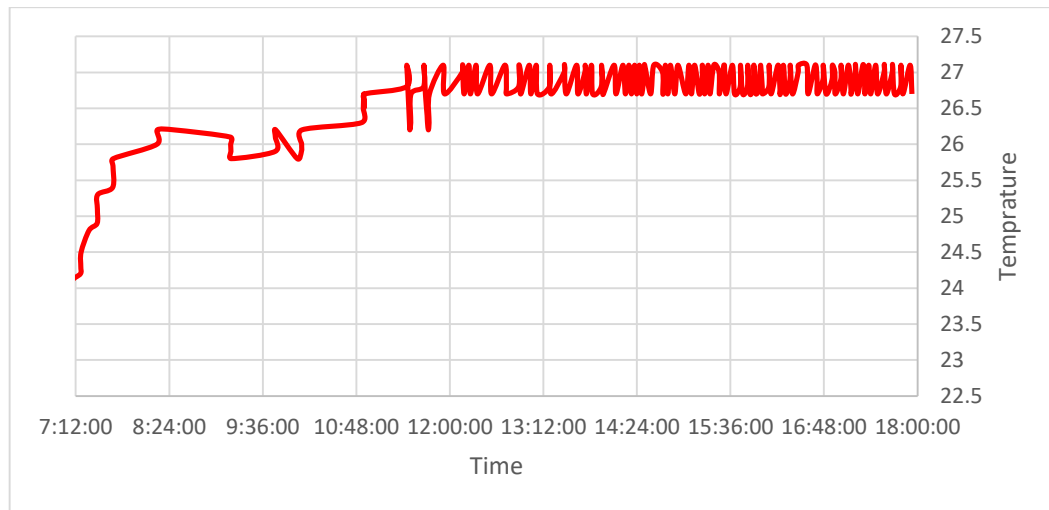


Figure 3.1: Mini Greenhouse inside temperature on 2022-12-31 7:00:00 to 18:00:00

The control system was set to maintain the temperature inside the greenhouse without exceeding 27 °C.

Mist generator automatically turned on and off depending on set humidity. The fluctuation of inside humidity on day 2022-12-31 during 7:00:00 to 18:00:00 was given in Figure 3.4.

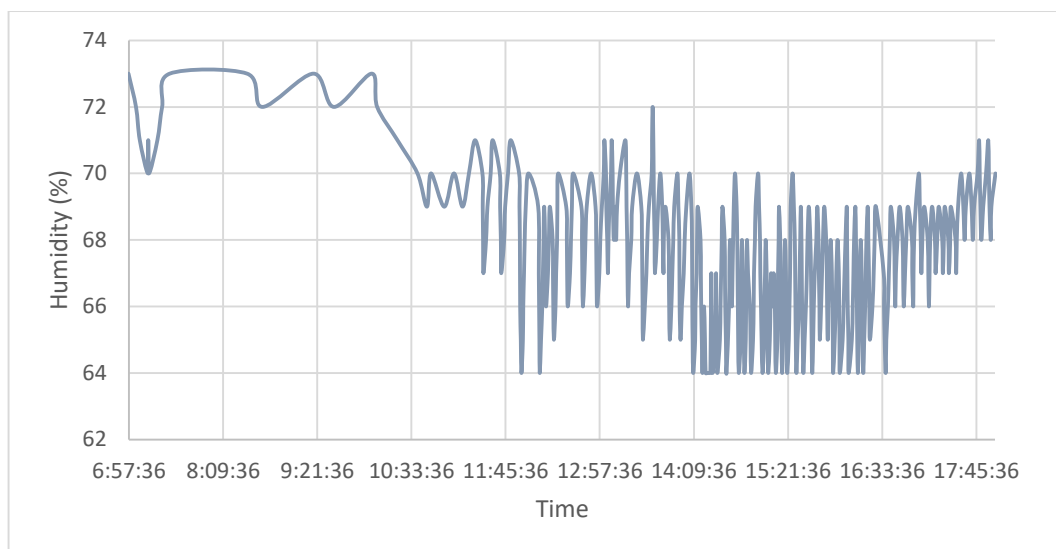


Figure 3.4: Mini Greenhouse inside humidity on 2022-12-31 7:00:00 to 18:00:00

The control system was set to maintain humidity between 64% and 70% inside the greenhouse.

Lights automatically turned on and off depending on both the light schedule plan and set light intensity. Water pump automatically turned on and off depending on both the water supply schedule plan and set soil moisture content. When the automatic mode was on for the fertilizer supply, it automatically turned on and off depending on both the fertilizer supply schedule plan and the set volume of fertilizer solution issued.

### 3.2 Crop performance

#### 3.2.1 Effect of different cropping systems on growth parameters of Lettuce

Table 3.1: Effect of different cropping systems on growth parameters of Lettuce

Cropping system	Observation			
	Leaf count	Plant height (cm)	Fresh weight (g)	Dry weight (g)
Mini Green house	7.00A*	19.66A	24.42A	1.16A
Outdoor	7.00A	12.00B	22.75A	1.14A
Least Significant Difference (LSD)	2.267	6.673	18.874	0.894
Probability %	1.00	0.0332	0.818	0.957

\*The average values with same letter showed similar performance and with different letters showed different performance of two cropping systems.

The leaf count, fresh weight of plant and dry weight of plant did not show significant different between two treatments. However, plant height varies significantly between two treatments where, highest value was observed with mini greenhouse cropping systems (Table 3.1).

### 3.2.2 Effect of different cropping systems on plant nitrogen (N) content and uptake of Lettuce

Table 3.2: Effect of different cropping systems on plant nitrogen (N) content and uptake of Lettuce

Cropping system	Parameter	
	Plant N content (%)	Plant N uptake (mg/pot)
Mini Green house	4.10A	52.43A
Outdoor	3.94A	51.03A
Least Significant Difference (LSD)	0.970	14.998
Probability %	0.674	0.808

No significance difference was observed between two cropping systems in relation to plant N content (Percentage of nitrogen in plant) and nitrogen uptake (N content \*Total dry matter). However, highest values were observed with green house cropping system (Table 3.2).

### 3.2.3 Effect of different cropping systems on growth parameters of Capsicum

Table 3.3: Effect of different cropping systems on growth parameters of Capsicum

Cropping system	Observation			
	Leaf count	Plant height (cm)	Fresh weight (g)	Dry weight (g)
Mini Green house	60.67A	58.67A	47.05A	9.56A
Outdoor	24.67B	37.66B	23.02B	2.76B
Least Significant Difference (LSD)	28.794	18.463	21.004	2.635
Probability %	0.0256	0.0343	0.0336	0.0020

Leaf count, plant height, fresh weight and dry weight vary significantly between two cropping systems. The highest values were observed with green house cropping system (Table 3.3). According to above the results, the lettuce plants grown in two different cropping systems showed similar performance in relation to growth parameters and N content and uptake.



### 3.2.4 Effect of different cropping systems on plant reproductive of Capsicum

Table. 3.4: Effect of different cropping systems on reproductive parameters of Capsicum

Cropping system	Parameter	
	Flower count	Pod count
Mini Green house	19.00A	1.00A
Outdoor	8.67B	0.00B
Least Significant Difference (LSD)	8.38	0
Probability %	0.0267	0

Both flower and pod numbers vary significantly between two cropping systems. The highest values were observed with mini greenhouse cropping system (Table 3.4).

### 3.2.5 Effect of different cropping systems on plant nitrogen content (N) and uptake of Capsicum

Table 3.5: Effect of different cropping systems on plant nitrogen (N) content and uptake of Capsicum

Cropping system	Parameter	
	Plant N content (%)	Plant N uptake (mg/pot)
Mini Green house	3.79A	133.57A
Outdoor	3.85A	66.13B
Least Significant Difference (LSD)	0.758	29.116
Probability %	0.845	0.003

Plant N content did not vary significantly between two cropping systems. However, plant N uptake significantly vary between two cropping systems (Table 3.5). According to the above results, the capsicum plants grown in mini greenhouse showed higher performance compared with the plant kept in outdoor in relation to both growth and reproductive parameters as well as N uptake.

## 4.0 CONCLUSION

The prototype has successfully demonstrated its capability to sense environmental factors in mini greenhouse such as temperature, humidity, and soil moisture content. The prototype also managed to implement the data gathered by the sensor and sent signal to devices i.e., fan, mist generator, water pump, led light, peristaltic pump and to take action when the threshold was reached.

As far as crop performance is concerned, the lettuce plants grown in two different cropping systems showed similar performance in relation to crop growth and nitrogen uptake and the capsicum plants grown in green house showed higher performance compared with the plant kept in outdoor.

Therefore, this design helps to ease much of the burden and challenge growers face having to manage every single environmental factor, without the need for constant monitoring and adjustment.

## **ACKNOWLEDGEMENT**

Authors appreciate the valuable help given to complete analytical part of this study not only providing chemicals and instruments but also training given for methodology of analysis by staff of the soils and plant nutrition division of Tea research institute of Sri Lanka.

## **REFERECES**

- [1]. Cruz, D., Rodrigues, C., Chase, O., Araújo, D., Almeida, J. F., IoT-based Smart Mini Greenhouse, *International Journal for Innovation Education and Research*, 7(10), (2019), 31–37
- [2]. Kodali, R. K., Jain, V., Karagwal, S. , IoT based smart greenhouse, Proc. In *2016 IEEE region 10 humanitarian technology conference (R10-HTC)*, 2016, 1-6
- [3]. Daily F.T., Why is Sri Lanka's youth stepping down from agriculture, 2017, <https://www.ft.lk/article/627465/Why-is-Sri-Lanka-s-youth-stepping-down-from-agriculture-> (Accessed date: 2023 January 18)
- [4]. Bremner, J.M., Determination of nitrogen in plants by the Kjeldahl method, *The Journal of Agricultural Science*, 55(1), (1960), 11-33
- [5]. Anon, *SAS/ETS user's guide, Version 6*, 2nd edition, SAS institute Cary, NC, 1995

## MULTIFUNCTIONAL LABORATORY POWER SUPPLY

L.S.K. Gunasinghe\*, L.D.R.D. Perera

*Department of Electronics, Wayamba University of Sri Lanka, Kuliyaipitiya, Sri Lanka*

\*lakshigunasinghe96@gmail.com

### ABSTRACT

Designing a single equipment that can provide dc power and generate essential wave forms for laboratory practical is reported in this paper. The low voltage dc power supply was designed with 7805, and LM 317 & LM 337 voltage regulator ICs. ICL 8038 integrated circuit was used as the core to design the signal generator. Circuits were simulated with Proteus 8 Professional software. The designed circuit has regulated fixed 5 V dc output and continuously variable, regulated dual rail  $\pm 12$  V output. The signal generator has square, sine and triangular wave outputs with provisions for amplitude, frequency and duty cycle adjustments. The design has high accuracy, simple structure and small size, and is suitable for many laboratory experiments in physics and electronics. The designed circuit is a low cost solution to replace the more expensive laboratory power supply and the signal generator. There is the potential to add more functions and enhance output parameters of the signal generator and thereby expand the range of applications.

**Keywords:** Power supply, Signal generator, ICL 8038

### 1.0 INTRODUCTION

Signal generators have a wide range of applications in the fields of research and development, communication, and control and measurement industry. Today's electronic systems require many signal waveform shapes. Signal generators are available in different types, each with different applications and purposes. They also have different designs and use different circuits, offering various levels of capability and functionality [1,2,3]. Common waveforms are the sine wave, square wave, triangular wave, and single pulse wave with a fixed duration. Fixed-duration pulses are used in communication and control systems. Square waves are used as clock pulses for digital systems. Triangular waves or saw tooth waves are used for scanning an electron beam on a CRT screen, in precise time measurements, and in time modulation. With the development of modern technology, the function generator with independent control of amplitude and frequency plays an important role in applied electronics, communications,

instrumentation, and signal processing applications [2].

Currently, most of the general purpose power supplies and signal generators used for educational purposes are very expensive. The low cost ones often have circuit failures resulting in a waste of resources. Local school and university laboratories face a huge problem due to high cost of these equipment and equipment breakdowns and malfunctioning. The multifunctional power supply is proposed as a result of background survey done in 2022. Major points identified there were that school laboratories and some university electronics laboratories lack these two basic laboratory equipment in required numbers and a majority of the school science labs do not have these equipment.

The main objective of this project was to design a multifunctional laboratory power supply, which is a combination of both a dc power supply and a signal generator combined into one device, to achieve cost effectiveness and versatility. A multifunctional power supply can replace the standard dc power supply and the signal generator with a low cost single device. With this low-cost power supply cum signal generator, students and undergraduates will have the opportunity to do a range of laboratory experiments individually or in small groups.

In a general purpose dc power supply, to convert line frequency ac to dc, a diode bridge rectifier is used. To reduce the ripple in the dc output voltage, large filter capacitors are used at the rectifier output [4]. For output regulation, use of voltage regulator ICs is the most appropriate way for low current applications [5].

The circuits in this study were designed with 7805 IC for fixed 5V output, LM 317 and LM337 ICs for dual rail dc voltage regulation and ICL8038 for wave form generation. The ICL8038 waveform generator is capable of producing high accuracy sine, square and triangular waveforms with a minimum of external components.

The designed power supply has continuously variable dual rail  $\pm 12\text{V}$  outputs. The signal generator can produce square wave, sine wave, and triangular/saw tooth wave outputs in the 20Hz to 100kHz range. It has provisions for frequency and duty cycle adjustments.

The designed multifunctional power supply is cost-effective and occupies less space, and is convenient to operate rather than using two equipment. The designed system can be further

improved to have additional functionalities and output wave form regulations.

## 2.0 EXPERIMENTAL

A laboratory power supply operates in one of the two modes. The proposed model has the constant voltage (CV) mode. In this mode, the lab power supply supplies the set voltage [4].

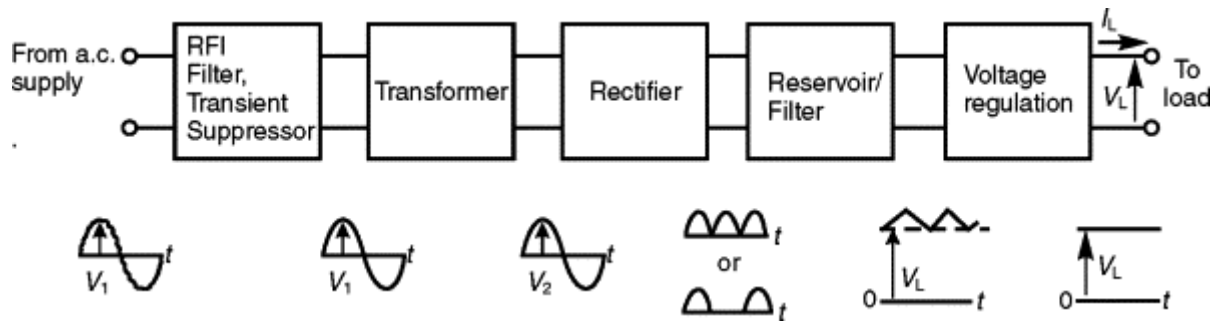


Figure 2.1. Main functional stages of a dc power supply

Main functional stages of a common dc laboratory power supply, shown in Figure 2.1, and explained below were incorporated in the proposed design.

**The Transformer:** A center-taped transformer first takes the input power supply of the alternating current (ac) mains voltage of 230V and brings it down to a lower voltage level of 24V ac (12V-0-(-12)).

**The Bridge Rectifier:** AC voltage of the transformer is rectified using a full-wave rectifier to give equal positive and negative voltage outputs.

**The Smoothing circuit (Filter Circuit):** The ripples in the rectifier output are smoothed using low-pass filtering of the waveform by a shunt capacitor.

**The Voltage regulator:** This stage delivers a stabilized DC voltage to the output as set by the control unit. 7805 voltage regulator IC was used for fixed 5 V output. LM 317 and LM 337 adjustable, three terminal voltage regulator ICs were used for dual rail +/- 12 V regulation.

The block diagram of the smart power supply and signal generator is shown in Figure 2.2. It is a combination of both a signal generator and a power supply. The unit is working with 230 V AC voltage and it outputs a +12 V/ -12 V voltage as the power supply unit. It also outputs three

different waveforms, namely, sine wave, square wave, and triangular waveform with different frequency values.

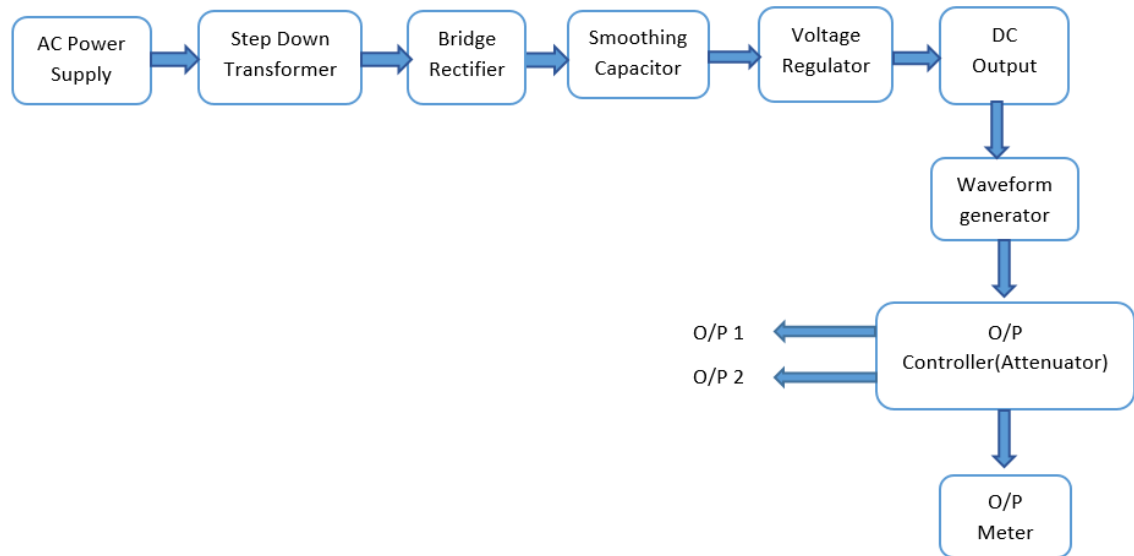


Figure 2.2: Functional block diagram of the proposed device

The circuit diagram of the regulated dual rail (+12) – 0 – (-12) V dc voltage generator is shown in Figure 2.3. It contains LM 317 and LM 337 ICs for dual rail voltage regulation, and the output can be continuously varied by means of a coupled potentiometer. The 7805 IC can be connected similarly in parallel with the bridge output to generate 5 V fixed output.

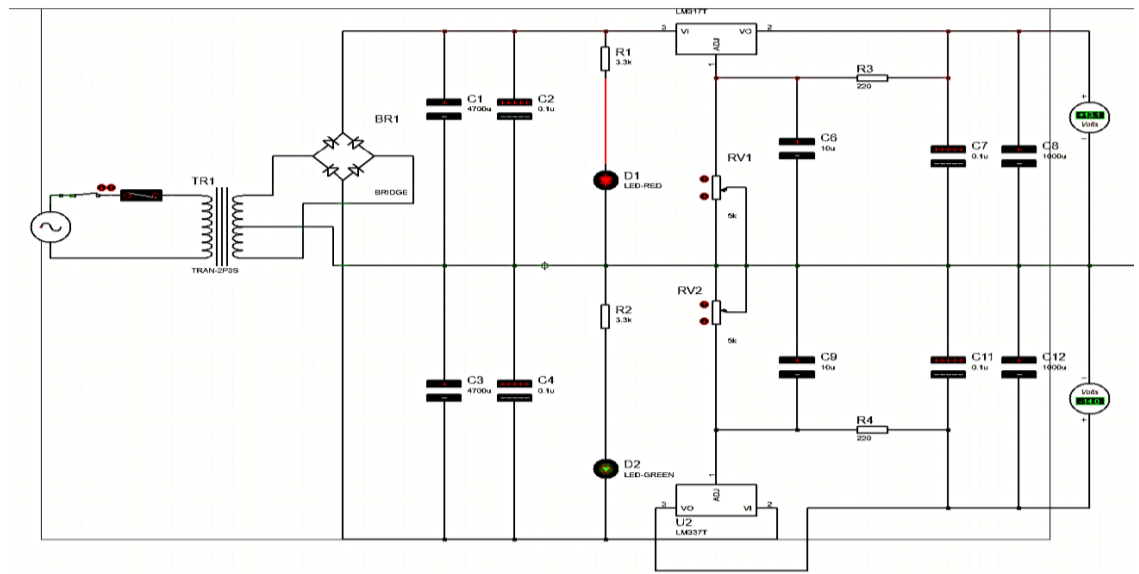


Figure 2.3: Circuit diagram of the variable 12-0-12V dc power supply

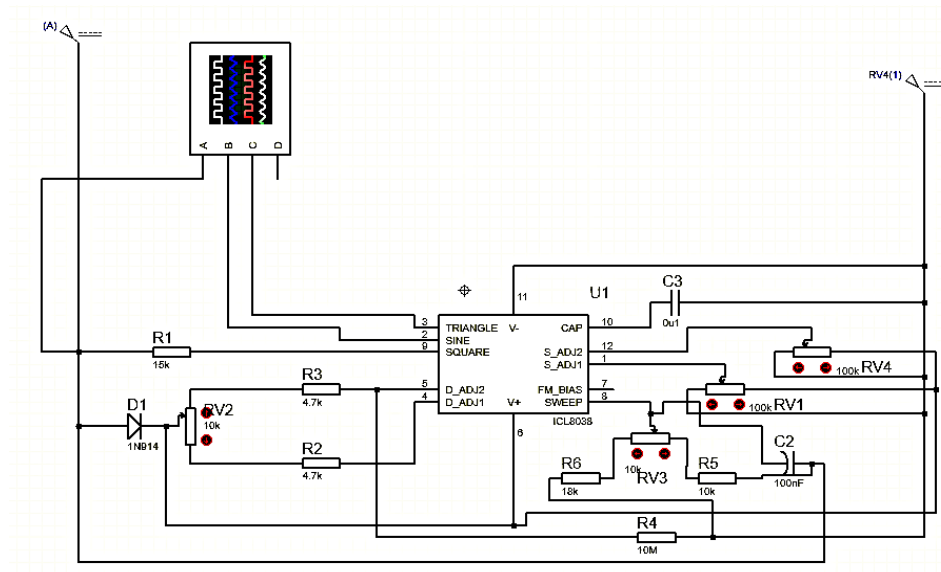


Figure 2.4: Circuit diagram of the signal generator

The signal generator circuit was designed as in Figure 4. It takes  $\pm 12\text{V}$  dc input for its operation from the previously designed power supply. The core component of this device is the ICL 8038 waveform generator IC. The frequency and the duty cycle of the waveforms can be adjusted through the potentiometers and its simulated outputs were observed on an oscilloscope.

### 3.0 RESULTS AND DISCUSSION

The designed system has 230 V ac voltage as its input. When in the dc power mode, simulated output characteristics showed balanced  $\pm 12\text{V}$  variation through the two voltmeters connected to the  $\pm$  rails. The positive and negative voltage outputs can be separately adjusted by means of the two potentiometers, or the dual rail output can be continuously varied by a single knob of a combined potentiometer. Additional 5 V fixed output can also be provided through incorporation of 7805 regulator IC.

The voltage regulator ICs used in this circuit can supply currents in excess of 500 mA, and hence, the power supply is suitable for many experiments generally found in physics and electronics courses.

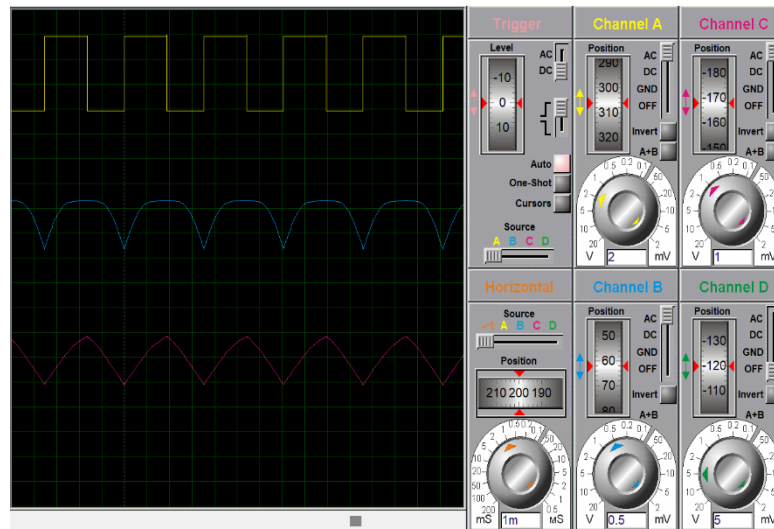


Figure 2.5: Signal generator outputs

The wave form generator can be operated either from a single power supply (10 V to 30 V) or a dual rail power supply (+/-5 V to +/-15 V). In the present design, the wave form generator is powered by already designed dual rail +/-12 V supply. The split power supply has the advantage that all waveforms move symmetrically about the ground level.

The designed signal generator circuit has square, sine and triangular waveform outputs, and the simulated outputs as observed through an oscilloscope, are shown in Figure 2.5.

The typical amplitudes of the triangular and sine waves are  $0.33 \times V_{\text{supply}}$  and  $0.22 \times V_{\text{supply}}$ , respectively. The sine and triangular wave amplitudes can therefore be varied in a limited range by adjusting the supply voltage. Alternatively, the amplitude adjustment range can be expanded by feeding the outputs to op-amp buffer amplifiers.

The square wave output is not specified. However, a load resistor can be connected to pin 9 and  $+V_{\text{supply}}$  or to a different power supply (<30V) to have desired output levels. Accordingly, the square wave output can be made TTL compatible by connecting the load resistor to +5 V.

The triangular waveform and the square waveform generated by the IC are fed to in-built buffer stages before making them available at pins 3 and 9. The maximum sink currents through pins 3 and 9 are 25 mA.



The sine wave output from the IC (pin 2) has relatively high output impedance, typically  $1\text{k}\Omega$ . Output from pin 2 can be fed to an Op-amp based buffer amplifier for buffering, and gain and amplitude adjustments. A simple op-amp voltage follower could also be used.

In the ideal case, frequency of the wave forms can be adjusted externally from  $0.001\text{ Hz}$  to more than  $300\text{ kHz}$  using either resistors or capacitors, and frequency sweeping can be accomplished with an external voltage applied to pin 8. The designed system has a variable frequency, and could output a maximum frequency of about  $100\text{ kHz}$ . Linearity of input sweep voltage versus output frequency can be significantly improved using an op-amp sweep input voltage stage and a voltage follower at the output.

The symmetry of all the waveforms can be adjusted with the external timing resistors connected to pins 4 and 5. For square pulses, duty cycles from less than 1% to greater than 99% are achievable. Typical values are 2% - 98%.

To minimize distortion of sine waves, a potentiometer has been connected between pins 11 and 12. With this arrangement distortion of less than 1% is achievable. The designed system is working correctly as expected with no noise or hysteresis.

#### **4.0 CONCLUSION**

A continuously variable, dual rail,  $\pm 12\text{V}$  dc power supply with a signal generator functions for laboratory applications was designed and the output characteristics were simulated using Proteus 8 Professional software. Power for both circuits can be derived from a common primary rectifier stage minimizing the equipment cost.

$\pm 12\text{ V}$  dc voltage regulation was achieved through the LM 317 and LM 337 ICs, and balanced dual rail variation can be obtained by employing a single combined potentiometer for voltage adjustment. Additional circuit for  $5\text{ V}$  fixed output can also be added.

Three types of waveforms; square, triangular and sine, could be generated using ICL 8038 IC as the core component. The frequency and the duty cycle of the waveforms can be varied by varying the resistances. Frequency is variable up to  $100\text{kHz}$  and the duty cycle of the square wave can be varied from 2%-98%. Amplitude and gain adjustments of sine and triangular waves can be performed by connecting ICL 8038 outputs to an op-amp buffer amplifier stage

or to a simple voltage follower depending on the intended applications of the signal generator.

The separately designed two circuits can be integrated in parallel to make it a single device operating with the same power supply.

The designed equipment is cost effective and eliminates the need for two equipment required for most of the undergraduate practicals in electronics. It further ensures maximum usage of components and prevents idling of equipment that could occur when a separate power supply and a signal generator are used. It could also save lab table space and is convenient to operate rather than using two equipment for the same purpose.

### ACKNOWLEDGEMENTS

Authors wish to extend their gratitude to staff of the Department of Electronics, Wayamba University of Sri Lanka for their assistance, and thank all who have supported to make this research a success.

### REFERENCES

- [1] Yash S.R., Kulkarani, S., Kumara, B., Waveform generation using Direct Digital Synthesis (DDS) Technique, *International Research Journal of Engineering and Technology (IRJET)*, volume: 06, 11 November (2019), 2001-2005.
- [2] Fleischer, M., Rosser, H., Neumann, U., A new family of pulse and Pulse/Function generator, *Hewlett Packard Journal*, (1983), 27-30.
- [3] Pranjali A., Charde, P.R.Lakhe, Akshay P. Nanote, Design of multiple waveform generator and Frequency counter based on DDS, , *International Research Journal of Engineering and Technology (IRJET)*, Volume:03, 07 July (2016), 268-271
- [4] Toich, F., A SHORT HISTORY OF THE EVOLVED POWER SUPPLY, *KepecoCurrents* Vol.7, No.1
- [5] Shoewu, O., Ogunleye, O.M., Design and Development of an Intelligent Variable Power Supply Device, *Pacific Journal of Science and technology*, (2011), 30-37.

## DEVELOPMENT OF A SMART PILL DISPENSER

M.A. Pathiraja\*, W.A.S. Wijesinghe

*Department of Electronics, Wayamba University of Sri Lanka, Kuliypitiya, Sri Lanka*

\*ashan.pathiraja@gmail.com

### ABSTRACT

Maintaining a correct consumption of medications daily become very difficult for the elder population in the society due to poor physical and mental conditions. Sometimes youngers also faces to the same problem. Also medication Non-adherence is one of a major causes of death and has risen in recent years. There are many people in the society who need constant help may it be elderly people, younger or others. But it is not always possible to remind them of their medicine's dosages regularly. There is a demand for a system that assists the patients to take medications correctly and overcome the medication non-adherence and negligence. As a solution to above problem, an IOT based, intelligent, user friendly and portable smart solution is proposed in this paper. The proposed system consists of a three sub systems each of which has specific task. The first sub system is a physical device that stores the medications and assists to the patient to take the medications correctly. Also, it sense the medication taken and update the system. The next sub system is the mobile application which is used by the patient's family member to configure the system and monitor the medication taken. As the third sub system is the cloud server which links the mobile application and the hardware device through the internet.

**Keywords:** Medication Dispenser, Medication Reminder, Internet of Things (IOT)

### 1.0 INTRODUCTION

Evolutions in smart healthcare technologies have led people to live a better lifestyle with each passing generation. The extent of benefits would have been even more prominent if the percentage of medication errors could be minimize and circumvented. In many cases, negligence has led to death and an increase in the expenditures by millions each year. Even though, more than 80% of the population above the age of 60 years are prescribed to take medicines multiple times a day, statistics indicate that 70% of adults do not follow a prescribed course of action, manipulate their dose or cease to continue drug therapy simply due to negligence or non-adherence. But another issue that has been in existence all along is no adherence [1,2].

The pill boxes are the traditional way to overcome this problems but it is static solution because it only organizes the medications according to the schedule and it doesn't reminder and not assists the patient to take medications which is the main disadvantage. To overcome the disadvantages of the traditional pill boxes, the electronic alarmed pill boxes were commercially available on the market which actively remind the patients to take medications, but those systems are not user friendly when changing the schedules and those systems not supported the tracking if the patient correctly took the medications or not [4,5].

There are couple of commercially available IOT based medications reminding systems available in the market, but those systems are complicated and expensive. Therefore those systems are not popular among consumers. Also, those systems are not actively assists when patients taking medications. A smart solution requires to overcome the weaknesses of the currently available solutions therefore new user-friendly, portable, real-time monitoring support and actively assistive medication reminding system is proposed in this paper.

## **2.0 METHODOLOGY**

The block diagram of the Smart Pill Dispenser System as shown in following Figure 2.1. According to the bock diagram the Smart Pill Dispenser System can be divides into to three sub systems Pill Dispensing device, cloud server and mobile application. The pill dispensing device interacts with patient and dispense the medications according to the schedule. The android application interacts with the user. The cloud server stores the user configurations and dispensing details and sync with the pill dispensing system.

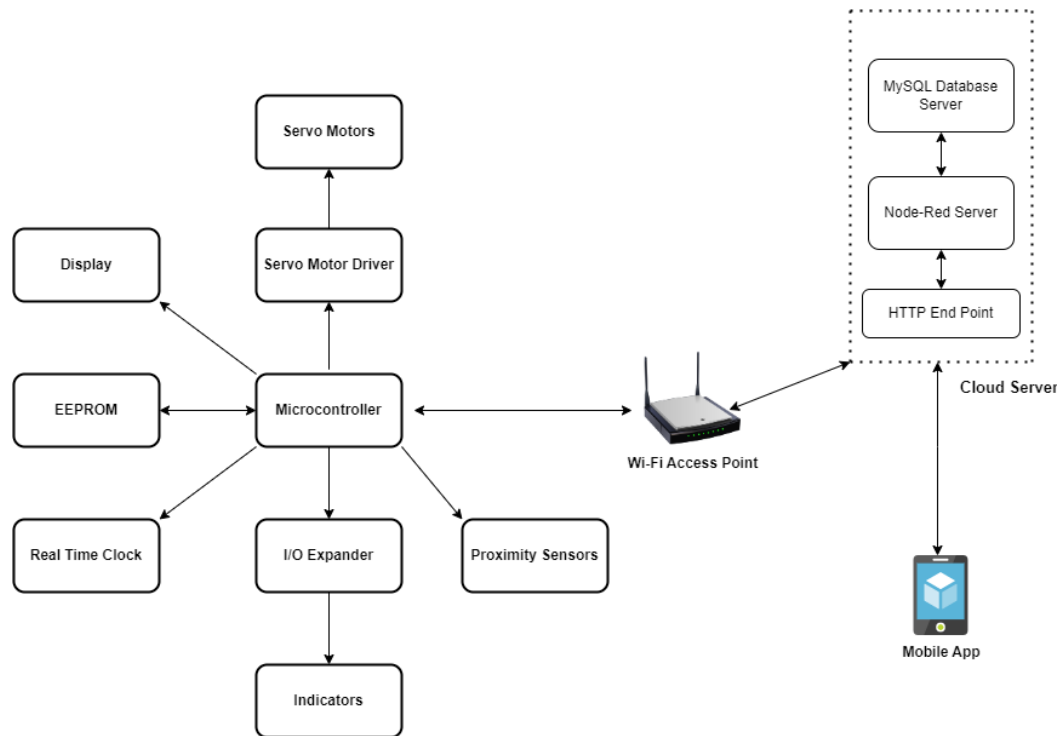


Figure 2.1: Block Diagram of the Smart Pill Dispensing System

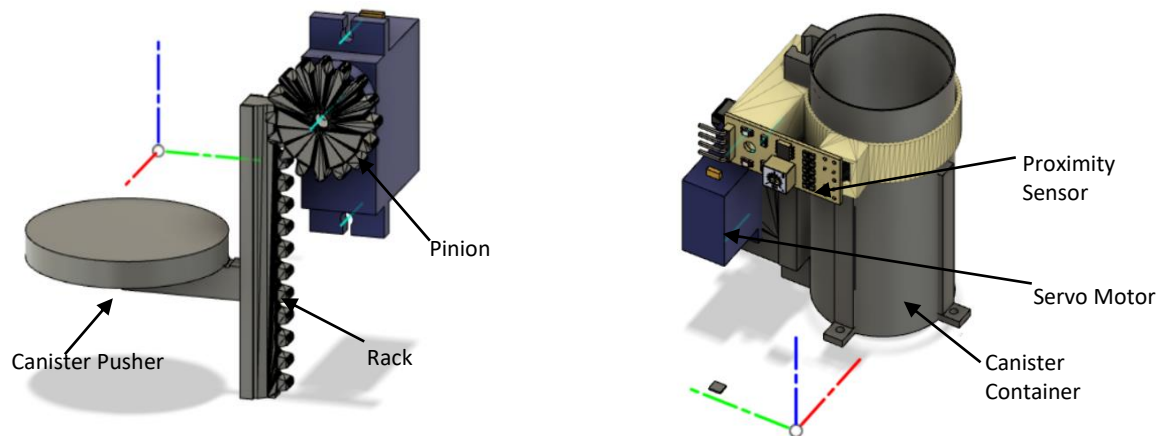


Figure 2.2: Expandable Canister Container Mechanism

The pill dispensing device consists of six expandable canister containers based on rack and pinion mechanism as shown in Figure 2.2, which controlled by servo motors. The each canister in a container can push upwards or downwards by controlling the rotation direction of the each servo motor. The proximity sensors were connected to each expandable canister container. Each proximity sensor was connected to the external hardware interrupt pin of a microcontroller therefore microcontroller detects each canister was inserted or extracted.

The LED was placed near to each canister for visually indicate the canister to be taken. Each LED was connected to the I/O expander to save the GPIO pins of the microcontroller. The I/O expander was connected to the microcontroller through the I2C communication protocol. The display was connected to the microcontroller through the UART protocol. The microcontroller displays all the necessary information and instructions to the patient through the display. The RTC module was used to keep the current date and time. Apart from keeping the time, RTC module generates an interrupt signal to the MCU (Micro Controller Unit) to initiate the dispensing process according to dispensing schedule.

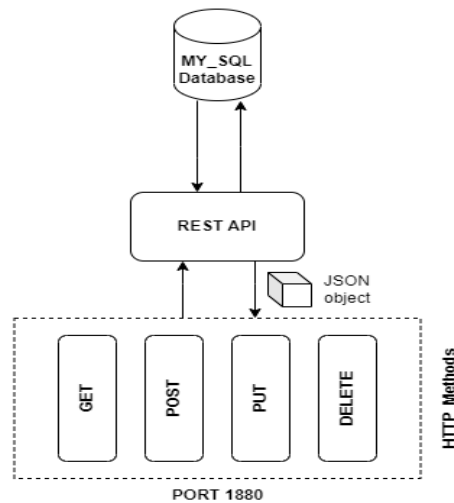


Figure 2.3: Cloud Server HTTP endpoint architecture

The Figure 2.3 shows the cloud server architecture which was implemented on the google cloud platform which has a public IP address. On the cloud server the Node-Red server and MySQL server was installed. The Node red server implements the backend control logic and provide HTTP endpoint on TCP port 1880 provide REST API for the clients to communicate with the backend.

The main steps of the smart pill dispenser firmware shown in the Figure 2.4. When device starts, first searches and connects to the Wi-Fi access point. Then it retrieves the schedule updates from cloud server and updates the EEPROM values. Then it retrieves the next dispensing time from the EEPROM and sets the alarm interrupt time on the RTC.

Then wait for the RTC interrupt and if the interrupt occurs the MCU initiates the medication dispensing process according to the EEPROM schedule. In the dispensing process MCU rotates the servo motors related to each canister to be dispense and turn on the related indicator LED and attaches the hardware interrupts to each proximity sensor to detect canister taken and insertion. Then waits some programmed time interval for patient to take the canisters.

After the time interval MCU updates the EEPROM values to the current state. After the medication dispensing process, MCU sends the medication dispensing status to the cloud server through the HTTP requests. Then repeats the process.

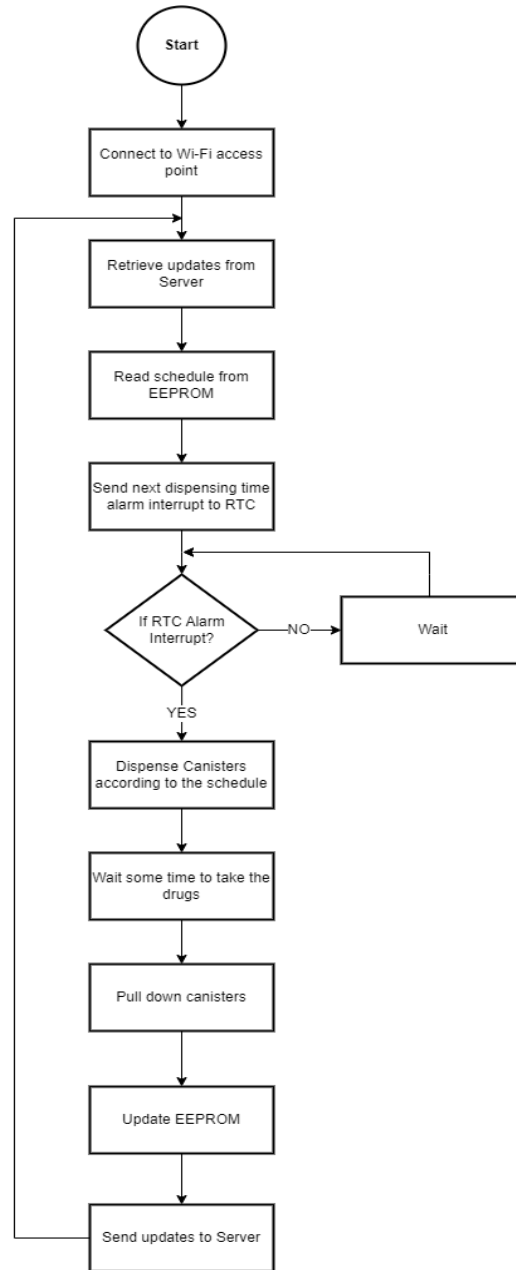


Figure 2.4: Flow Chart of the Main Process of the pill dispensing device

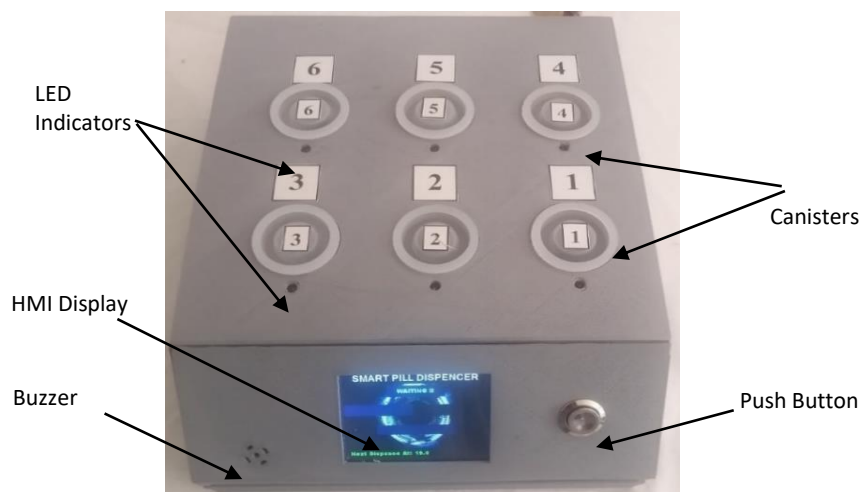


Figure 2.5: Smart Pill Dispenser Final Prototype

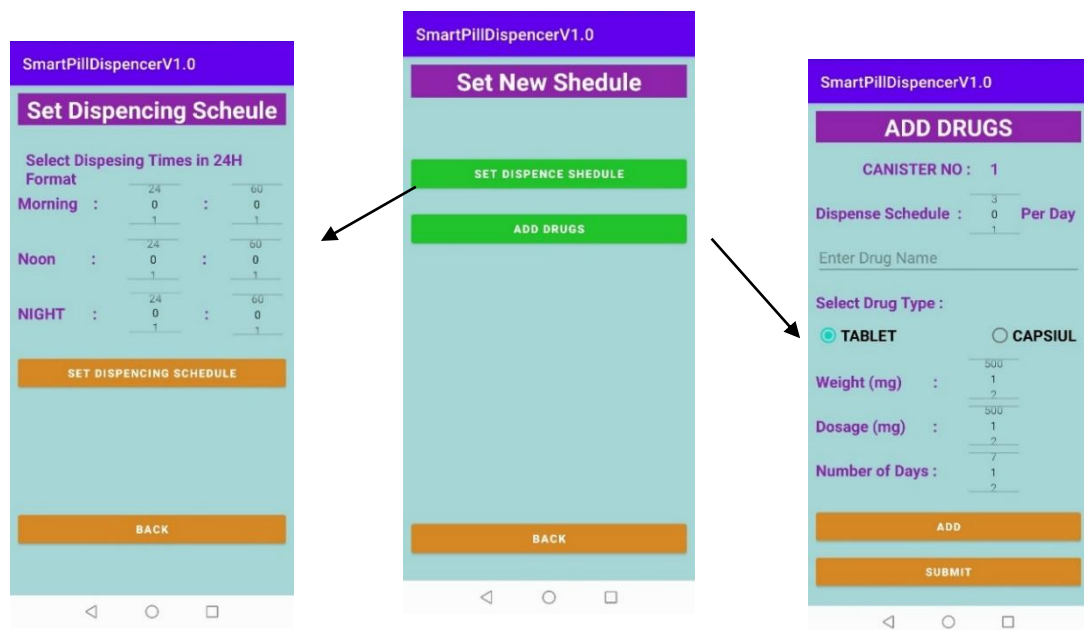


Figure 2.6: Mobile Application User Interfaces

### 3.0 RESULTS AND DISCUSSION

The hardware device prototype and mobile application were developed and tested multiple times without bugs. The schedule was added using the mobile application user interface and added schedule was correctly stored in the cloud server context database as shown in Figure 3.1.



Flow	
1/29/2023, 10:03:55 AM	
Q1H	"21"
Q1M	"11"
Q2H	"0"
Q2M	"0"
Q3H	"0"
Q3M	"0"
T0	"1"
T0_DName	"PARACETAMOL"
T0_DType	"true"
T0_MG	"500"
T0_ND	"7"
T0_NOPT	"1"
T1	"2"
T1_DName	"PIRITON"
T1_DType	"true"
T1_MG	"20"
T1_ND	"14"
T1_NOPT	"1"
T2	"3"
T2_DName	"CLOXIL"
T2_DType	"false"
T2_MG	"500"
T2_ND	"21"
T2_NOPT	"1"
T3	"2"
T3_DName	"CITAZINE "
T3_DType	"true"
T3_MG	"10"

Figure 3.1: Image of the Node-Red platform context database

The medication storing device correctly dispenses the medication according the added schedule as shown in Figure 3.2 and when patient has taken each canister, the dosage and the other important details were displayed on the HMI display.

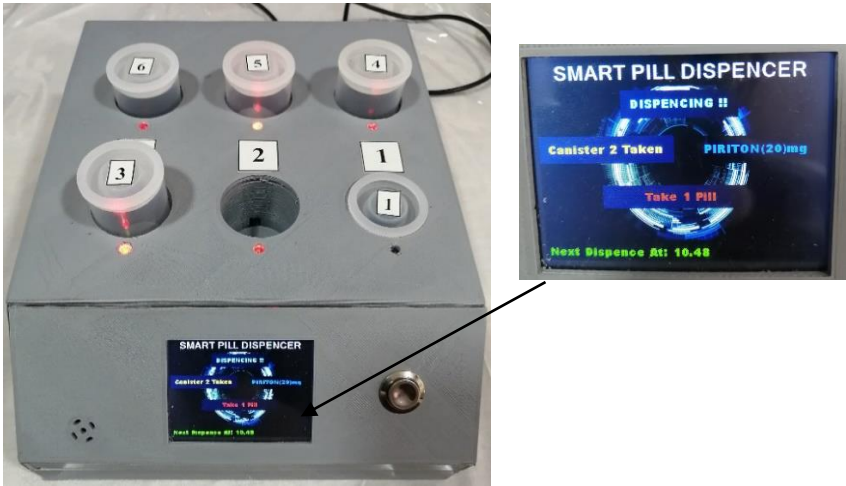


Figure 3.2: Image of the pill dispensing device after canisters taken.

Under the work carried out, some significance capabilities were identified which helps the patients to take the medications correctly according the schedule. There were few key points that should be overcome in the next level of development. One is the canister container locking

mechanism for prevent the patients to take wrong canisters mistakenly. The other main point is the use of audible instructions to assists the patients who are having visual diseases. The next point is the use of high quality gear wheels in the rack and pinion mechanism to decreases the jerks of the linear motion of the canisters.

#### **4.0 CONCLUSION**

The main objective of this work, is to develop a user friendly and portable system that reminding the medications according to the schedule and assists to take medications for the patients who requires special care. The prototype of the “Smart pill dispenser” system was designed and tested successfully, which ensure that the aged and the patients would take medicines on time as prescribed by the doctor. Hence the overall health of the society can be improved.

#### **ACKNOWLEDGMENTS**

Authors would like to express their gratitude to academic and non-academic staff of Department of Electronics, Faculty of Applied Sciences, and Wayamba University of Sri Lanka.

#### **REFERENCES**

- [1]. Nananda, C., Fanale, J.P.,Kronholm, P., The Role of Medication Non-Compliance and Adverse Drug Reactions in Hospitalizations of the Elderly, *Archives of Internal Medicine*, 1990, pp:841-845.
- [2]. Sokol, Michael C., Impact of Medication Adherence on Hospitalization Risk and Healthcare Cost. , *Medical Care*, vol. 43, no.6, 2005, pp: 521–530
- [3]. Jayavardhana R.B., Gubbi, Internet of Things (IOT): A vision, architectural elements, and future directions, *Science Direct*, 2013
- [4]. Hayes T.L., Hunt J.M., Adami A., Kaye J.A., An electronic pillbox for continuous monitoring of medication adherence, *Proc. The 28th IEEE EMBS annual international conference*, 2006
- [5]. Othman, Binti N., Ek O.P., Pill dispenser with alarm via smart phone notification, *Proc. IEEE 5th Global Conference on Consumer Electronics*, Kyoto, Japan, 2016, pp: 1-2

## ARDUINO BASED RECHARGEABLE BATTERY TESTER

Y.G Chandrasiri\*, K.K.C.S Kiriella

*Department of Electronics, Wayamba University of Sri Lanka, Kuliyaipitiya, Sri Lanka*

\*gayanchandrasiri12all@gmail.com

### ABSTRACT

This research project offers a viable solution to check the battery capacities of Tozed M60 and V10 hybrid routers. Tozed M60 and Tozed V10 respectively comprised of 2000 mAh and 1000mAh Li-ion battery packs. The proposed design is able to test the battery capacity, voltage, current and battery warning alerts when necessary with the help of an Arduino nano microcontroller and discharge the battery voltage through the load resistor which is switched by n-channel metal oxide semiconductor field effect transistor (MOSFET). A voltage divider method was used to check the voltage level of the battery pack through microcontroller unit (MCU). An Arduino code was developed to process the input data. As output methods, an organic light emitting diode (OLED) display and a buzzer were used to indicate the parameters and transmit warning alerts respectively. A prototype was developed and tested with sample batteries. Test results suggest that the realized system has good accuracy and high sensitivity. Moreover, this design can be considered a user friendly one because it does not require much technical knowledge to operate. but the Heat generation of the system is high so planned to implement a cooling system to work with different capacity batteries for future development.

**Keywords:** Battery tester, Hybrid routers, Li-ion battery packs

### 1.0 INTRODUCTION

Comparatively, hybrid routers have a higher demand than normal routers as it offers both telephone and internet router. Furthermore, the hybrid router has a battery backup (Portable device) which makes it more reliable. There are main two types of hybrid routers. Those are Tozed M60 and Tozed V10. Tozed M60 router is comprised of a 7.4 V and 2000 m Ah lithium-ion rechargeable battery and Tozed V10 has a 3.7 V and 1000 mAh rechargeable battery.

The capacities of the batteries reduce with time. Accordingly, backup time from the battery is also reduced. As a result, batteries need to be replaced from time to time. Normally, new batteries are replaced with faulty batteries. However, due to the high cost of rechargeable

batteries, medium-conditioned (used) batteries are used as replacements for faulty ones. So, there is a need to check the battery capacity of used batteries before they use. However, there is no proper method to measure battery capacity to identify the conditions of a battery. The rest of this paper discusses the characteristics of Li-ion batteries, a literature review of battery testers, methods used to obtain battery parameters, realized the system and obtained results.

## 2.0 EXPERIMENTAL

### 2.1 Literature review

#### 2.1.1 Lithium-ion battery

Typically, a lithium-ion cell consists of a separator, anode, and cathode submerged in the electrolyte solution. Lithium ions and electrons travel from the cathode to the anode during charging. The electrolyte acts as a conduit for the movement of ions. However, the electrons move through the external circuit using current collecting plates at both electrodes. The cell's primary functions during charge and discharge are to store electrochemical energy and release it. Below is a detailed explanation of each part of a lithium-ion cell, which is seen in figure 2.1 [1].

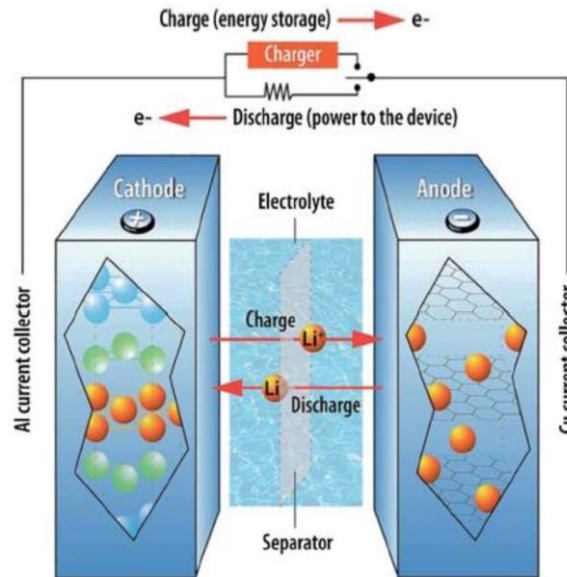


Figure 2.1 Internal structure of Li-ion Battery [1]

In the reduction process, a lithium ion is trapped in the interphase for each electrolyte molecule that reacts and breaks down. The battery's capacity decreases as more and more lithium becomes trapped. Because the lifetime of Li-ion batteries is limited to some time.

### 2.1.2 Lithium-ion Battery testing system (Umer khalid, Ali fasal Murtaza (2018))

This testing system's two main building parts are the control circuit board and GUI. The load is connected to the batteries using the relay section, which is subsequently utilized to detach the load from the batteries. When several batteries are being tested at once, a liquid crystal display (LCD) is utilized to indicate the overall number of passed batteries in a single try. MAX232 is used to link the control board to the personal computer (PC). The microcontroller sent the date to the GUI over a serial connection. Figure 2.2 shows a system of the block diagram [2].

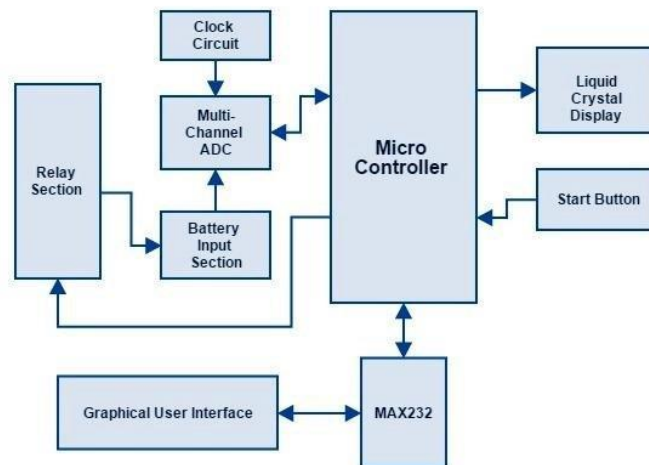


Figure 2.2 Block diagram of Lithium-ion Battery testing system [2]

This system is relatively complex as it uses different components for multi-channel ADC and clock circuits. This can be further developed using a newer version of the microcontroller which simulates the above components. Instead of LCD, it is proposed to use OLED panels to get more clear graphical output.

Figure 2.3 is shown in the block diagram of the developed testing system.

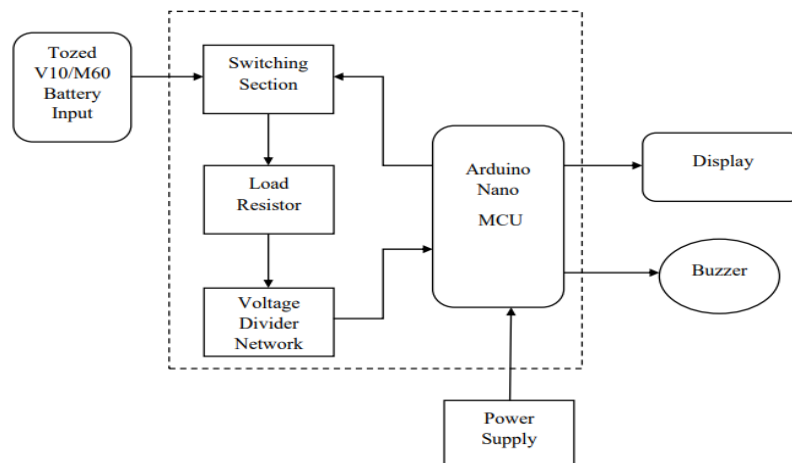


Figure.2.3 Block diagram of the design

There, input to the system is the Tozed V10/M60 rechargeable battery. System outputs are display and buzzer. The display indicates current, voltage and capacity while the buzzer indicates warning alerts. The system is processed by an Arduino nano MCU.

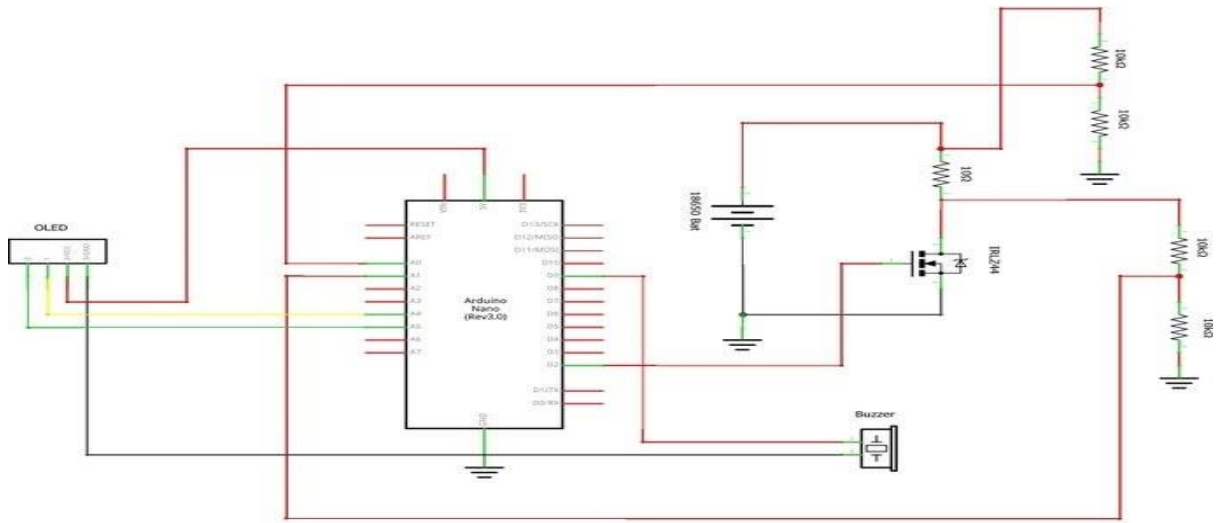


Figure 2.4 Schematic design of the project

Figure 2.4 shows the design is based on Arduino Nano. An OLED display is used to display the battery parameters. Three screw terminals are used for connecting the battery and the load resistance. A buzzer is used for giving different alerts. Two voltage dividers circuit is used to monitor the voltages across the load resistance. The function of the MOSFET is to connect or disconnect the load resistance with the battery.

Arduino checks the battery condition, if the battery is good, give the command to switch ON the MOSFET [3]. It allows current to pass from the positive terminal of the battery, through the resistor, and the MOSFET then completes the path back to the negative terminal. This discharges the battery over a period of time. Arduino measures the voltage across the load resistor and then divided by the resistance to find out the discharge current. Multiplied this by the time to obtain the milliamp-hour (capacity) value.

## 2.2 Voltage Measurement

The voltage across the load resistor must be determined so the voltages are measured by using two voltage divider circuits. It consists of two resistors with values of 10 kΩ each. The output from the divider is connected to Arduino analog pins.

Arduino analog pin can measure voltage up to 5 V but the highest voltage of the battery pack

is 7.4 V. (Fully charged). Therefore, a voltage divider circuit was used.

The sensitivity of the displayed battery voltage value, in terms of fractional points, was set using the developed Arduino code. The fractional point can be adjusted by editing the Arduino code, allowing for customization according to the size of the OLED display.

### 2.3 Current Measurement

Current (I) = (Voltage (V) - Voltage drop across the MOSFET) / Load Resistance (R) ----- (1)

Note: Assumed the voltage drop across the MOSFET is negligible.

Here, V = Voltage across the load resistor and R = 10  $\Omega$

The result obtained is in amperes. Multiply 1000 to convert it into milliamperes.

So maximum discharge current = 7.4 / 10 = 0.74 A = 740 mA

The sensitivity of the displayed discharge current value of the battery was determined by utilizing an Arduino-based system. The fractional point can be adjusted by modifying the developed code, which enables adapting the fractional points to the OLED display size.

### 2.3 Capacity Measurement

Stored Charge (Q) = Current (I) x Time (t) ----- (2)

The current (I) was calculated already therefore the only unknown in the above equation is time (t). The millis () function in Arduino can be used to measure the elapsed time [4].

Battery Capacity value sensitivity is also set by the Arduino coding environment and its sensitivity (value fractional points) depends on the size of the OLED display.

### 2.4 Selecting the Load Resistor

The selection of a load resistor depends on the amount of discharge current. So maximum discharge current is 2000 mA, then the resistor value is,

Resistance (R) = Max Battery Voltage / Discharge Current = 7.4 / 2 = 3.7  $\Omega$  ----- (3)

The resistor needs to dissipate a bit of power, so size does matter in this case.

Heat dissipated =  $I^2 \times R = 2^2 \times 3.7 = 14.8$  W

Therefore 5  $\Omega$ , 20 W load resistor was selected.

### 3.0 RESULTS AND DISCUSSION

#### 3.1 Results

The designed system has an OLED display, buzzer, and battery holder shown in figure 3.1. Users can easily connect the router battery to the battery holder. Then the designed system displays battery voltage, current and capacity in the OLED display as shown in figure 3.2. If the connected battery has low voltage, the OLED display shows the warning alert in figure 3.3. The buzzer also activates that movement. This system can be powered up by any DC voltage source having a 9-12 V range.

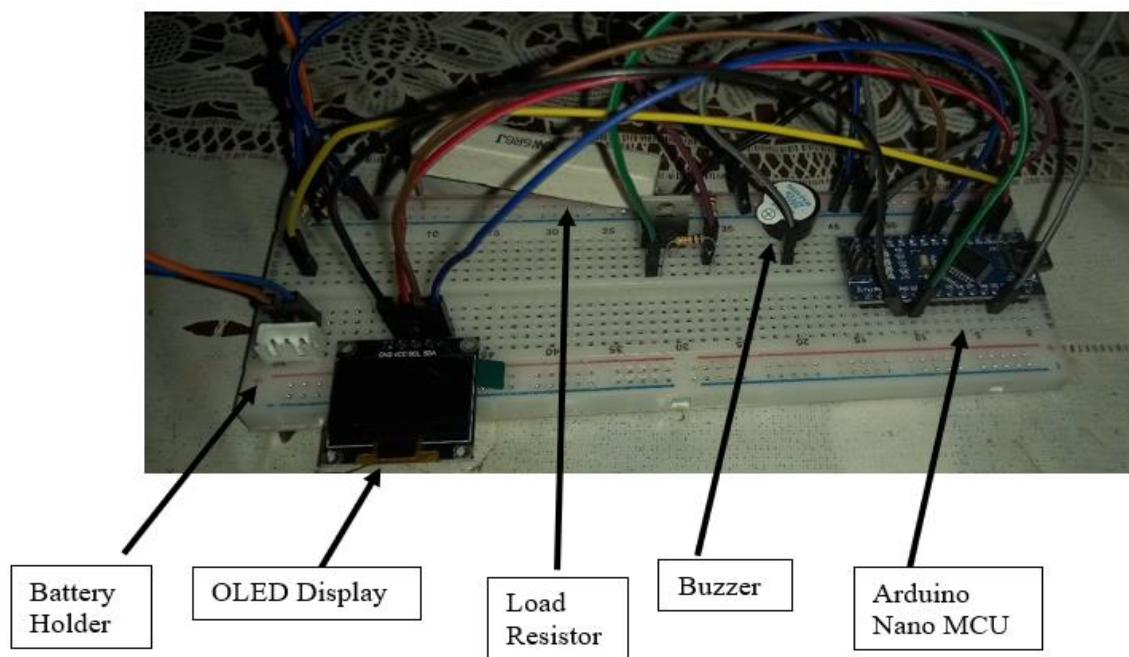


Figure 3.1 Picture of the entire circuit diagram

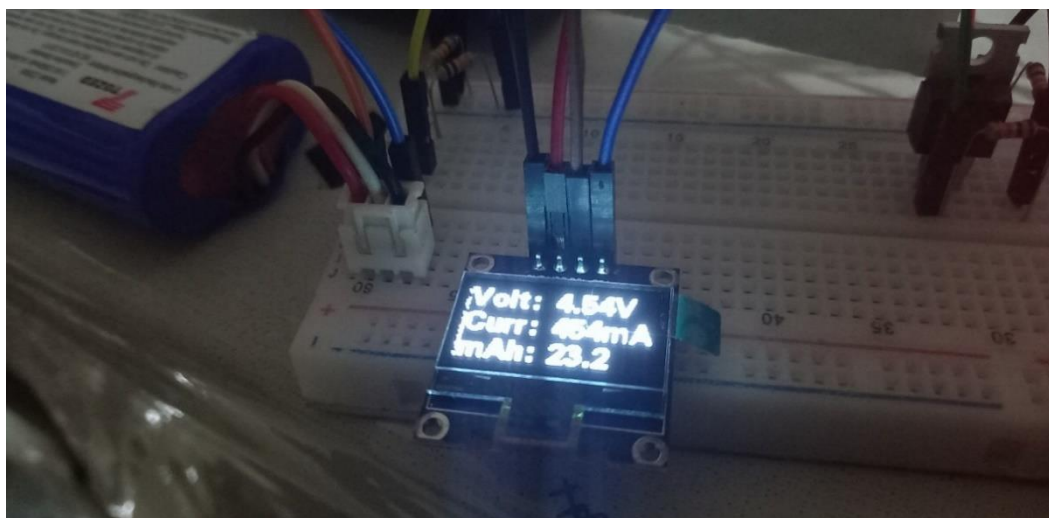


Figure 3.2 Picture of the displaying Battery Parameters



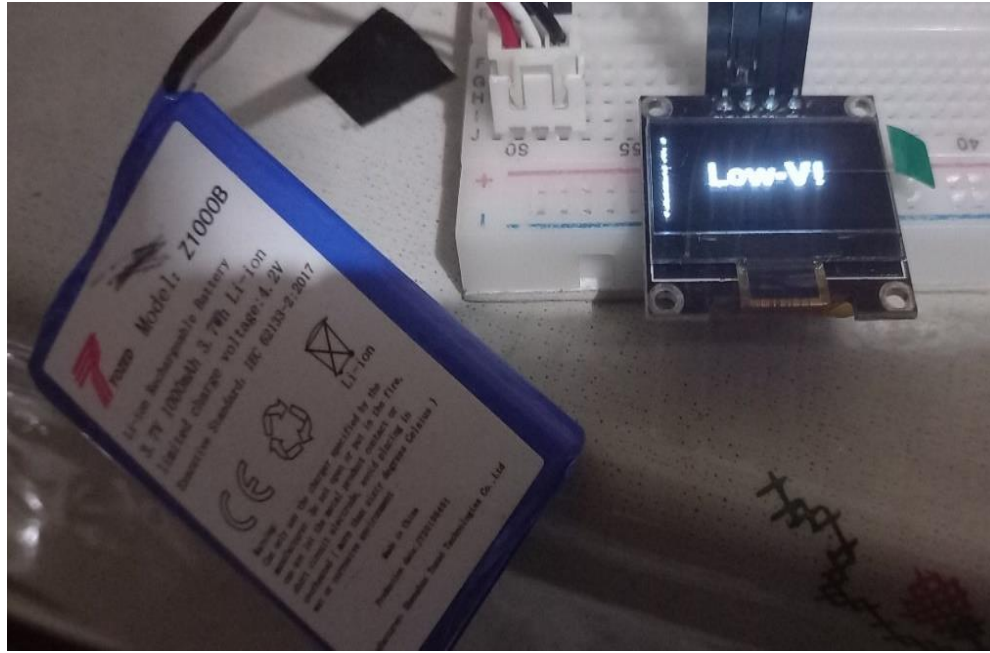


Figure 3.3 Picture of the displaying Battery Low voltage

### 3.2 Discussion

According to the results, the accuracy of the instrument is high, and it indicates the results to a voltage of 0.01 V, current of 1 mA and capacity of 0.1 mAh. Furthermore, the system is very user friendly and does not require any specific knowledge to operate.

On the other hand, there are some weaknesses identified through the testing and processing of the instrument such as the heat generation of the system being high as load resistor power is less than the required value. Moreover, Tozed M60 battery has a 2000 mAh capacity which takes much time to discharge. Therefore, the waiting time to get the capacity reading is high. However, it can be concluded that the instrument carries many strengths than weaknesses which makes it a viable solution.

## 4.0 CONCLUSION

This research project aimed to design and develop an Arduino based rechargeable battery tester to test the used Tozed M60 and V10 hybrid router batteries. This equipment can be used in Telecom LTE Unit where they troubleshoot the 4G routers. In the current system, the capacity level of the batteries is not displayed which confuses the customers with battery levels. By implementing a such system, battery capacity and discharge current and voltage can be displayed. In addition to that, dead batteries can be identified by checking the voltage levels of the batteries. To reduce the heat generated by the system, a cooling mechanism can be designed as a further improvement.

## ACKNOWLEDGEMENTS

The authors would like to express their appreciation to the staff of the Department of Electronics at the Faculty of Applied Sciences, Wayamba University of Sri Lanka, for their support in the successful completion of this project, both academic and non-academic.

## REFERENCES

- [1]. Chapman, B., How does a lithium-Ion battery work, *Let's talk science*, (2019), <https://letstalkscience.ca/educational-resources/stem-in-context/how-does-a-lithium-ion-battery-work>, (Accessed 2022.12.20)
- [2]. Khalid, U., Design of Low Cost Multi Channel Lithium ion Battery Testing System, *Researchgate*, (2016), [https://www.researchgate.net/publication/315696319\\_Design\\_of\\_Low\\_Cost\\_Multi\\_Channel\\_Lithium\\_ion\\_Battery\\_Testing\\_System](https://www.researchgate.net/publication/315696319_Design_of_Low_Cost_Multi_Channel_Lithium_ion_Battery_Testing_System), (Accessed 2022.12.2-3)
- [3]. IRLZ44N Power MOSFET: Pinout, Parametrics, Applications, *apogeeweb*, (2019), <https://www.apogeeweb.net/circuitry/irlz44n-power-mosfet-pinout-parametrics-applications.html>, (Accessed 2022.12.29)
- [4]. Tan, C., millis() function and Arduino, *Little Bird Electronics*, (2021), <https://littlebirdelectronics.com.au/guides/129/millis-function-and-arduino>, (Accessed 2022.12.19)

## IOT BASE REAL TIME VEHICLE TRACKING SYSTEM

S.H.D. Dananjani\*, M.A.A. Karunarathna

*Department of Electronics, Wayamba University of Sri Lanka, Kuliyaipitiya, Sri Lanka*

\*dananjani955@gmail.com

### ABSTRACT

Nowadays, security systems and navigators have always been a necessity of human life. The primary goal of the vehicle tracking system is to provide all vehicles with pre-programmed security. As a theft prevention and recovery tool, vehicle tracking systems are also widely used by people. This research describes the IoT-based vehicle tracking system. This system includes NODEMCU (ESP8266), GPS module, power supply, etc. The proposed system is used for positioning and navigating the vehicle with an accuracy of 10 m. The system tracks the location of a particular vehicle and sends it to the user's Web Page in form of data. The arrived data, in the form of latitude and longitude is used to locate the vehicle on Google maps and also the output can be seen on the android phone by using thingspeak.com. This project consists of a GPS receiver and an ESP8266 module. The tracking hardware's fitted onto the vehicle in such a manner that it is not visible to anyone who is inside or outside of the vehicle. Thus, it is used as a covert unit that continuously or by any interrupt to the system, sends the location data to the monitoring unit. On the other end (main vehicle station) the mobile phone is attached to the computer with thingspeak.com. So the GPS will send the longitudinal and altitude values corresponding to the position of the vehicle to Node MCU (ESP8266). When the device gets a Wi-Fi connection, the data send to the GPS module. After that, the data send to ESP8266 and which manages the data. It calculates the latitude and longitude and speed of the near vehicle. It also shows the location of the vehicle on the map. This research has two main aims. When the SLT vehicle is stolen, the location data from the tracking system can be used to find the location and can be informed to the police for further action. Then manage the SLT working and evaluation of driver's performance.

**Keywords:** IoT, Vehicle Tracking, ESP8266

### 1.0 INTRODUCTION

The new technology, popularly called Vehicle Tracking Systems created many wonders in the security of the vehicle. Vehicle Security is a primary concern for all vehicle owners. Both owners and researchers are constantly looking for new and improved vehicle security

technologies. With the modernization of technology, it is now possible to track and closely monitor the vehicle in real-time as well as to check the history of vehicle movements. One must be grateful for the Vehicle Tracking System, which has made a significant contribution to preserving the security of the vehicle by continuously monitoring its actions [06]. The system uses Global Positioning System [GPS], to find information about the location of the vehicle that is to be monitored and then send the latitude and longitude to the monitoring center through satellite. At the monitoring center, different software is used to display the vehicle on Google Maps. This is how our system tracks automobiles in real time. Due to real-time tracking facilities, vehicle tracking systems have become increasingly popular among owners of vehicles as they can monitor their vehicles continuously [01]. This research has two main aims. When the SLT vehicle is stolen, the location data from the tracking system can be used to find the location and can be informed to the police for further action. Then manage the SLT working and evaluation of driver's performance.

## 2.0 EXPERIMENTAL

GPS is a system that is used to track and monitor mobile objects using a set of satellites. It also shows the location of the vehicle on the map. There are two primary goals for this study. When the SLT vehicle is stolen, the tracking system's location data can be utilized to locate the vehicle and can be given to the authorities for follow-up action. After that, manage SLT operations and driver performance reviews [05].

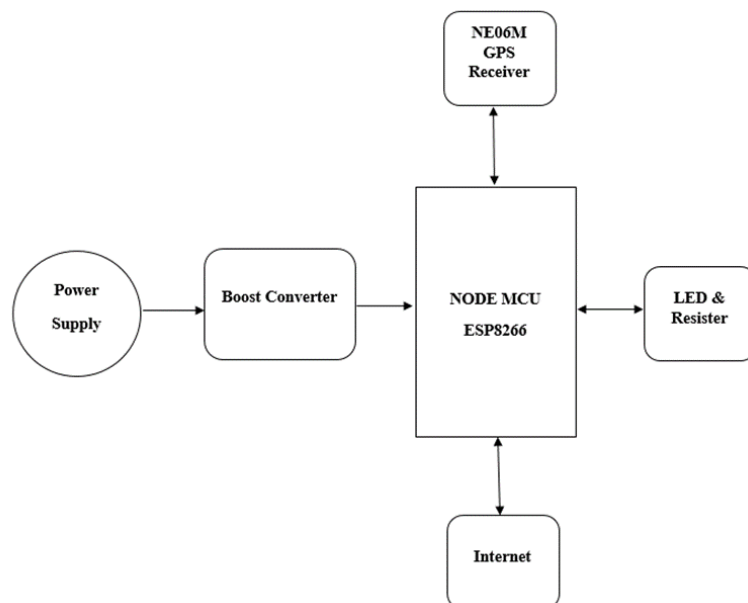


Figure 2.1: Block Diagram of Vehicle Tracking System

Figure 2.1 Block Diagram of the proposed Vehicle Tracking System which is used for tracking and positioning of SLT vehicles by using Global Positioning System (GPS) [03].

Table 2.1: Component description used to design a prototype of Vehicle Tracking System

Used Component List for Design Proposed Prototype	
Device	Description
ESP8266 NODEMCU	an embedded controller chip
NE06M GPS Receiver	Identifies locations anywhere in the world.
Boost Converter	Wide output voltage 5V~35V.
18650 Battery	Power Supply

In Figure2.2 shows the flowchart of vehicle tracking system given below.

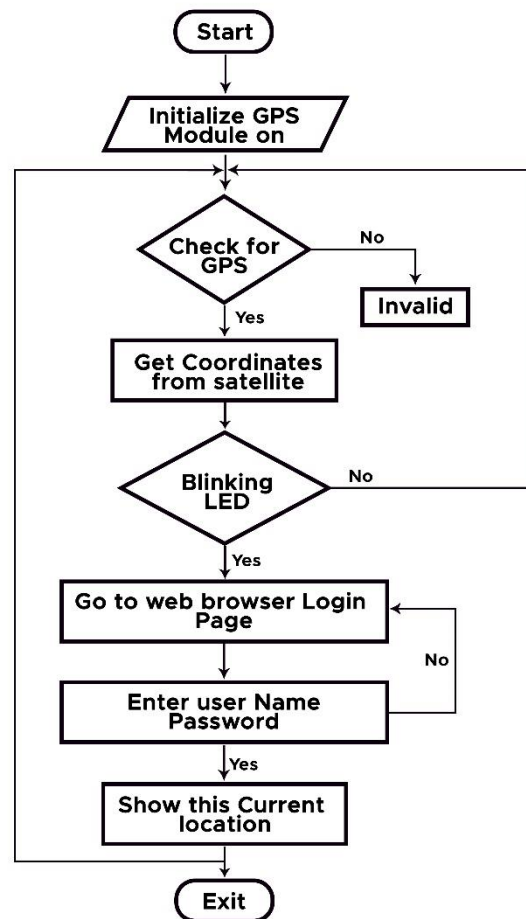


Figure 2.2: Flow Chart of Real-time Vehicle Tracking

Power is supplied when the system is started. The device gets a Wi-Fi connection, the data send to the GPS module. After that, the data send to Esp8266 and which manages the data. It

calculates the latitude and longitude of the near vehicle. It also shows the location of the vehicle on the map. At that time, Go to the web browser, enter the correct username and password then logging the web page. Then go to the page that can show the live location on the SLT vehicles.

Figure 2.3 shows the overall circuit diagram of the Vehicle Tracking System. This project consists of a GPS receiver and ESP8266 module.

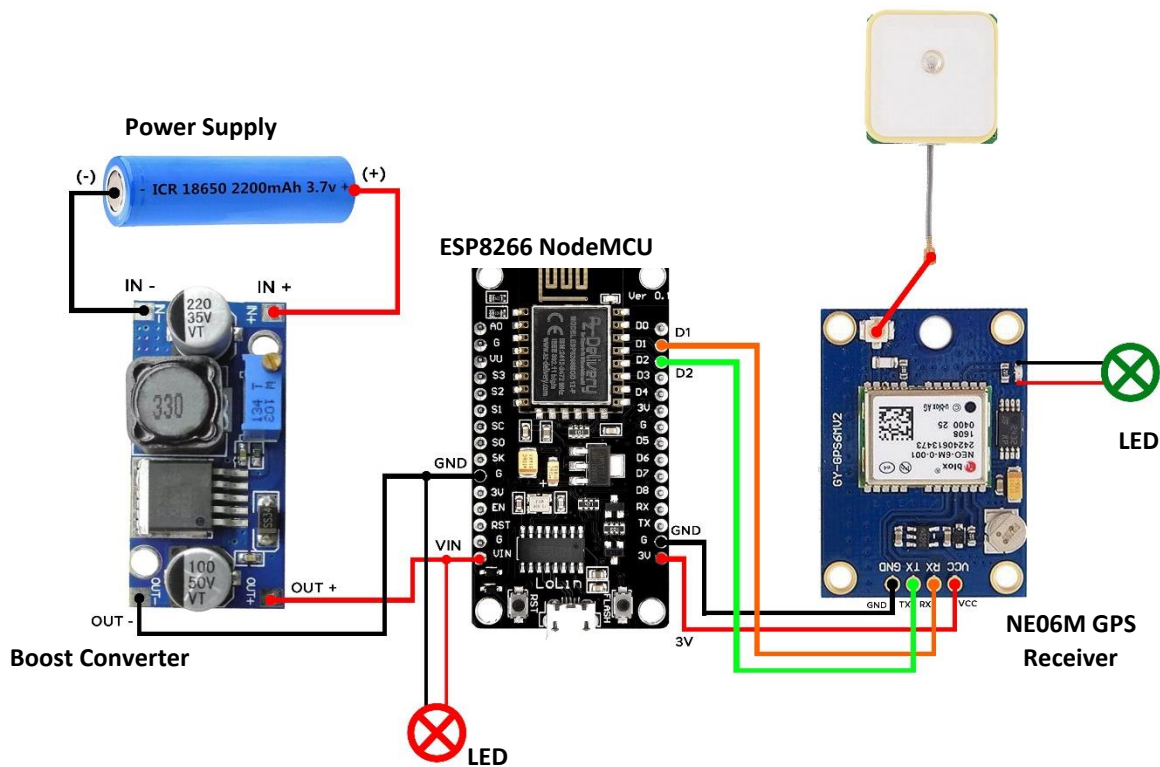


Figure 2.3: Circuit Diagram of the system

### 3.0 RESULTS AND DISCUSSION

The vehicle tracking device is configured with NODE MCU EPS8266, GPS module. The core part of a tracking system is ESP8266. The Google location of a vehicle can be captured through a GPS receiver and that data system will be transmitted by using GSM technology. For monitoring the location of the vehicle on the map, a web application has been developed. The device gets a Wi-Fi connection, the data send to the GPS module. After that, the data send to Esp8266 and which manages the data. It calculates the latitude and longitude of the near vehicle. It also shows the Real time location of the vehicle on the map.

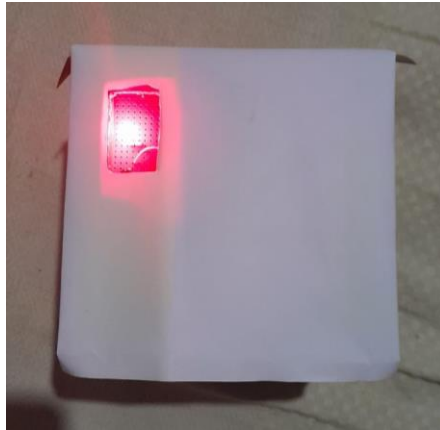


Figure 3.1: Vehicle Tracking System Front View

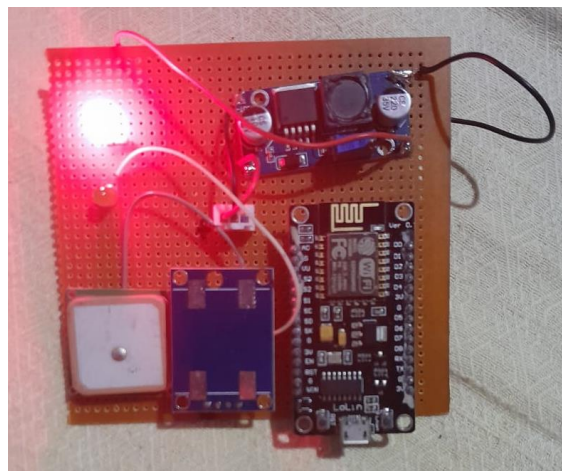


Figure 3.2: Inside View from Top

The application is programmed using PHP Language and the application developed User Interface is designed using HTML, CSS, and PHP. The application operates on a local server developed on XAMPP using MySQL.

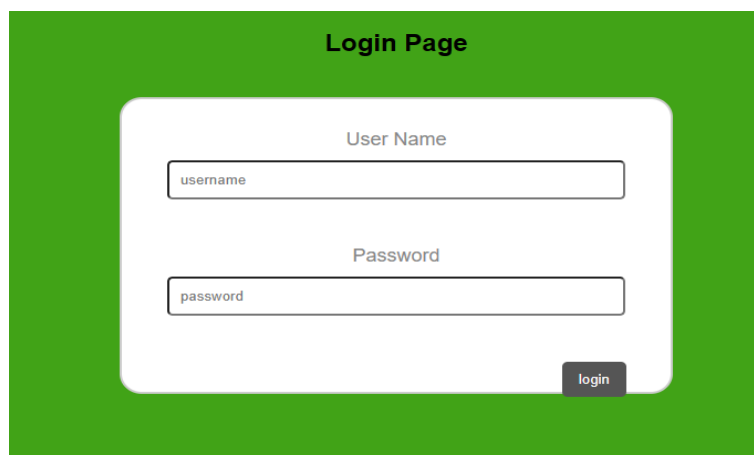
A screenshot of a web application's login page. The page has a solid green background. At the top center, the text "Login Page" is displayed in white. Below this, there is a white rectangular form with rounded corners. Inside the form, there are two input fields: the first is labeled "User Name" and contains the placeholder text "username"; the second is labeled "Password" and contains the placeholder text "password". At the bottom right of the form, there is a dark gray button with the word "login" in white text.

Figure 3.3: Login Page



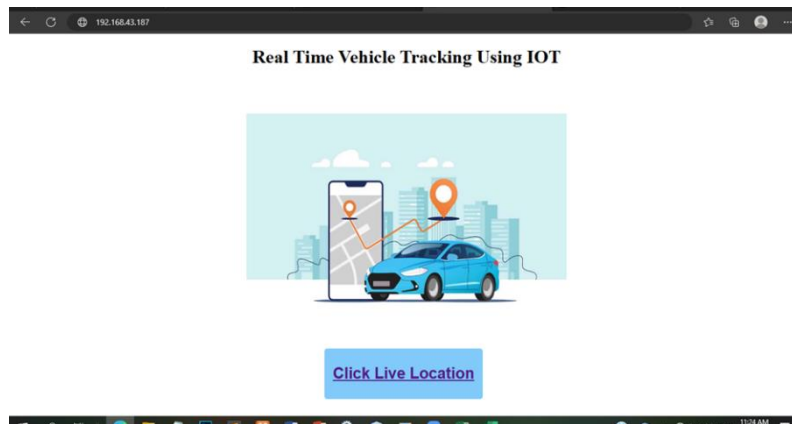


Figure 3.4: Web Browser Page

After connecting the hardware and uploading the code, just the device gets a Wi-Fi connection, the data send to the GPS module. After that, the data send to Esp8266 and which manages the data. It calculates the latitude and longitude of the near vehicle. It also shows the location of the vehicle on the map.

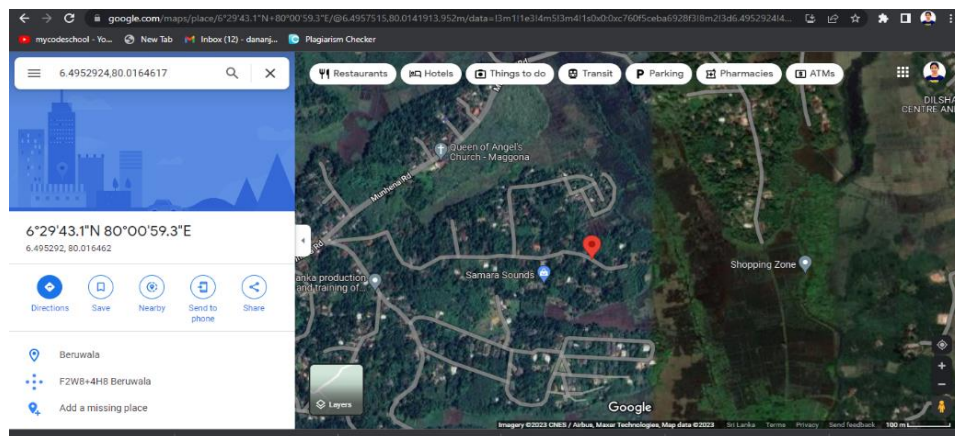


Figure 3.5: Open the Google Map Current Location

At the same time, Thing Speak will also log the Latitude and Longitude of the vehicle and present them in the graphs as shown above in Figure 3.6 and Figure 3.7.



Figure 3.6: The Latitude Graphs of using Thing Speak



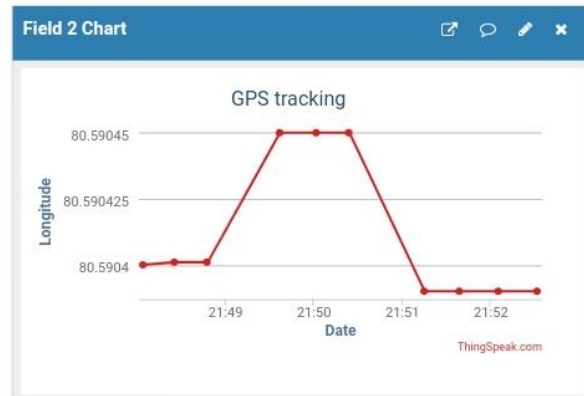


Figure 3.7: The Longitude Graphs of using ThingSpeak

#### 4.0 CONCLUSION

In this research, a vehicle tracking system has been developed that is flexible, customizable, and accurate. This tracking system can monitor the vehicle's location via mobile and online on Google Maps. To display the position on Google Maps, Google Map API has been used on the map. It is useful for managing the SLT working and evaluating the driver's performance. GPS tracking device to monitor the real-time location of the vehicle from anywhere. Here Thing Speak IoT cloud will be used to store the history of locations from where the vehicle has traversed. Interfaced with GPS with Node MCU ESP8266 and displayed the location coordinates on a webpage. Here this IoT Vehicle Tracking System will also display a link on the webpage which will take the user to Google Maps showing the vehicle's location. Then we can get information about where the SLT Vehicles and it also shows the location of the vehicle. The majority of users of vehicle tracking systems are commercial fleet operators. These systems are created for operational tasks like routing, security, dispatching, and gathering onboard data. These are also used for fire detector in large vehicles like the train, bus, etc. because vehicle like train contains a large number of people, and sending an alert about a fire accident can save many lives. The applications for this project are in the military, navigation, automobiles, aircraft, fleet management, remote monitoring, remote control, security systems, etc.

#### ACKNOWLEDGEMENTS

Authors would like to thank all the staff of Department of Electronics, Faculty of Applied Sciences, Wayamba University of Sri Lanka, and others who have supported to make this research a success.

## REFERENCES

- [01] IOT BASED VEHICLE TRACKING SYSTEM USING NODEMCU AND ARDUINO IDE,  
<https://iotdesignpro.com/projects/iot-based-vehicle-tracking-system-using-nodemcu-and-arduino-ide>  
(Accessed 2023-01-05)
- [02] Google map vehicle tracking system using GPS & GSM modem  
<https://www.projects8051.com/vehicle-tracking-system-using-gps-and-gsm-modem/>, (Accessed 2023-01-05)
- [03] Track a vehicle on Google maps using Arduino, ESP32 & GPS  
<https://circuitdigest.com/microcontroller-projects/arduino-vehicle-tracker-on-google-maps-using-esp8266> (Accessed 2023-01-10)
- [04] Getting Started with ESP32 | Introduction to ESP32, <https://www.electronicshub.org/getting-started-with-esp32/> , (Accessed 2023-01-10)
- [05] Design and Implementation of IOT Based Vehicle Tracking System,  
[https://www.academia.edu/42909622/Design\\_and\\_Implementation\\_of\\_IOT\\_Based\\_Vehicle\\_Tracking\\_System](https://www.academia.edu/42909622/Design_and_Implementation_of_IOT_Based_Vehicle_Tracking_System), (Accessed 2023-01-10)
- [06] IoT-BASED VEHICLE TRACKING SYSTEM FOR KHULNA UNIVERSITY  
[https://www.researchgate.net/publication/365876505\\_IoT\\_BASED\\_VEHICLE\\_TRACKING\\_SYSTEM\\_FOR\\_KHULNA\\_UNIVERSITY](https://www.researchgate.net/publication/365876505_IoT_BASED_VEHICLE_TRACKING_SYSTEM_FOR_KHULNA_UNIVERSITY), (Accessed 2023-01-10)
- [07] ESP8266 and Arduino Based IoT Vehicle Tracking System ,  
<https://www.engineersgarage.com/esp8266-and-arduino-based-iot-vehicle-tracking-system/>,  
(Accessed 2023-01-12)
- [08] Internet of Things-based Vehicle Tracking and Monitoring System ,  
<https://ieeexplore.ieee.org/document/9683883>, (Accessed 2023-01-12)

## QUALITY CHECKING AND DATA ANALYZING HARDWARE SYSTEM WITH IOT FOR APPAREL INDUSTRY

K.P. Gunaratne\*, Y.A.A. Kumarayapa

*Department of Electronics, Wayamba University of Sri Lanka, Kuliyaipitiya, Sri Lanka*

\*kalanagune96@gmail.com

### ABSTRACT

Quality control in the garment industry and apparel is a crucial factor that helps to maintain consistency and quality and ensure that all garments meet a specific set of standards and specifications. But currently, quality checking, recording data and analyzing those data are being done manually [1]. It usually takes a long period of time to address the root cause of the defects. In order to give a solution to this problem, IoT based automated quality checking and data analyzing system was proposed and implemented for the production line. Thus, it can be used to be mark the quality of each garment that was passed through the quality section. The quality information was recorded in the database and current and hourly defect rates for the production were calculated. Then, using navel web applet, the end results were visualized with analyzed graphs. Hence, using proposed and constructed equipment, the defect rate of the production process per operator can be reduced by identifying the rate of decline in the quality of the product due to the error of the machine or the error of the operator. Then, by considering an error prone case, by taking timely remedy to the root cause of the error, it was possible to decrees the defect rate up to 51.03%.

**Keywords:** IoT based automation, Appeal Industry, Quality checking

### 1.0 INTRODUCTION

Sri Lankan textile and apparel industry have gained a strong reputation worldwide for ethical manufacturing of high-quality apparels. In the apparel industry, quality control of produced garments is a crucial factor that helps to maintain consistency, and quality. Also, those procedures help to ensure that all the garments meet a specific set of standards and specifications [2].

Rather than checking at after production stage, inspection during production is crucial for ensuring that garments are produced to meet customer expectations and specifications. According to available literature, about 20% of defects occur during the production.

Mainly two factors effect on the rejection of a garment at quality inspection level. They are;

- Team member (Operator) Mistakes
- Machine malfunctioning

Currently, there is a system of manually recording the number of defects of each team member, but due to the change in the size of the input panel received by the team member, it is not possible to get an idea about team member's efficiency.

The best way to measure the efficiency of a team member is to calculate the defect rate. But it is difficult to calculate defect rates in real-time using manual method. It takes a long time to address the root cause of the defects, most probably at the following day. Hence, the management could not be able to get quick decisions by analyzing real time data. Therefore, there was a huge waste of resources, time and money.

In order to address this problem, design and construction of an IoT based system for automatically quality checking and data analyzing system for apparel industry production line is discussed in this study.

## 2.2 EXPERIMENTAL

### 2.3 Usual Quality Checking (QC) process in production line

The last part of the production line is quality checking. Garments that are rejected by this process test are known as rejected.

For explaining the overall process, with reference to following Figure 2.1, we use the abbreviation TM, where TM - team member.

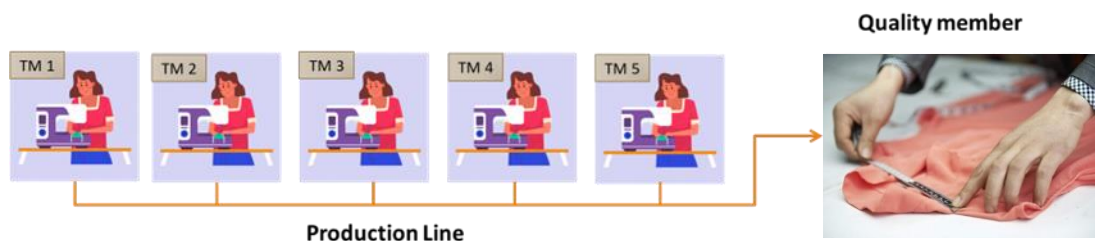


Figure 2.1: Usual Formal quality checking process in apparel production line

### 2.4 Selected operation: Collar Linking process

Collar linking operation was chosen for the proposed study.

Linking Machine allows to quickly and easily link together the seams of knitted garments such as sleeves, body, collars, and bands. Collar linking is a very stern task prone to errors and

defects which should be done with proper training and attention. Hence, its defect rate is also very high. Therefore, there is a strong need to reduce the defect rate for this particular operation.



Figure 2.2: The focused collar linking process

## 2.5 System design and functionality for the selected malfunction process

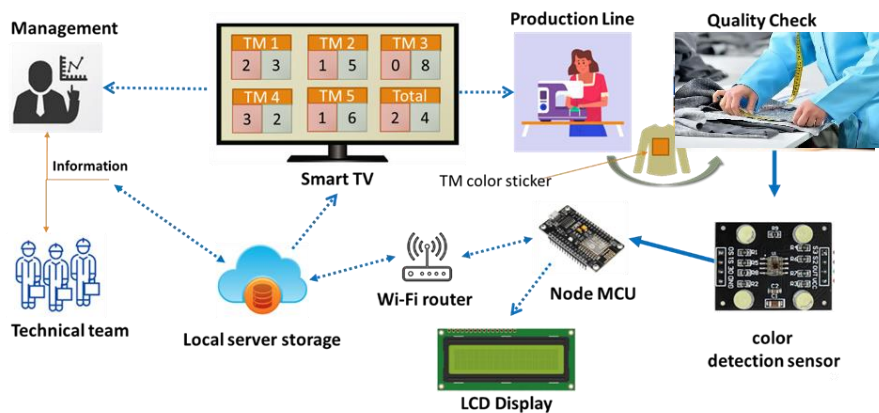


Figure 2.3: System design data flow diagram for the proposed QC technology

The overall process illustrated in figure 2.3 which can be given in the following steps

1. After linking, a colored sticker tag which is unique to identify the operator of the team with a unique color for each team member were pasted on the garment. (Team members were slicked a color tag that color identical to each team member).
2. The stitched garment was sent for quality inspection along with the tag.
3. ESP 8266 Node MCU was used to detect the team member who sent the garment by detecting the color of the tag using the designed and constructed color sensing module.
4. After inspection, the quality checking officer can mark whether it was accepted or rejected by simply pressing the accept button or reject button.
5. LCD display was used to indicate the team member's ID number and whether it is accepted or rejected.
6. ESP 8266 Node MCU was updated the reject/accept garment count of relevant team member then the result was stored in local server SQL database.
7. Smart TV / Desktop computer could be used to view rejected/accepted garment counts

and defect rates via web interface.

8. Then the stored data can be further analyzed for making final decisions.

## 2.6 Defect rate for the focused process

Defect rate is a measurement of how many units of production are defective, or unusable, out of a specific number of units. Defect rate use as the. In this study defect rate use as a measurement to determine product quality for production line. Defect rate calculate as follows.

$$\text{defect rate} = \frac{\text{No.of defects}}{\text{No.of outputs tested}} \times 100 \% \text{ ----- (1)}$$

## 3.0 RESULTS AND DISCUSSION

### 3.1 Collected data from the system

Total accept and reject count, defect rates for each operator and mean defect rate and production were obtained using main dashboard.



Figure 3.1. The GUI of Main dashboard of system

Hourly defect rates were calculated and displayed for each team member in Hourly defect rate dashboard. then team member's defect rates were compared using the chart. The fluctuation in defect rates of each team member was shown in the graph. (Figure 3.2)

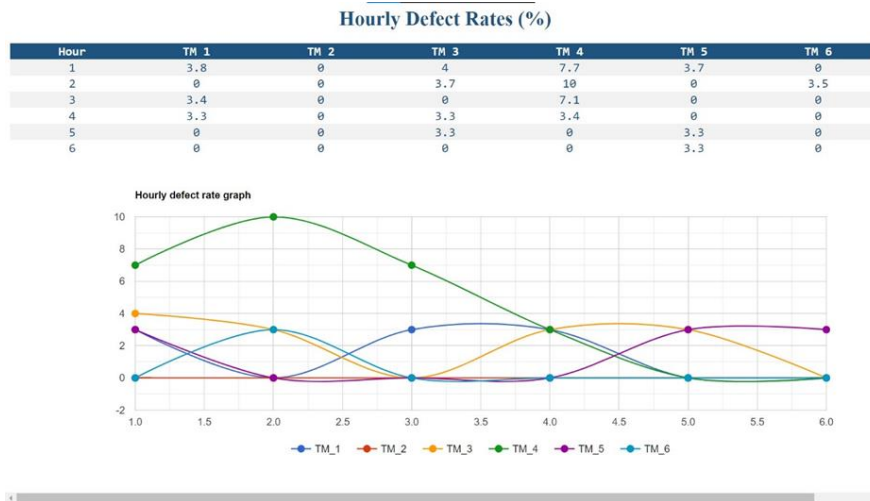


Figure 3.2. The calculated hourly defect rate and corresponding graph for each team member

Hourly productions were calculated and displayed for each team member in Hourly production dashboard. Each team member's production was compared using the chart. The fluctuation in production of each team member was shown using the graph (Figure 3.3).

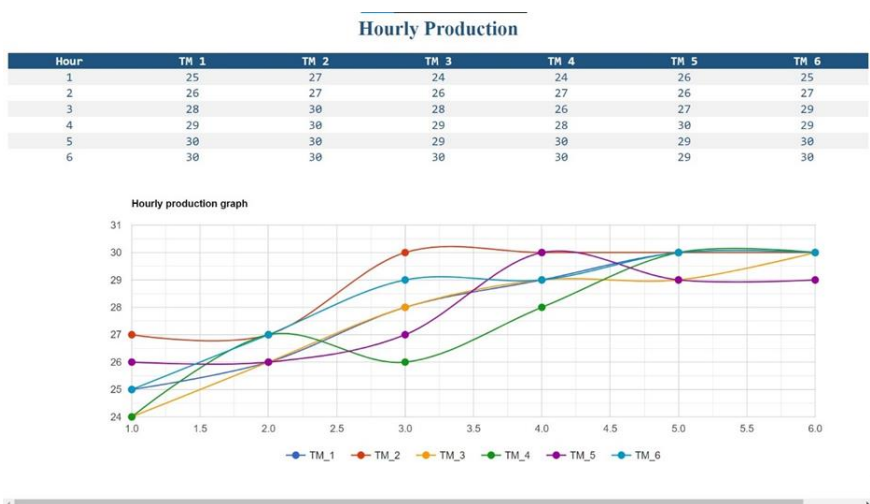


Figure 3.3. Hourly production and graph for each team member

### 3.2 Identify quality degradation

Following graph (Figure 3.4) shows that hourly defect rates of the first four hours of the day. A significant increase in the defect rate of the team member 4 was observed the first hour. It was also automatically indicated in red color on the main dashboard.

But considering the variation in quantity of accepted items produced, no significant variation was shown during the first hour for team member number 4. Quality degradation could quickly be identified by focusing on the defect rate rather than the number of accepted items.



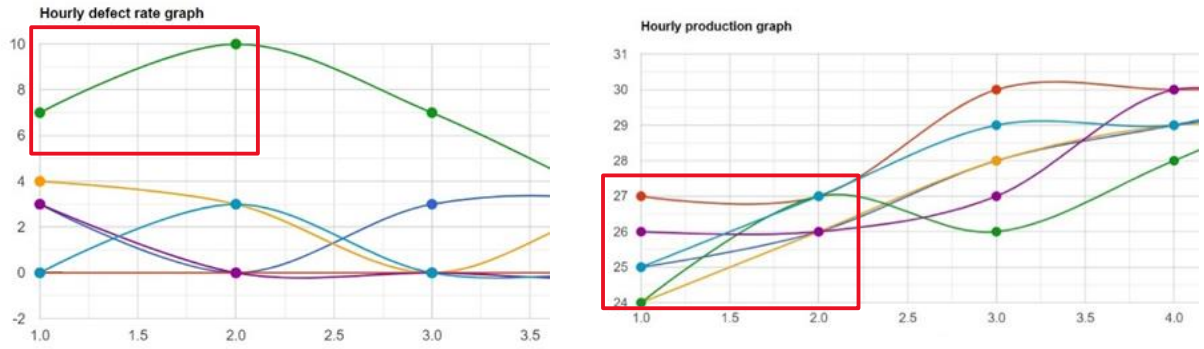


Figure 3.4. Variation of defect rate and production rate for team member 4

### 3.3 Reduce quality degradation

After identifying the quality degradation, the reason for it was investigated. In this case study it was caused by a very minor technical fault in the machine. After fixing that fault, the defect rate returned to normal.

Following graph (Figure 3.5) shows that team member number 4's defect rate after the identifying and solving of quality degradation by using the quality checking system (QCS) against projected defect rate without identifying quality degradation (without QCS).

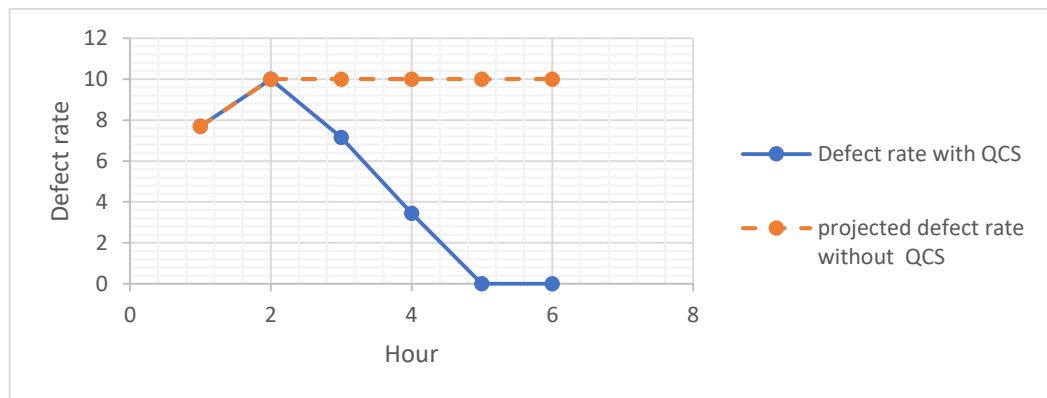


Figure 3.5. Member 4 defect rate with QCS against projected defect rate without QCS

Assume,

D1 = Mean defect rate after the identified quality degradation (with QCS)

D2 = Mean defect rate without identified quality degradation (without QCS)

By considering the data stored in database during the first 6 hours,

D1 = 4.71

D2 = 9.62

$$\begin{aligned} \text{Estimated percentage reduction in defect rate due to use of QCS} &= \frac{D2 - D1}{D1} \times 100 \% \\ &= 51.03 \% \end{aligned}$$



### 3.4 The observation increases of the production.

An increase in production was observed along with the decrease in defect rate of the team member number 4. Estimated production was calculated if QCS was not used (Table 3.1). Following graph (Figure 3.6) shows that team member 4's production after the identify and solve of quality degradation by using the quality checking system (QCS) against projected production without identify quality degradation (without QCS).

Table 3.1. Team member 4 production with QCS and projected production without QCS

Hour	Total Production (Accept + Reject)	Defect rate with QCS (%)	Production with QCS	Projected defect rate without QCS (%)	Estimated production without QCS
1	26	7.69	24	7.69	23
2	30	10	27	10	27
3	28	7.14	26	10	25
4	29	3.45	28	10	26
5	30	0	30	10	27
6	30	0	30	10	27
<b>Mean</b>	<b>29</b>	<b>4.71</b>	<b>27.5</b>	<b>9.62</b>	<b>26</b>

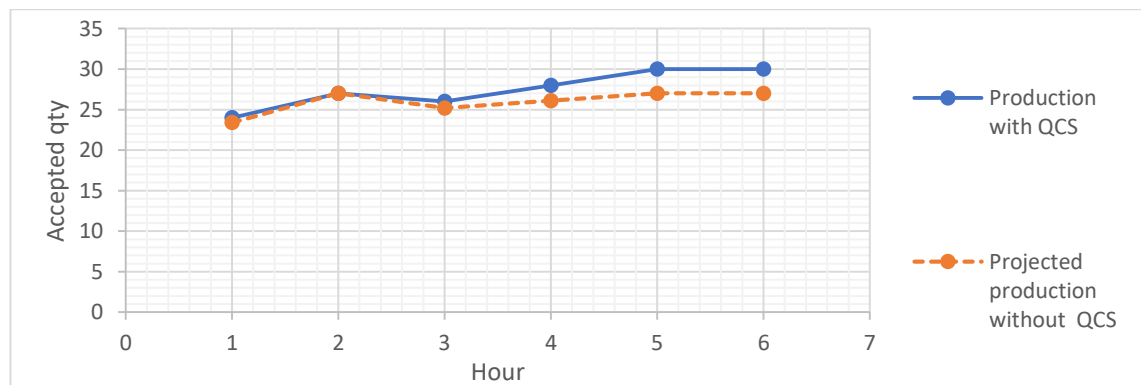


Figure 3.6. Member 4 production with QCS against estimated production without QCS

We have done following calculations in order to evaluate the increase in production.

Assume,

P1 = Production rate after the identifying quality degradation

P2 = Estimated production without identified quality degradation

$$\begin{aligned}\text{Estimated percentage increment in production due to use of QCS} &= \frac{P_1 - P_2}{P_2} \times 100 \% \\ &= 6.4 \%\end{aligned}$$

#### 4.0 CONCLUSION

Decisions were made based on defect rate rather than number of accepted productions is more effective. Hence, it can be used to detect quality degradation quickly rather than inspection of production rate. To increase the quantity of production, the speed of the team member as well as the reduction of the defect rate were mainly influence. An increase in the production rate of team members over the initial situation was observed as they continued to engage in the same operational task. Therefore, the increase in production speed can be used effectively by reducing the defect rate.

The defect rate of the concerned member was reduced by about 50% and the production rate was increased approximately 6%, by on time solving the defect related root course by using quality degradation indications of this device.

It was concluded that IoT based automated quality checking and data analyzing system can be used for apparel industry to enhance the quality control process.

#### ACKNOWLEDGEMENTS

Authors would like to thank all staff of the Department of Electronics of Wayamba University of Sri Lanka and to the all the staff in MAS Fabrics Matrix, Thulhiriya.

#### REFERENCES

1. Industry 4.0, Disruptive Technology & MAS Matrix: An Example For Way Forward In Sri Lanka, <https://www.colombotelegraph.com/index.php/industry-4-0-disruptive-technology-mas-matrix-an-example-for-way-forward-in-sri-lanka/>, (Accessed date: 18/12/2023 )
2. Why sri lankan apparel? <https://www.srilankabusiness.com/apparel/why-sri-lankan-apparel.html>, (Accessed date: 18/ 12 /2023)
3. All About Garment Quality Assurance & Quality Control, <https://techpacker.com/blog/manufacturing/all-about-quality-assurance-control/>, (Accessed date: 20/11/2023 )
4. Sihombing, P., Tommy, F., Sembiring, S., Silitonga, N., The citrus fruit sorting device automatically based on color method by using tcs320 color sensor and arduino uno microcontroller, *Journal of Physics*, Vol. 1235, No. 1, (2019), p. 012064

## SMART MONKEY REPELLENT SYSTEM FOR TELECOM WIRES

L.S.K. Gunasinghe<sup>1\*</sup>, J.M.J.W. Jayasinghe<sup>2</sup>, K.G. Welagedara<sup>3</sup>

<sup>1,2</sup>*Department of Electronics, Wayamba University of Sri Lanka, Kuliyaipitiya, Sri Lanka*

<sup>3</sup>*Sri Lanka Telecom PLC, Kandy, Sri Lanka*

\*lakshigunasinghe96@gmail.com

### ABSTRACT

Monkeys and other animals in telephone wires are becoming a serious problem in the telecommunication industry. The main objective of this research work is to develop a prototype of a variable frequency ultrasonic monkey repellent. Establishing a low input voltage and upholding a desired operating distance range has been listed along with retentive an effective range of random frequency operating on a wide bandwidth region. This work was simulated with PROTEUS software and built a prototype to study and ensure its operating characteristics. This device is more humane and sanitary to use near homes as they do not involve traps and poisons. Also, the varying ultrasonic frequencies emitted are inaudible to man.

**Keywords:** Monkey repellent, Frequency band, Ultrasonic Transmitting

### 1.0 INTRODUCTION

A telephone line or telephone circuit (or just a line or circuit within the industry) is a single-user circuit on a telecommunication system. This is the physical wire or other gesturing medium connecting the user's telephone devices to the telecommunications network, and usually also infers a single telephone number for billing purposes reserved for that user. Telephone outlines are used to bring wired telephone service and Digital Subscriber Line (DSL) phone cable service to the premises [1]. Telephone lines are exchanged to the public connected switch network. Usually, those wires are between a few hundred meters to a few kilometers. Those wires are connected in the central office to the telephone center/exchange. Normally, there is only the 48 V DC voltage from the central office battery in the line, and when the phone ring there is 70-130 V AC voltage in the line [2]. Normally the ring voltage can be 110 V AC. A telephone wire generally operates at 200-3400 Hz frequency [2]. Two

different types of wires are used in Sri Lanka to operate the Asymmetric Digital Subscriber Line (ADSL) function; namely, copper wires and Fiber optic cables.

Telephone wires are more advanced and cost highly. Therefore, damaging the wires cause not only costs but also highly affects the continuous flow of ADSL and internet connections of the end user. Since, the world becoming a global village, internet and mobile connections are highly important in their day-to-day activities. SLT – Kandy OPMC has identified a few major issues for the disconnection of ADSL and FTTH. Monkey bites or damaged cables by a monkey is one of the most common incidents reported in the 2018-2022 period. SLT – Kandy OPMC has identified a few major issues for the disconnection of ADSL and FTTH. Monkey bites or damaged cables by monkeys are one of the most common incidents reported in the 2018-2022 period.

This paper focuses on improving the features of the ultrasonic animal deterrent device to make it more efficient and consistent for current human needs. A random operating frequency is established to ensure that particular types of animals don't get used to a constant frequency. And the use of repeaters has been highlighted to increase the operating distance range and cover a vast area.

## **2.0 EXPERIMENTAL**

### **2.1 Related Work**

Scientists and engineers have come up with different solutions for animal deterrent methods and devices. AI-based animal repelling method was developed by [9]. By using a panel of cameras, it detects the animal using image processing. The study was conducted in a harvesting field. A similar method was used in for crop protection [10]. The AI-based approach is used to identify the animal.

Jhon D. introduce a method to repulse animals using laser beams [11]. Also, a method introduces a repulsive voice. Some bugs were identified in that system such as the frequency was not defined by the authors for the defined animals. Therefore, all animals can affect this system. In India, researchers found that monkeys bite wires due to their taste. Therefore, as a solution, they have made a wire with non-tasting coating wire [12].

## 2.2 Common Methodology

Ultrasound has been used as a deterrent technique for huge range of animals like monkeys, stray dogs, rodent, birds etc. due to its remarkable features while maintaining cost. The device activates on a frequency band of 10 kHz – 100 kHz. The sound is not pleasant but the volume is well under any level of intensity (loudness, decibels) that would cause injury, whether or not it is “heard.” It makes animals leave by making the space uncomfortable, not dangerous [3]. Table 2.1 defines the hearing range of different species of animals on the basis of their operating frequency range. Therefore, emitting a frequency closest to the given bands makes corresponding animals uncomfortable, making them leave the area.

Table 2.1: Different Frequency ranges for animals [10]

Index No.	Animal	Frequency Range (kHz)
1	Human	0 - 20
2	Birds, Squirrels, Monkeys	10 - 35
3	Dog, Cat Beetles, Ants, Boars	36 - 65
4	Rat, Mouse	66 - 100

The design structure was constructed as in figure 2.1. Input power to the system is 9 V DC. Using the PIR sensor, it detects an obstacle in front of the device. The sensor data is input into the Arduino controller. The program was constructed according to the requirements (Output frequency is set to 25 kHz). Then the voltage regulator regulates the output voltage and inputs it into the ultrasonic sound transmitter. Repeaters are used here to increase the range.

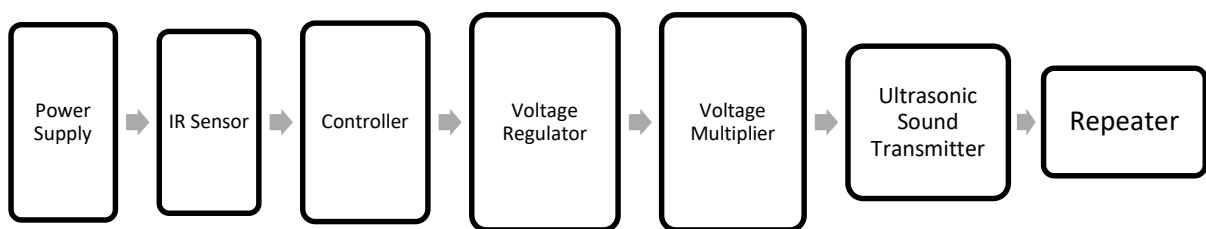


Figure 2.1: Design Structure of the project

A battery supply is used respectively to provide the input to the circuit. IR Sensor is used to detect the motion. Controller is used to control the frequency by using Arduino. Voltage regulator is connected to ensure the constant supply of the voltage at +3 V. The voltage multiplier (here, voltage triple) to amplify the source voltage. Voltage multipliers are AC-to-

DC power conversion devices, comprised of diodes and capacitors that produce a high potential DC voltage from a lower voltage AC source. Ultrasonic transmitter produces a variable frequency ranging from 10 kHz to 100 kHz a series of capacitors. Repeaters boost the strength of the signals and extend their range to the concept of implementation.

The circuit was set up as in figure 2.2. The frequency of the circuit can be changed by changing the frequency value of the Arduino program.

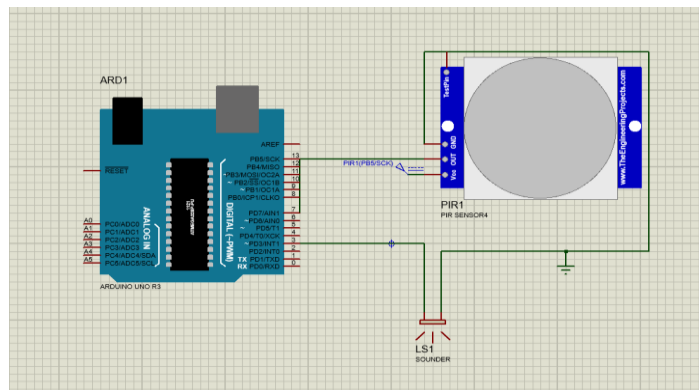


Figure 2.2: The Circuit Diagram

### 3.0 RESULTS AND DISCUSSION

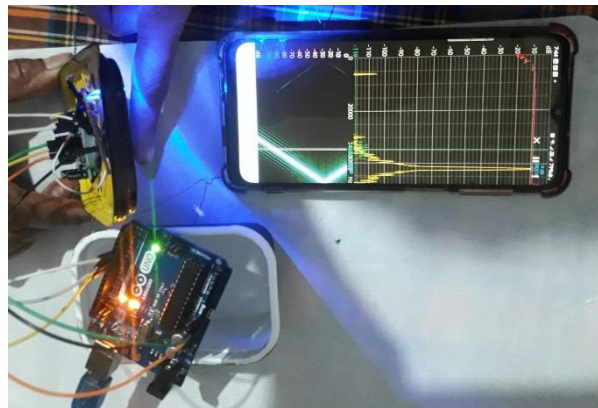


Figure 3.1: The working Circuit with output frequency

A pre-defined frequency was output when the circuit was powered as in figure 3.1. The output frequency can only change with the change of the Arduino program. It was a bit difficult to change in different scenarios. For future improvement, the circuit and the attachment can be built to change the frequency externally.

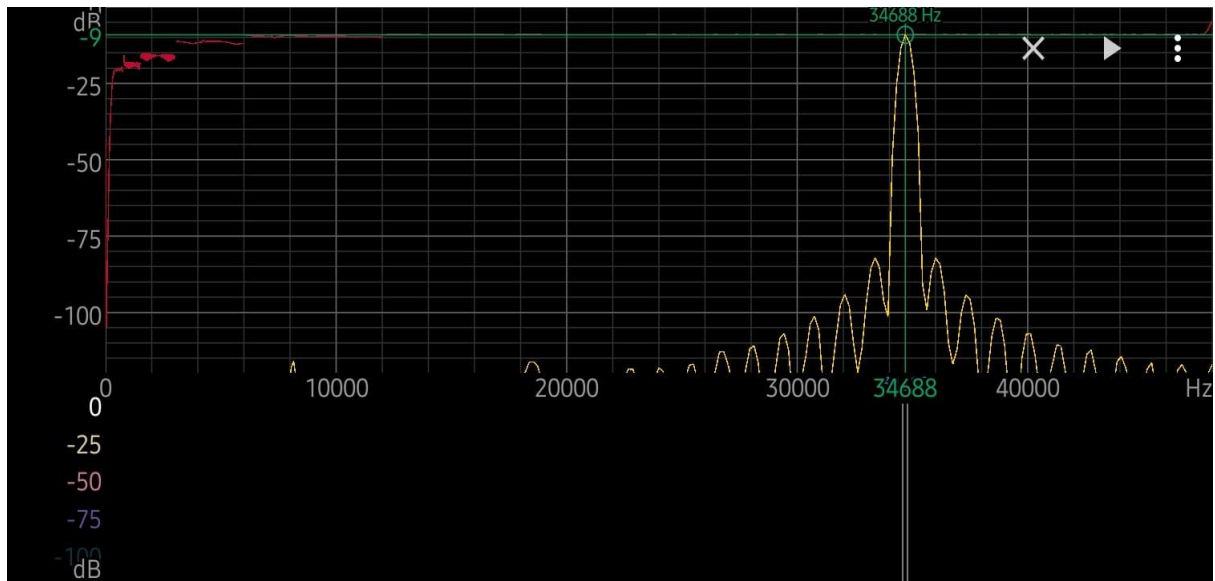


Figure 3.2: Output Frequency

The output frequency of the unit as in figure 3.2 is 34.68 kHz. This indicates the output of this system can only be hearable only for monkeys, and squirrels [10]. The monkey-repellent unit was installed in the telephone tower to get feedback.

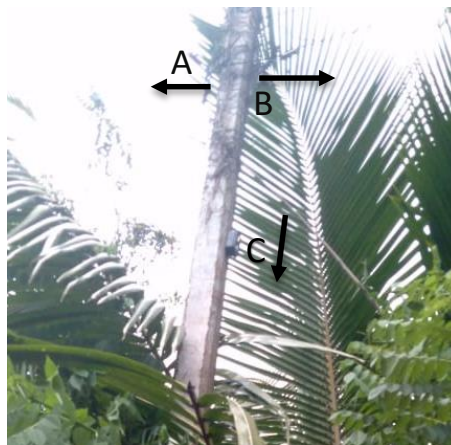


Figure 3.3: Unit Installation

The repellent unit was installed on the telephone tower as in figure 3.3. It was identified that the placement or installed direction is more critical for its function. A one-week observation was done to finalize the fixing location and the results were as below.

Table 3.1: Device installation Observations

Location	Direction	Placed Duration	Reason for placement	Comments
A	Facing trees and buildings	3 days	To avoid moving animals from trees to telephone wires	A few monkeys (7,8 monkeys) were identified on wires
B	Straight to the telephone wire	3 days	To direct the frequency to animals on wire	No monkeys and squirrels were detected on the 50m range
C	Downwards the wire	3 days	To avoid moving animals from trees to telephone wires	Animals on wire (Monkeys and squirrels)

Following observations direct to place the ultrasonic unit to “B” place; which directly faces the telephone line. The unit can control an area of 50m range. Therefore, another unit needs to be placed opposite the same tower.

#### 4.0 CONCLUSION

This paper describes a methodology to protect telephone wires from monkeys. The major damages reported to the SLT OPMC are due to animal bites; especially monkey bites of the telephone cables. We can conclude that the use of frequency bands which hearable for the relevant animal category is the best method for animal deterrent devices in the communication industry. It can conclude that the proposed system can be used in telephone wires more effectively than previously used methods. Proper grounding and the use of surge protection methods are critical to avoid damage from electrostatic charges and lightning. A solar-powered system can be suggested as a future improvement for successfully maintaining the continuous function to power up the unit.

#### ACKNOWLEDGEMENTS

The authors wish to extend their gratitude for the assistance given by the Department of Electronics at the Wayamba University of Sri Lanka and thank all who have supported making this research a success.



## REFERENCES

1. Leo Louis, Working Principle of Arduino and using IT as a tool for study and research, *International Journal of Control, Automation, Communication and Systems*, no.02 (2016), 21, [https://www.researchgate.net/publication/326316390\\_Working\\_Principle\\_of\\_Arduino\\_and\\_Using\\_it\\_as\\_a\\_Tool\\_for\\_Study\\_and\\_Research](https://www.researchgate.net/publication/326316390_Working_Principle_of_Arduino_and_Using_it_as_a_Tool_for_Study_and_Research), (Accessed date : 2022.11.12)
2. Bera, R., Pradhan, P. C., Liu, C.M., *Advances in Communication, Devices, and Networking*, Springer Nature, 2019, E-book
3. Arduino Uno, *Components101*, (2021), <https://components101.com/microcontrollers/arduino-uno>, (Accessed date : 2022.11.12)
4. Arduino UNO R3, <https://docs.arduino.cc/hardware/uno-rev3> (Accessed date : 2022.11.05)
5. What is Arduino, <https://www.arduino.cc/en/guide/introduction> (Accessed date : 2022.10.23)
6. Richard A. Lopchinsky, MD, FACS and Nancy H. Van Name, RDMS, RTR, and Marlene Kattaron, RDMS, “Physical Principles of Ultrasound”, 2000.
7. Ultipliers, Design Guide, Introduction, 281.
8. Fay R.R., *Hearing in Vertebrates: a Psychophysics Data book*, Hill-Fay Associates, Winnetka IL, ,1988.
9. Adami, D., Ojo, M.O, Giordano, S., Design, development and evaluation of an intelligent animal repelling system for crop protection based on embedded edge-ai, Digital Object Identifier 10.1109/ACCESS.2021.3114503, 07
10. Sabina N., Haseena P.V. , An Intelligent Animal Repellent System for Crop Protection: A Deep Learning Approach, *International Journal of Engineering Research in Computer Science and Engineering (IJERCSE)*, Vol 9, Issue 9, (2022)
11. Warakapitiya K., Too much monkey business causing havoc on many fronts, The Sunday times, ,<https://www.sundaytimes.lk/180610/news/too-much-monkey-business-causing-havoc-on-many-fronts-297445.html>, (Accessed date: 2022-10-02)
12. Kumar, V., Kumar, M., Sharma, S., Upgraded Ultrasonic Animal Deterrent Device, Page No:2

## DEVELOPMENT OF A SMART AGRO SOIL ANALYZER

M.A. Pathiraja<sup>1\*</sup>, W.A.S. Wijesinghe<sup>1</sup>, A.P. Kumara<sup>2</sup>

<sup>1</sup>*Department of Electronics, Wayamba University of Sri Lanka, Kuliyaipitiya, Sri Lanka*

<sup>2</sup>*SLT Digital LAB, Sri Lanka Telecom PLC, Lotus Road, Colombo 01*

\*ashan.pathiraja@gmail.com

### ABSTRACT

Chemical fertilizer plays an essential role in enhancing crop productivity and soil fertility. However, continuous utilization of chemical fertilizers is responsible for the decline of soil organic matter (SOM) content coupled with a decrease in the quality of agricultural soil. To overcome the chemical fertilizer overuse and protect the soil health, soil micronutrient content, and soil health have to be measured, and soil parameters have to be analyzed. Typical soil health and micronutrient content assessment require intensive field sampling and laboratory analysis. Although this approach yields accurate results but only suitable for static measurements of the soil properties and not suitable for continuous tracking of soil properties and micronutrient content because some of the soil properties (Soil moisture, temperature, conductivity, PH value) changes after taking the soil samples. Therefore typical laboratory analysis is not suitable for predicting the soil health accurately. Advances in an integrated soil sensors and wireless technologies, IOT based and offline soil analyzing systems are commercially available in the market to replace physical sampling, but those systems are expensive and suitable for large scale farms. This paper presents the development of portable and both online and offline mode supported consumer grade soil analyzing system which has low power consumption, for small scale and large scale farmers by combining cellular based low power wide area network technologies and commercially available integrated soil sensor.

**Keywords:** Soil analyzing system, Low Power Wide Area Network (LPWAN)

### 1.0 INTRODUCTION

Over 40% of global croplands are managed by smallholder farms (typically less than 2 hectare), mainly located in the developing world Compared to large-scale farms in developed countries (usually more than 20 hectares) [1]. Farms in developing countries are more likely to significantly over- or under-apply fertilizers, due to lack of knowledge about soil health and

micronutrient content of the soil due to not availability of low cost soil sampling services and devices.

The IOT based and offline soil analyzing systems are commercially available in the market for continuous monitoring of soil parameters. There are different types of wireless systems currently available for monitoring the soil parameters based on various technologies [2]. The most of the commercially available soil condition monitoring systems use low power wide area network (LPWAN) wireless technologies like LoRaWAN, SIGFOX, and NB-IOT can achieve long communication range (in the order of kilometers) while consuming low power and without the need for intermediate nodes. The LoRaWAN based soil condition monitoring systems suitable for large scale farms because it contains multiple sensor network connected by LoRaWAN local area network [4]. Also initial cost of LoRaWAN based soil condition system is expensive. Therefore currently available soil condition monitoring systems are not suitable for small scale farms which requires expensive initial cost and lack of portability. As a solution, low power and portable low cost soil analyzer system was proposed which supported the both online and offline soil monitoring capability to overcome the weaknesses of the currently available solutions therefore a by combining cellular based low power wide area network technologies and commercially available integrated soil sensor [5].

## **2.0 METHODOLOGY**

### **2.1 General Description of the overall system**

Smart agro soil analyzer system contains soil analyzer device and cloud server as shown in Figure 2.1. The integrated soil sensor reads seven soil parameters required to calculate soil health and micronutrient. The collected data is transmitted to the cloud server through the NB-IOT LPWAN technology using SIM7000X series Multi-Band 4G LTE cellular communication module.

Also, soil analyzer device supported the local data storage, if the cellular network coverage is not available. The soil analyzer device stores the soil parameters with the date and time in the microSD memory card. The locally stored readings automatically sends to the cloud server when cellular network available. The soil analyzer device normally operates in two modes - sleep mode and active mode to reduce the power consumption. In the sleep mode MCU (Microcontroller Unit) goes to the sleep mode and disables the power to the each peripheral accepts the RTC module and minimizes the power consumption of the hardware device.

According the RTC alarm interrupts MCU goes to active mode and enables the power to the peripherals and takes the readings and sends to the cloud server or store to local storage.

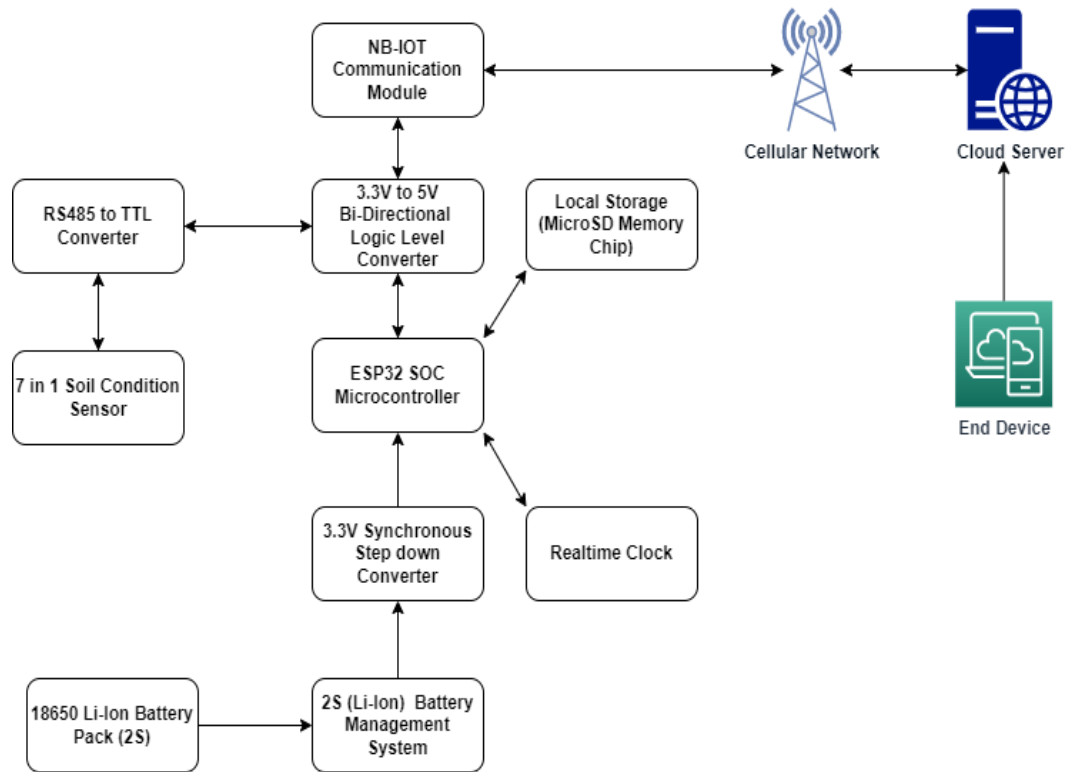


Figure 2.1: Block diagram of the design

According to the Figure 2.1 the soil analyzer device control logic is implemented by the Espressif systems ESp32 SOC MCU, which contains in built Wi-Fi and Bluetooth features. ESp32 also features excellent deep sleep current less than 60  $\mu$ A. The 7 in 1 integrated soil sensor connects to the MCU through the RS485 interface and the NB-IOT module connects to the MCU through the UART interface. The NB-IOT module uses the UDP protocol to transfer the data to the cloud server. The Li-Ion battery pack created by connecting two 3.7 V Li-Ion cells in series (2S) configuration. The battery management module is used to protect the battery pack from over charge, over discharge and short circuit protection. The synchronous buck converter module uses for efficiently converts the battery voltage to 3.3 V.

## 2.2 Description of the firmware

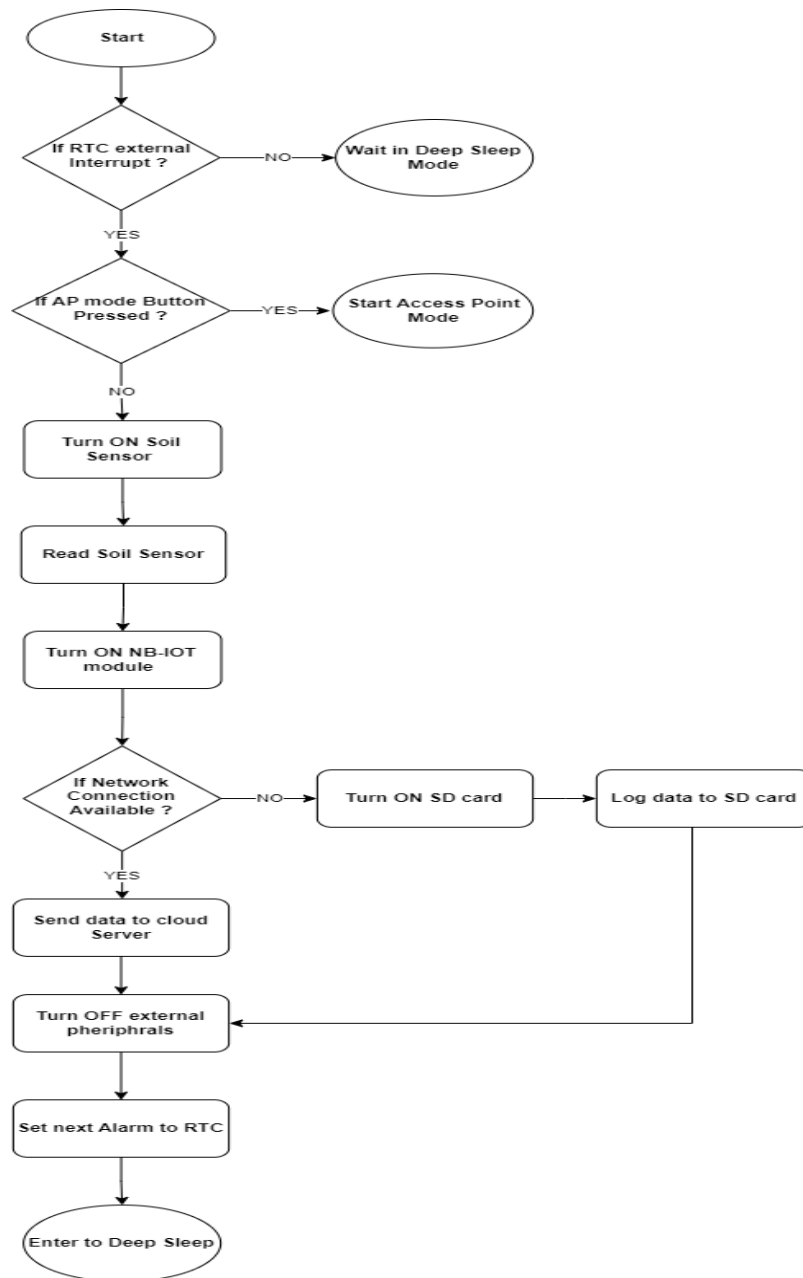


Figure 2.2: Flow of the Smart Agro Soil analyzer Firmware

The main steps of the Smart soil analyzer device firmware is shown in the Figure 2.2. When the device starts first, MCU configure the RTC alarm interrupt and disables all external peripherals except the RTC then enters to the deep sleep mode.

When RTC interrupts occurs MCU wakes up from the deep sleep mode and then checks, if the AP mode button is pressed. Thereafter it creates the Wi-Fi access point and starts a web server and host configuration HTML page to the connected clients, else it enables the soil condition sensor and reads the soil parameters. Then the MCU enables the NB-IOT module and checks

the network connectivity. If network connectivity is available, then it sends the readings to the cloud server, or else stores the reading to the local storage and goes to deep sleep mode.

### 2.3 Soil analyzer PCB Design



Figure 2.3: Populated PCB of the Smart Agro Soil Analyzer

As shown in Figure 2.3, A Printed Circuit Board (PCB) was designed and manufactured by integrating all the peripherals in to double side PCB. Then PCB soldered and tested by writing test firmware for each peripheral.

### 2.4 Soil analyzer Prototype



Figure 2.4: Top view and Bottom view of the completed soil analyzer Prototype

The soil analyzer PCB, battery pack and NB-IOT module was inserted in to the water proof enclosure and soil analyzer device finalized as show in Figure 2.4.

## 3.0 RESULTS AND DISCUSSION

Prototype of the soil analyzer hardware device was developed and tested multiple times without bugs. The system was setup and soil sample was tested as shown in the Figure 3.1. The Figure 3.2 shows the real time soil parameters in the cloud server web dashboard.



Figure 3.1: Smart Agro Soil Analyzer test setup



Figure 3.2: Screen shot of the cloud server real time Web Dashboard

Table 3.1: Measured average current consumption of the device

Active Mode (mA)	Sleep Mode (mA)
130mA	5mA

The table 3.1 shows the active and sleep mode average current consumptions of the soil analyzer. The theoretical estimated device run time calculated according to the equation 1.

$$\text{Battery Run time (Hours)} = \frac{\text{Battery Capacity (mAh)}}{\text{Load Current (mA)}} \quad (1)$$

The capacity of the battery was 8600mAh, and the run time of the device is approximately 45 days.

Under the work carried out, some significance capabilities were identified which increase the device operation time, durability and the usability. There were few key points that should be overcome in the next level of development. One is the use of ultra-low power MCU and power management integrated circuit to reduce the power consumption of the device and increase the operating time. The next point is the use of stable and well documented NB-IOT module which increases the stability of the device. The use of industrial grade water proof enclosure, water proof buttons and connectors to increase the durability of the device.

#### **4.0 CONCLUSION**

The main objective of this research is to develop a low power, portable and low cost soil condition monitoring system which supported the both online and offline soil monitoring capability. The soil analyzer device able to operate outdoor conditions long time period by minimizing the power consumption using low power wide area network. The real time soil parameters updates in the web dashboard therefore users can view the data from any mobile device through the internet. Therefore the “Smart Agro Soil Analyzer” system was suitable for small scale farmers to analyze the soil micronutrient content and the soil health.

#### **ACKNOWLEDGMENTS**

Authors would like to express their gratitude to academic and non-academic staff of Department of Electronics, Faculty of Applied Sciences, Wayamba University of Sri Lanka and to the team members of the SLT Digital LAB research and development unit, Sri Lanka Telecom PLC.

#### **REFERENCES**

- [1]. Adamopoulos, T., Restuccia, D., The Size Distribution of Farms and International Productivity Differences, *AMERICAN ECONOMIC REVIEW*, vol. 106 (2014), pp:1667-97.
- [2]. Feng, X., Yan, F., Liu, X. Study of Wireless Communication Technologies on Internet of Things for Precision Agriculture, *Wireless Personal Communications*, vol.:108 (2019), pp:1785–1802.
- [3]. Bhatnagar V., Chandra R., IOT-Based Soil Health Monitoring and Recommendation System, *Internet of Things and Analytics for Agriculture*, vol.:02 (2019), pp:1-21.



[4]. Ramson, S. R. J., A Self-Powered Real-Time, LoRaWAN IoT-Based Soil Health Monitoring System, *IEEE Internet of Things Journal*, vol. 8 (2021), pp: 9278-9293.

[5]. JXCT,7 in 1 Integrated Soil Sensor EC PH NPK Moisture Temperature Meter, [http://www.jxctiot.com/product/showproduct.php?id=197&gclid=Cj0KCQiAn4SeBhCwARIsANeF9DK6lQqz53\\_y7wSPInYeVTmBXrfHDsZNpi3n97KaM-n7J6oGMtyot-MaAsqnEALw\\_wcB](http://www.jxctiot.com/product/showproduct.php?id=197&gclid=Cj0KCQiAn4SeBhCwARIsANeF9DK6lQqz53_y7wSPInYeVTmBXrfHDsZNpi3n97KaM-n7J6oGMtyot-MaAsqnEALw_wcB),  
[Accessed: 15-September-2022].

ISSN 2362-0560



9 772362 056001